Probing the meV QCD Axion with the SQWARE Quantum Semiconductor Haloscope

Pheno 2026

Jaanita Mehrani, Tao Xu, Andrey Baydin, Michael J. Manfra, Henry O. Everitt, Andrew J. Long, Kuver Sinha, Junichiro Kono, Shengxi Huang

based upon work in
arXiv:2509.14320

Axions are a promising DM model

- Several theoretical dark matter models with unique properties of mass, spin, charge, couplings!
- Axions could additionally solve the strong charge parity problem in quantum chromodynamics (QCD)

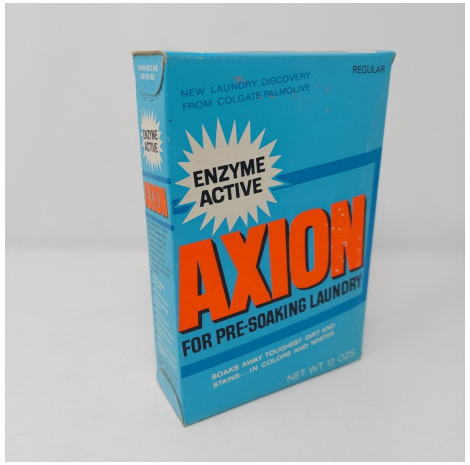

How can we detect axions? with photons!

- Axions can couple to photons under different models (KSVZ/DFSZ)

$$\mathcal{L}_{a\gamma\gamma} = \frac{g_{a\gamma\gamma}}{4} a F_{\mu\nu} \tilde{F}^{\mu\nu}$$

How can we detect axions? with photons!

- Axions can couple to photons under different models (KSVZ/DFSZ)

$$\mathcal{L}_{a\gamma\gamma} = \frac{g_{a\gamma\gamma}}{4} a F_{\mu\nu} \tilde{F}^{\mu\nu}$$

- Inverse Primakoff effect: axions can convert into photons in a magnetic field

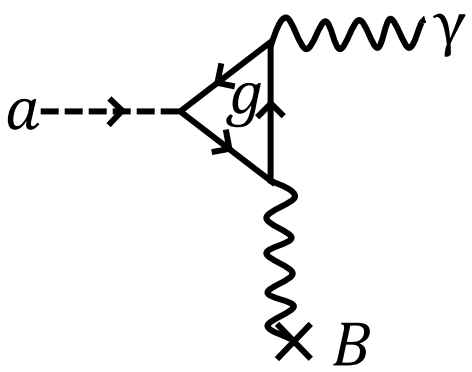

How can we detect axions? with photons!

- Axions can couple to photons under different models (KSVZ/DFSZ)

$$\mathcal{L}_{a\gamma\gamma} = \frac{g_{a\gamma\gamma}}{4} a F_{\mu\nu} \tilde{F}^{\mu\nu}$$

- Inverse Primakoff effect: axions can convert into photons in a magnetic field

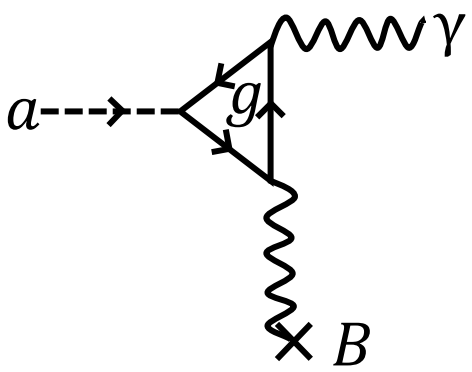

Inverse Primakoff effect

- Classical Maxwell's equations are modified under axion field a

$$\partial_\mu F^{\mu\nu} = J^\nu - g_{a\gamma} \tilde{F}^{\mu\nu} \partial_\mu a$$
$$\left(\partial_\mu \partial^\mu + m_a^2\right) a = -\frac{g_{a\gamma}}{4} F_{\mu\nu} \tilde{F}^{\mu\nu}$$

Inverse Primakoff effect

- Classical Maxwell's equations are modified under axion field a

$$\partial_\mu F^{\mu\nu} = J^\nu - g_{a\gamma} \tilde{F}^{\mu\nu} \partial_\mu a$$
$$\left(\partial_\mu \partial^\mu + m_a^2\right) a = -\frac{g_{a\gamma}}{4} F_{\mu\nu} \tilde{F}^{\mu\nu}$$

- To first order, axions convert to photons

$$\hat{\varepsilon}\mathbf{E}(t) = -g_{a\gamma}\mathbf{B}ae^{-im_a t}$$

Axion Search Strategies

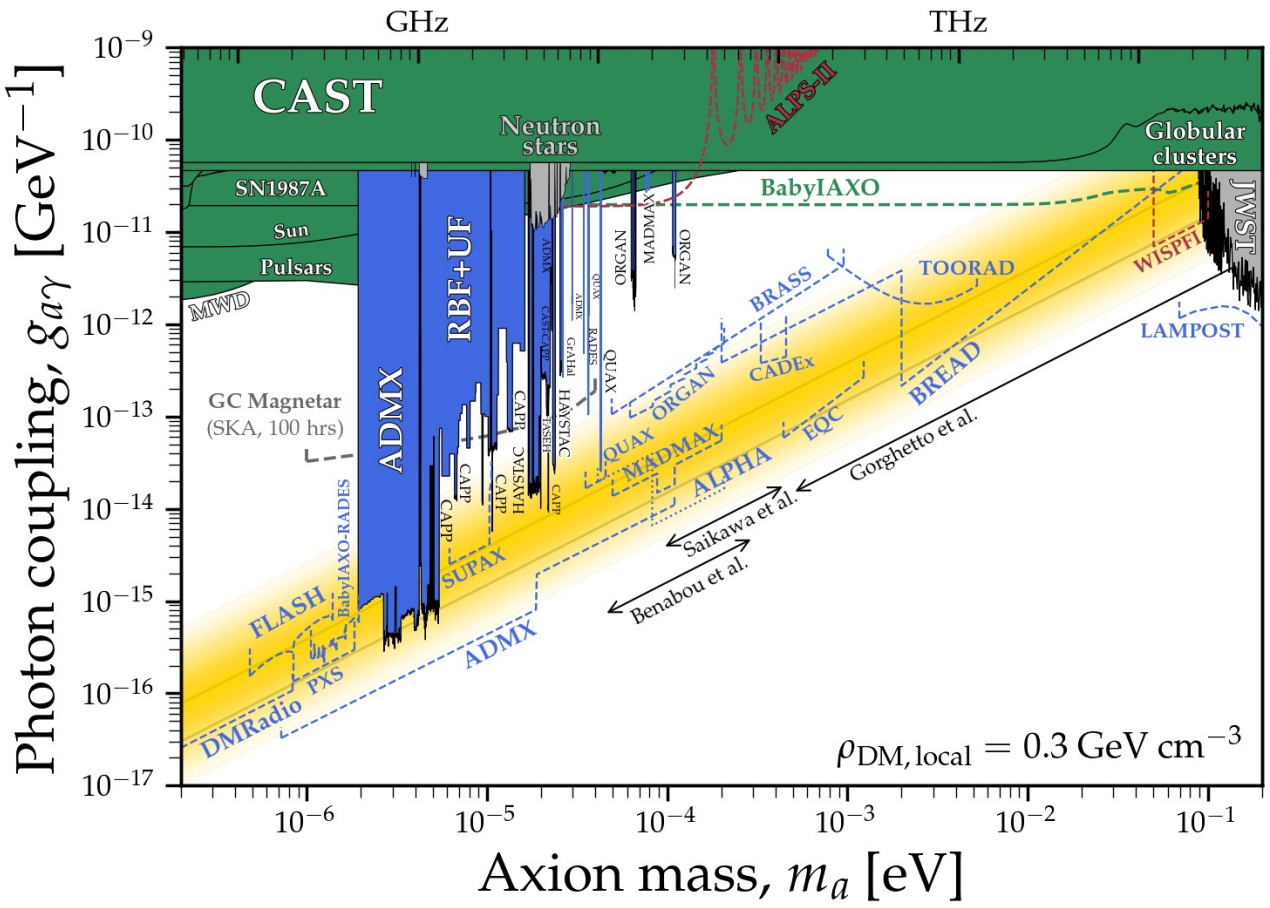

C. O'Hare

Axion Search Strategies

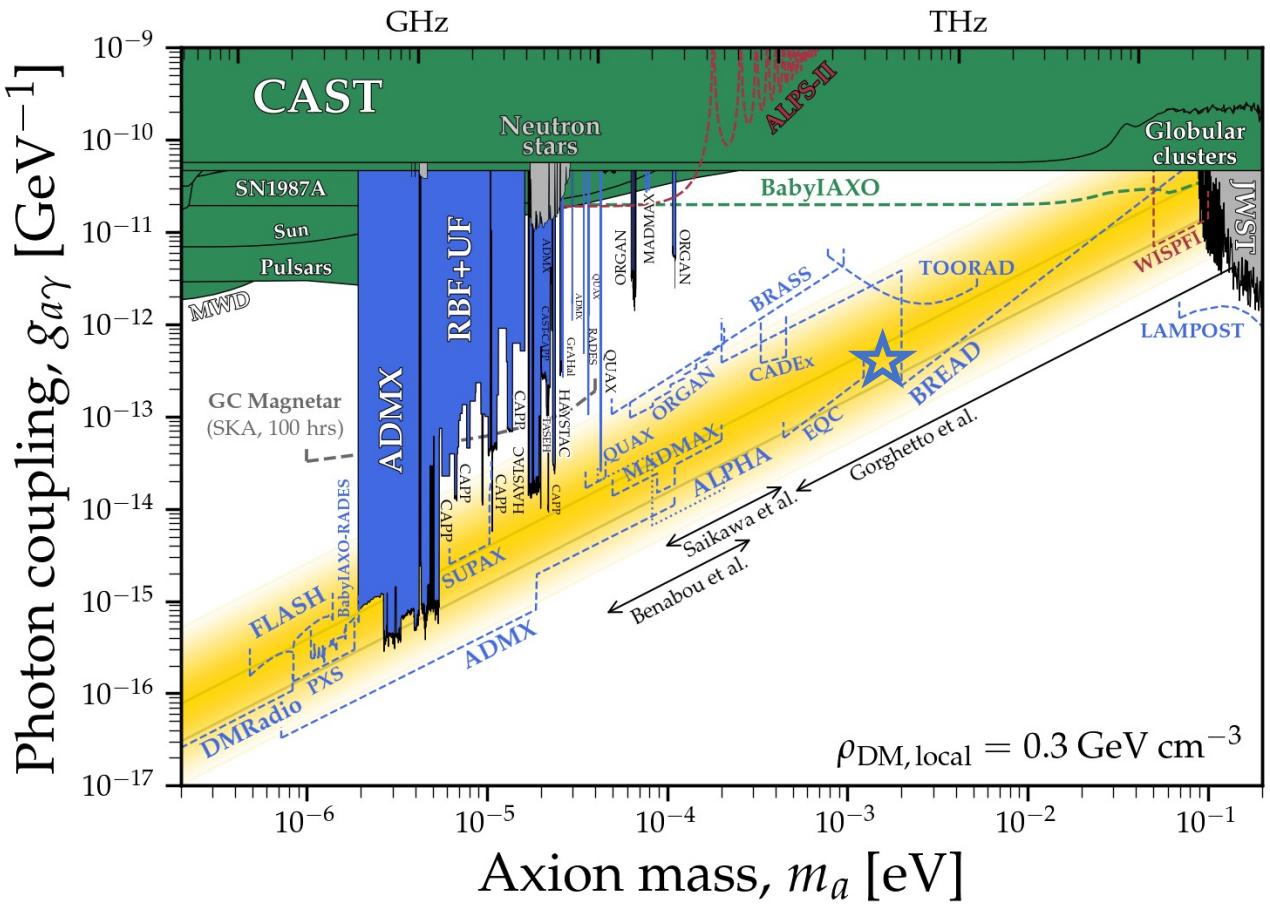

C. O'Hare

Axion Search Strategies

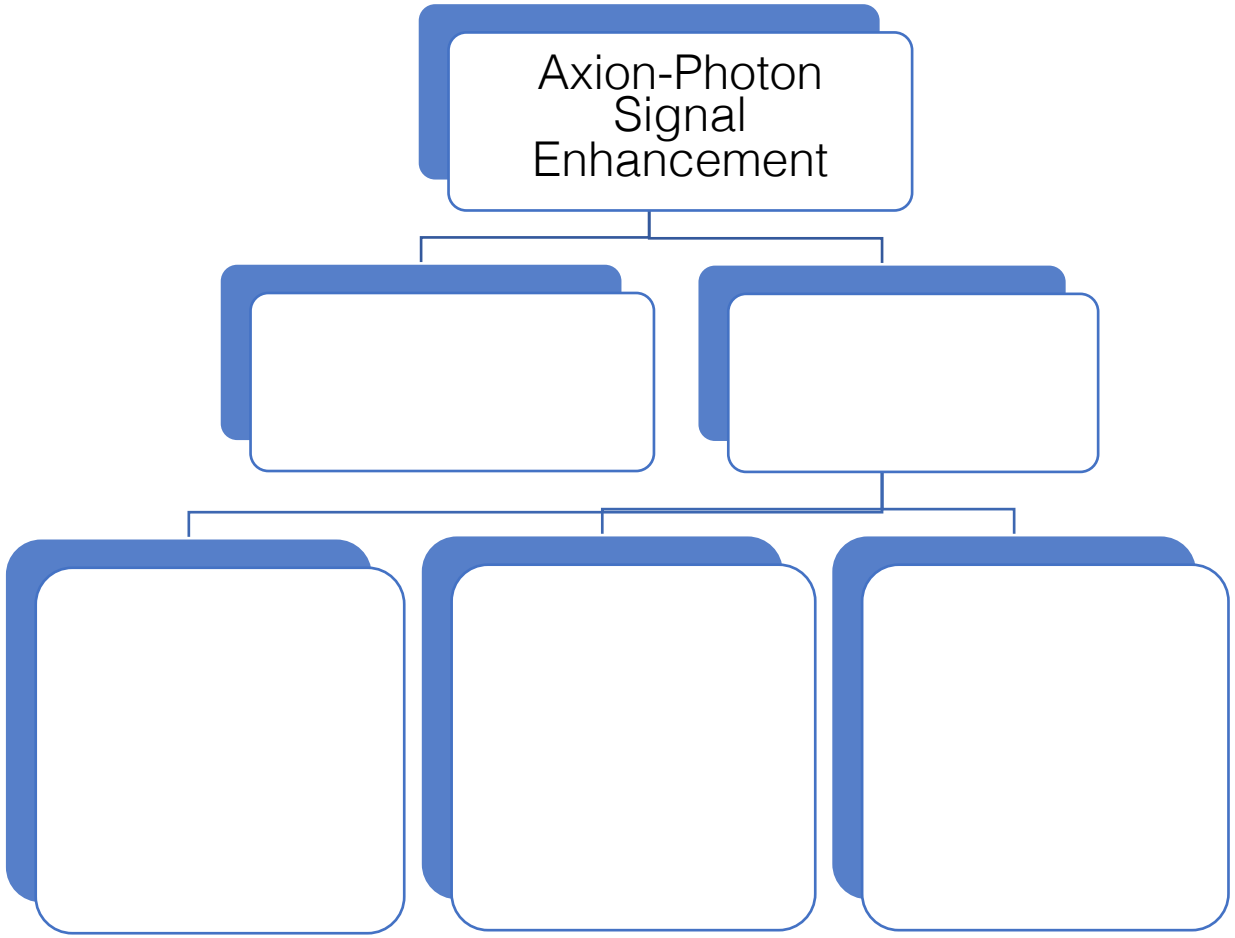

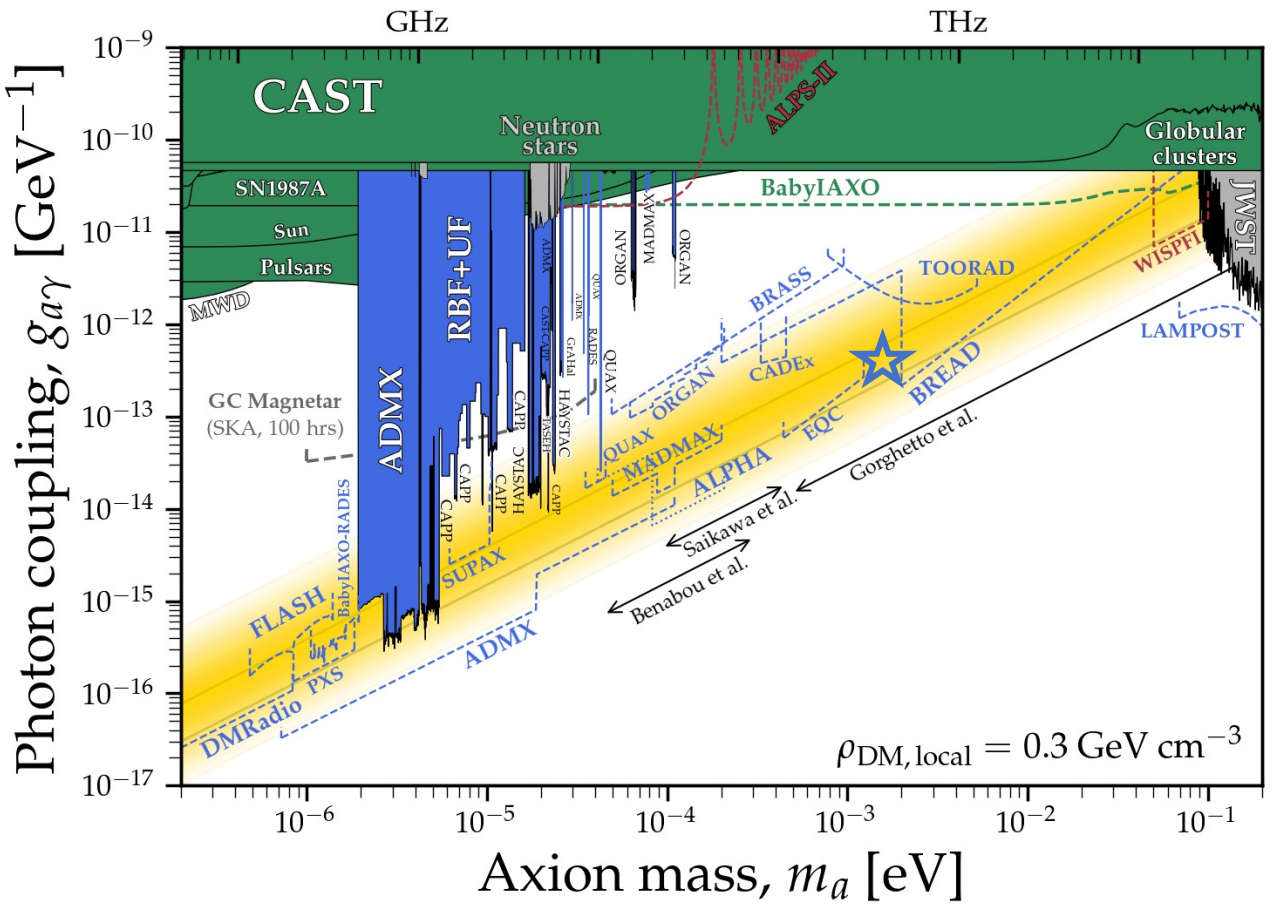

C. O'Hare

Axion Search Strategies

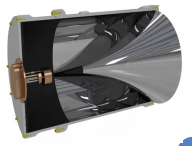

BREAD

Axion-Photon Signal Enhancement

Broadband: focus photons from large volume

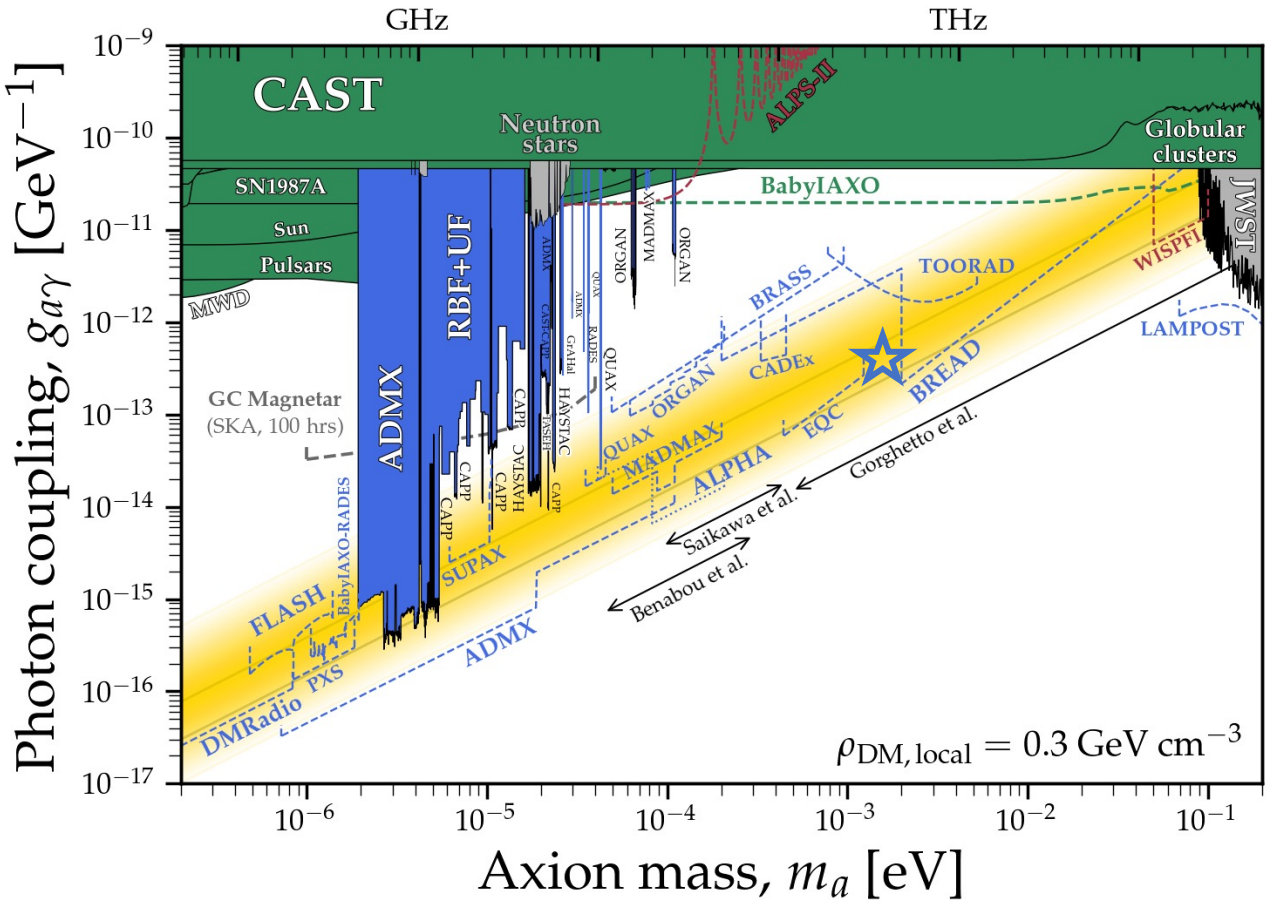

C. O'Hare

Axion Search Strategies

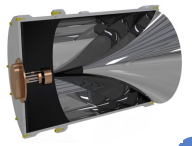

BREAD

Axion-Photon Signal Enhancement

Broadband: focus photons from large volume

Resonant: cavities resonate at axion mass

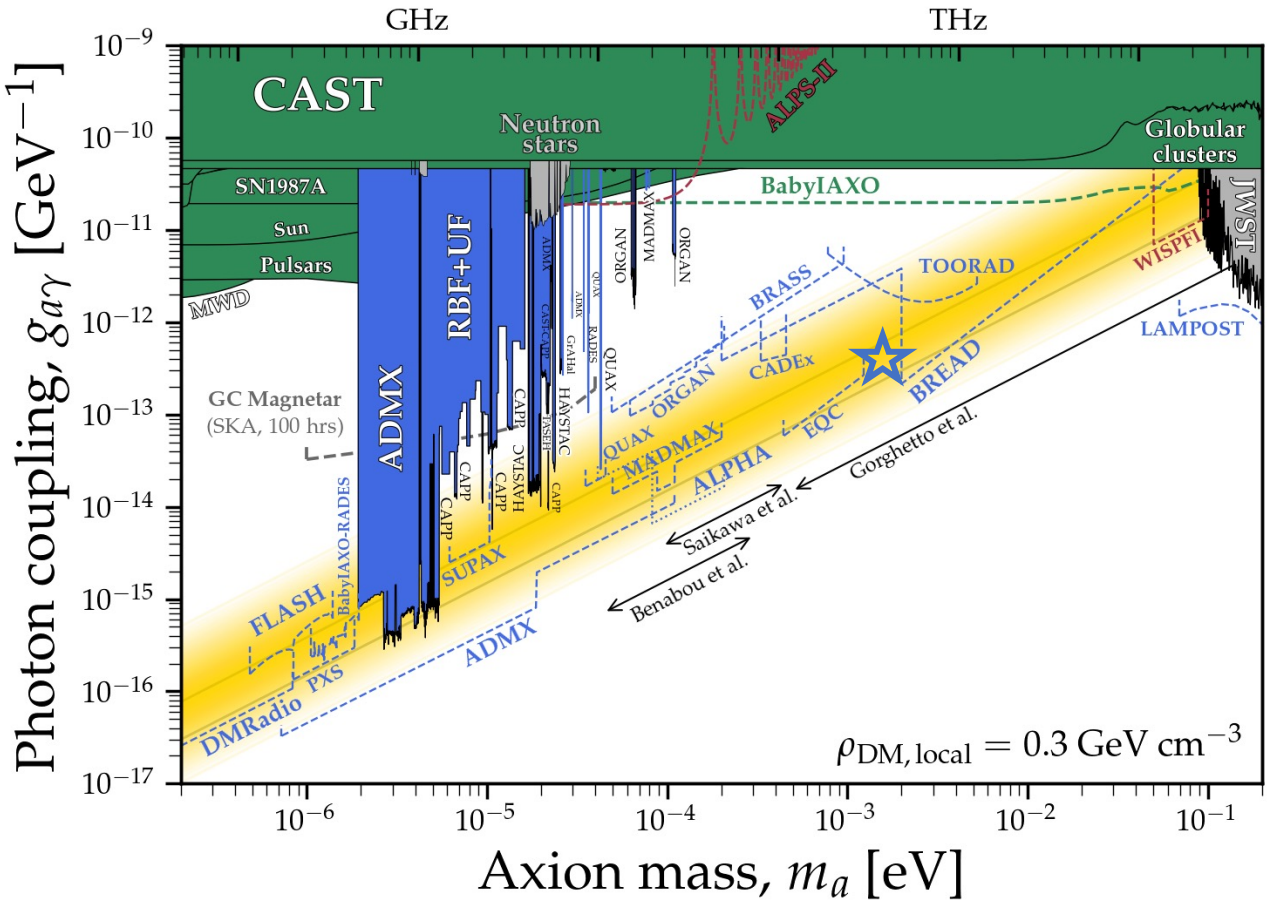

C. O'Hare

Axion Search Strategies

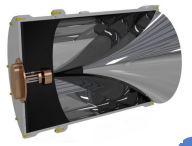

BREAD

Axion-Photon Signal Enhancement

Broadband: focus photons from large volume

Resonant: cavities resonate at axion mass

Vacuum

- reduced volume
- reduced quality
- mechanical tuning (moving rods)

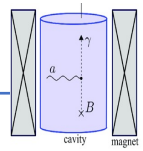

ADMX

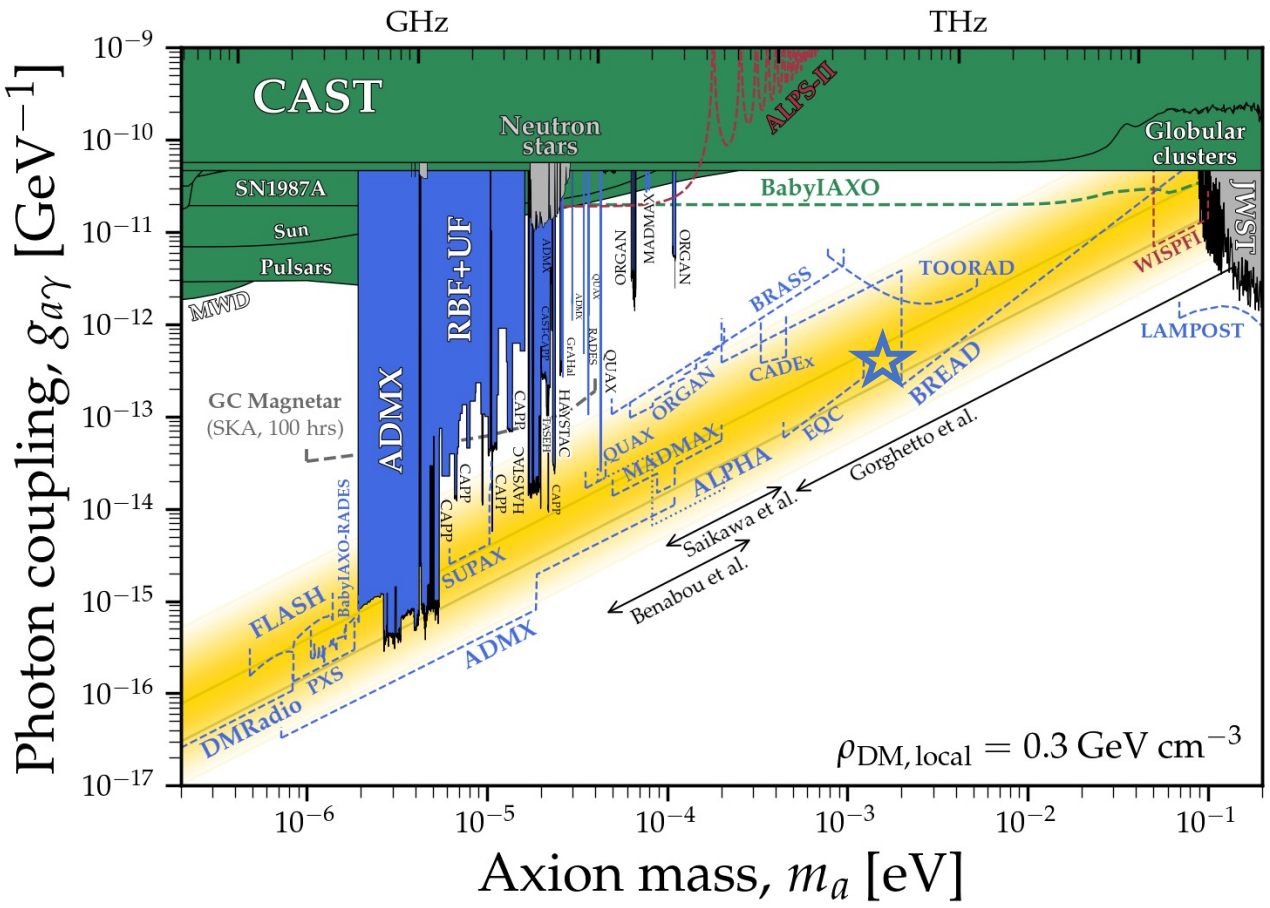

C. O'Hare

Axion Search Strategies

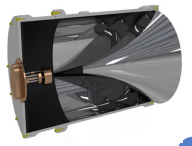

BREAD

- Axion-Photon Signal Enhancement
  - Broadband: focus photons from large volume
  - Resonant: cavities resonate at axion mass
    - Vacuum
      - reduced volume
      - reduced quality
      - mechanical tuning (moving rods)
    - Dielectric
      - reduced volume
      - low structural integrity
      - mechanical tuning (moving thin disks)

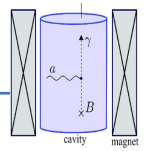

ADMX

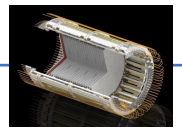

MADMAX

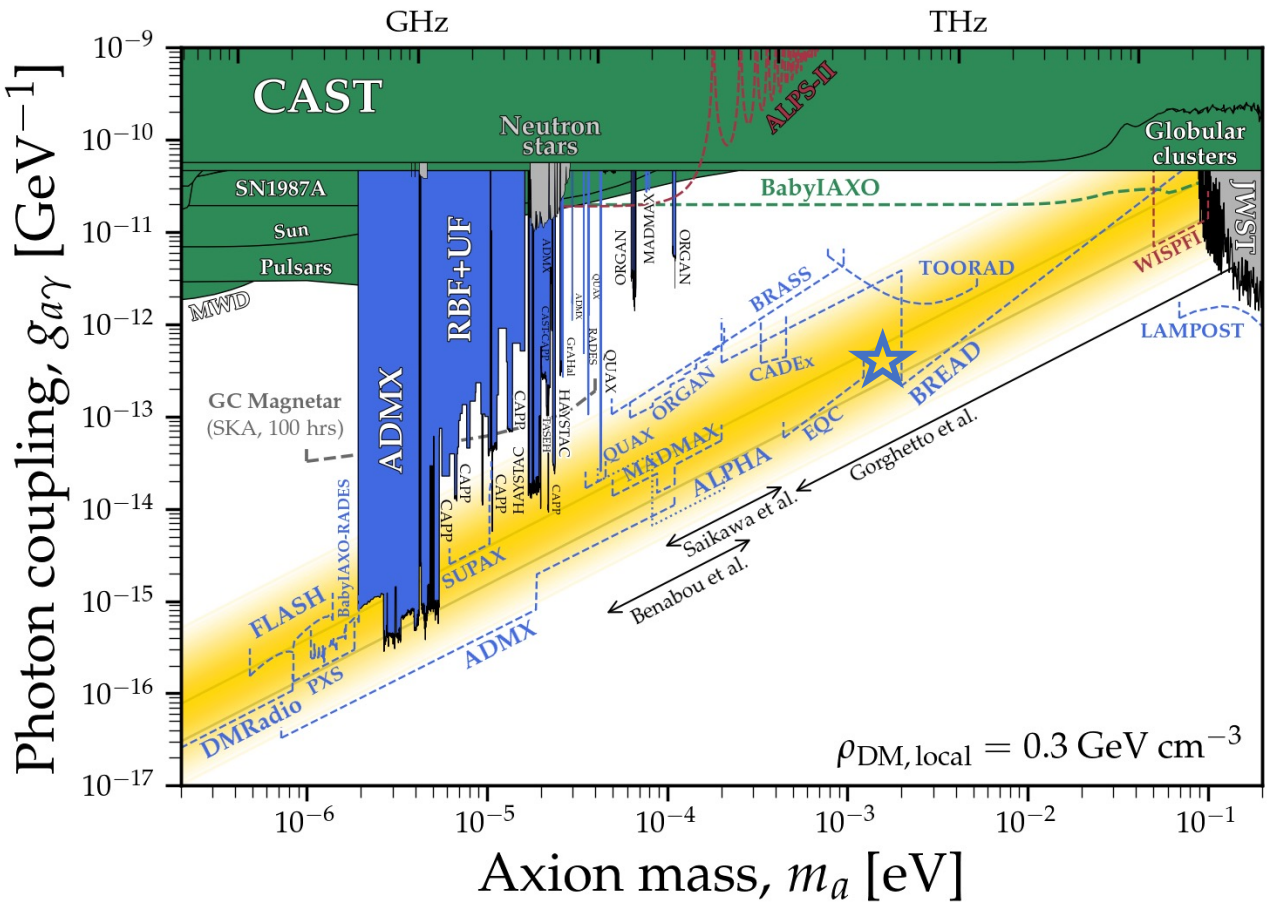

C. O'Hare

Axion Search Strategies

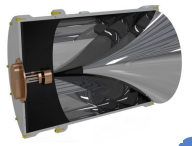

BREAD

Axion-Photon Signal Enhancement

Broadband: focus photons from large volume

Resonant: cavities resonate at axion mass

Vacuum

- reduced volume
- reduced quality
- mechanical tuning (moving rods)

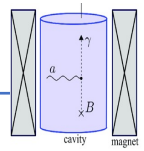

ADMX

Dielectric

- reduced volume
- low structural integrity
- mechanical tuning (moving thin disks)

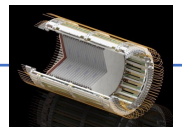

MADMAX

Material

- lack of low-loss materials
- often mechanical tuning (strain or pressure)

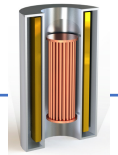

ALPHA

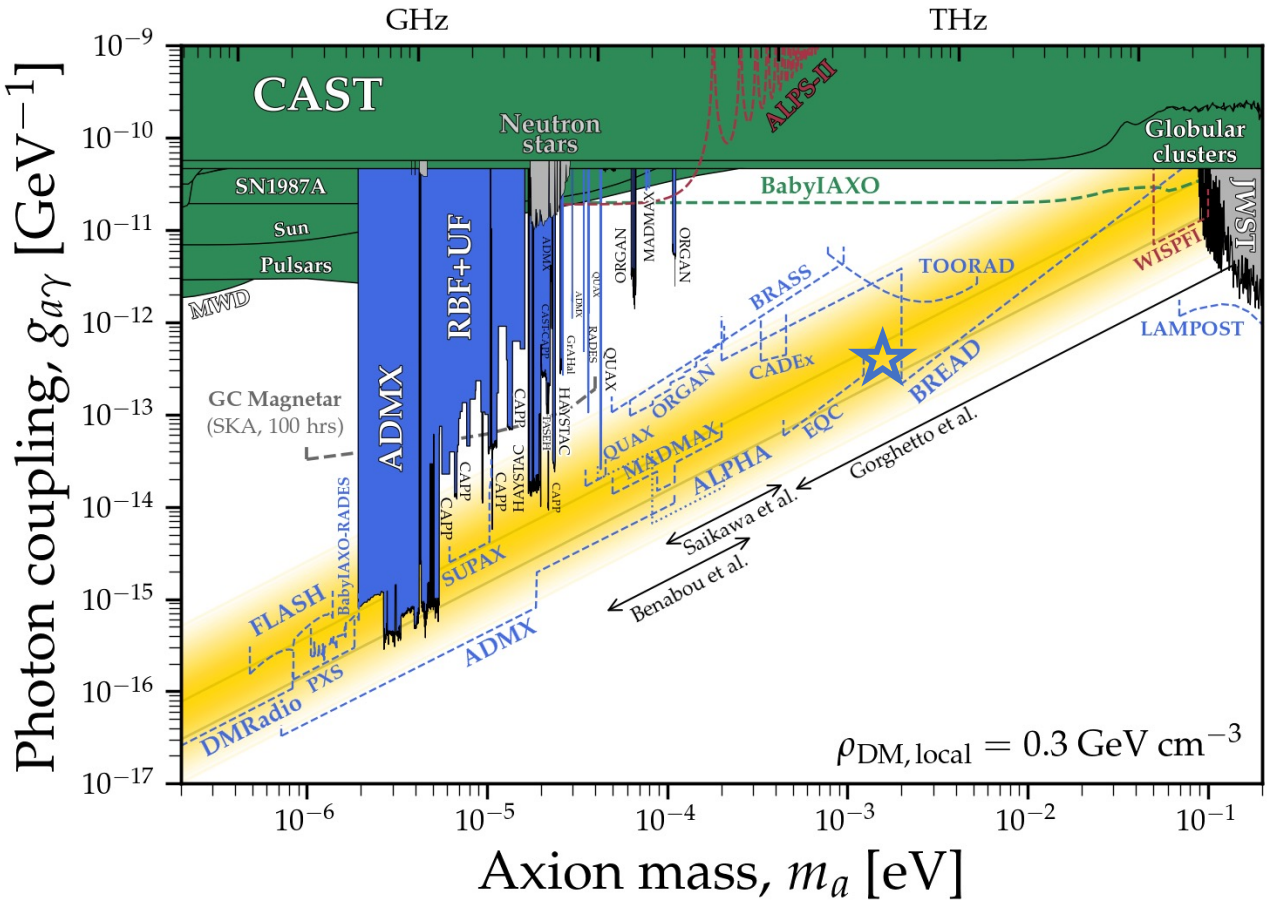

C. O'Hare

Material Resonances Enhance Axion-Photon Conversion

- Fermi's Golden Rule: Probability of axion → photon

Ara N. Ioannisian et al JCAP09(2017)005

Material Resonances Enhance Axion-Photon Conversion

- Fermi's Golden Rule: Probability of axion → photon

$$\Gamma_{a\to\gamma} = 2\pi \sum_{\mathbf{k}} |\mathcal{M}|^2 \delta(\omega_{\boldsymbol{a}} - \omega_{\mathbf{k}})$$

Ara N. Ioannisian et al JCAP09(2017)005

Material Resonances Enhance Axion-Photon Conversion

- Fermi's Golden Rule: Probability of axion → photon

$$\Gamma_{a\to\gamma} = 2\pi \sum_{\mathbf{k}} |\mathcal{M}|^2 \delta(\omega_{\boldsymbol{a}} - \omega_{\mathbf{k}})$$

Energy Conservation

Axion: $\omega_a = \sqrt{\mathbf{p^2} + m_a^2}$,

Photon: $\omega_{\mathbf{k}} = |\mathbf{k}|$

Ara N. Ioannisian et al JCAP09(2017)005

Material Resonances Enhance Axion-Photon Conversion

- Fermi's Golden Rule: Probability of axion → photon

$$\Gamma_{a\to\gamma} = 2\pi \sum_{\mathbf{k}} |\mathcal{M}|^2 \delta(\omega_{\boldsymbol{a}} - \omega_{\mathbf{k}})$$

Energy Conservation

Axion: $\omega_a = \sqrt{\mathbf{p^2} + m_a^2}$,

Photon: $\omega_{\mathbf{k}} = |\mathbf{k}|$

$$\mathcal{M} = \frac{g_{\alpha\gamma}}{2\omega V} \int d^3\mathbf{r}\, e^{i\mathbf{p}\cdot\mathbf{r}} \mathbf{B}(\mathbf{r}) i\omega_{\mathbf{k}} e^{-i\mathbf{k}\cdot\tilde{n}\cdot\mathbf{r}}$$

Ara N. Ioannisian et al JCAP09(2017)005

Material Resonances Enhance Axion-Photon Conversion

- Fermi's Golden Rule: Probability of axion → photon

$$\Gamma_{a\to\gamma} = 2\pi \sum_{\mathbf{k}} |\mathcal{M}|^2 \delta(\omega_{\boldsymbol{a}} - \omega_{\mathbf{k}})$$

Energy Conservation

Axion: $\omega_a = \sqrt{\mathbf{p^2} + m_a^2}$,

Photon: $\omega_{\mathbf{k}} = |\mathbf{k}|$

$$\mathcal{M} = \frac{g_{\alpha\gamma}}{2\omega V} \int d^3\mathbf{r}\, e^{i\mathbf{p}\cdot\mathbf{r}} \mathbf{B}(\mathbf{r}) i\omega_{\mathbf{k}} e^{-i\mathbf{k}\cdot\tilde{n}\cdot\mathbf{r}}$$

Momentum Mismatch

$$\mathbf{q} = \mathbf{p} - \mathbf{k}' = \sqrt{\omega_a^2 - m_a^2} - \tilde{n}\omega_{\mathbf{k}}$$

Ara N. Ioannisian et al JCAP09(2017)005

Material Resonances Enhance Axion-Photon Conversion

- Fermi's Golden Rule: Probability of axion → photon

$$\Gamma_{a\to\gamma} = 2\pi \sum_{\mathbf{k}} |\mathcal{M}|^2 \delta(\omega_{\boldsymbol{a}} - \omega_{\mathbf{k}})$$

Energy Conservation

Axion: $\omega_a = \sqrt{\mathbf{p^2} + m_a^2}$,

Photon: $\omega_{\mathbf{k}} = |\mathbf{k}|$

$$\mathcal{M} = \frac{g_{\alpha\gamma}}{2\omega V} \int d^3\mathbf{r}\, e^{i\mathbf{p}\cdot\mathbf{r}} \mathbf{B}(\mathbf{r}) i\omega_{\mathbf{k}} e^{-i\mathbf{k}\cdot\tilde{n}\cdot\mathbf{r}}$$

Momentum Mismatch

$$\mathbf{q} = \mathbf{p} - \mathbf{k}' = \sqrt{\omega_a^2 - m_a^2} - \tilde{n}\omega_{\mathbf{k}}$$

- Suppressed conversion due to momentum mismatch

Ara N. Ioannisian et al JCAP09(2017)005

Material Resonances Enhance Axion-Photon Conversion

- Fermi's Golden Rule: Probability of axion → photon

$$\Gamma_{a\to\gamma} = 2\pi \sum_{\mathbf{k}} |\mathcal{M}|^2 \delta(\omega_{\boldsymbol{a}} - \omega_{\mathbf{k}})$$

Energy Conservation

Axion: $\omega_a = \sqrt{\mathbf{p^2} + m_a^2}$,

Photon: $\omega_{\mathbf{k}} = |\mathbf{k}|$

$$\mathcal{M} = \frac{g_{\alpha\gamma}}{2\omega V} \int d^3\mathbf{r}\, e^{i\mathbf{p}\cdot\mathbf{r}} \mathbf{B}(\mathbf{r}) i\omega_{\mathbf{k}} e^{-i\mathbf{k}\cdot\tilde{n}\cdot\mathbf{r}}$$

Momentum Mismatch

$$\mathbf{q} = \mathbf{p} - \mathbf{k}' = \sqrt{\omega_a^2 - m_a^2} - \tilde{n}\omega_{\mathbf{k}}$$

- Suppressed conversion due to momentum mismatch

Ara N. Ioannisian et al JCAP09(2017)005

Material Resonances Enhance Axion-Photon Conversion

- Fermi's Golden Rule: Probability of axion → photon

$$\Gamma_{a\to\gamma} = 2\pi \sum_{\mathbf{k}} |\mathcal{M}|^2 \delta(\omega_{\boldsymbol{a}} - \omega_{\mathbf{k}})$$

$$\mathcal{M} = \frac{g_{\alpha\gamma}}{2\omega V} \int d^3\mathbf{r}\, e^{i\mathbf{p}\cdot\mathbf{r}} \mathbf{B}(\mathbf{r}) i\omega_{\mathbf{k}} e^{-i\mathbf{k}\cdot\tilde{n}\cdot\mathbf{r}}$$

Energy Conservation

Axion: $\omega_a = \sqrt{\mathbf{p^2} + m_a^2}$,

Photon: $\omega_{\mathbf{k}} = |\mathbf{k}|$

$\tilde{n} = \sqrt{\tilde{\varepsilon}} \to 0$

Momentum Match

$$\mathbf{q} = \mathbf{p} - \mathbf{k}' = \sqrt{\omega_a^2 - m_a^2} - \tilde{n}\omega_{\mathbf{k}}$$

- Resonant conversion due to momentum matching

Ara N. Ioannisian et al JCAP09(2017)005

Material Resonances Enhance Axion-Photon Conversion

- Fermi's Golden Rule: Probability of axion → photon

$$\Gamma_{a\to\gamma} = 2\pi \sum_{\mathbf{k}} |\mathcal{M}|^2 \delta(\omega_{\boldsymbol{a}} - \omega_{\mathbf{k}})$$

$$\mathcal{M} = \frac{g_{\alpha\gamma}}{2\omega V} \int d^3\mathbf{r}\, e^{i\mathbf{p}\cdot\mathbf{r}} \mathbf{B}(\mathbf{r}) i\omega_{\mathbf{k}} e^{-i\mathbf{k}\cdot\tilde{n}\cdot\mathbf{r}}$$

Energy Conservation

Axion: $\omega_a = \sqrt{\mathbf{p^2} + m_a^2}$,

Photon: $\omega_{\mathbf{k}} = |\mathbf{k}|$

$$\lambda_{\text{med}} = \frac{\lambda_{\text{vac}}}{\tilde{n}} \to \infty$$

$$\tilde{n} = \sqrt{\tilde{\varepsilon}} \to 0$$

Momentum Match

$$\mathbf{q} = \mathbf{p} - \mathbf{k}' = \sqrt{\omega_a^2 - m_a^2} - \tilde{n}\omega_{\mathbf{k}}$$

- Resonant conversion due to momentum matching

light hybridizing with matter, gaining effective mass

Ara N. Ioannisian et al JCAP09(2017)005

Multiple Quantum Wells (MQW)!

Multiple Quantum Wells (MQW)!

- Low-loss THz plasmonic resonances that are electromagnetically tunable…

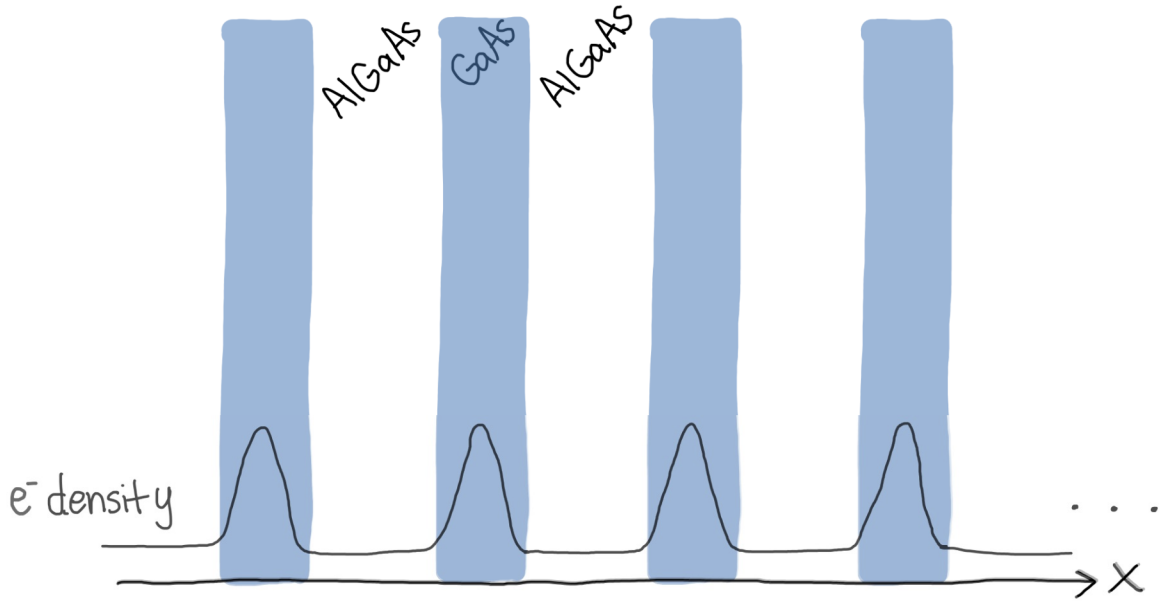

Multiple Quantum Wells (MQW)!

- Low-loss THz plasmonic resonances that are electromagnetically tunable… and well-studied!!

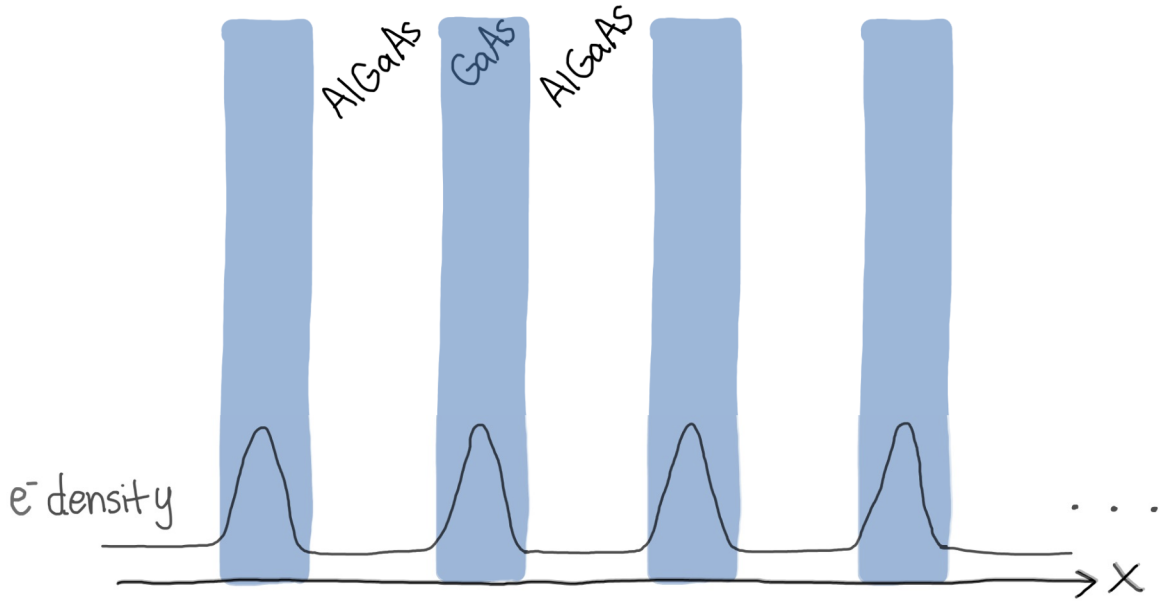

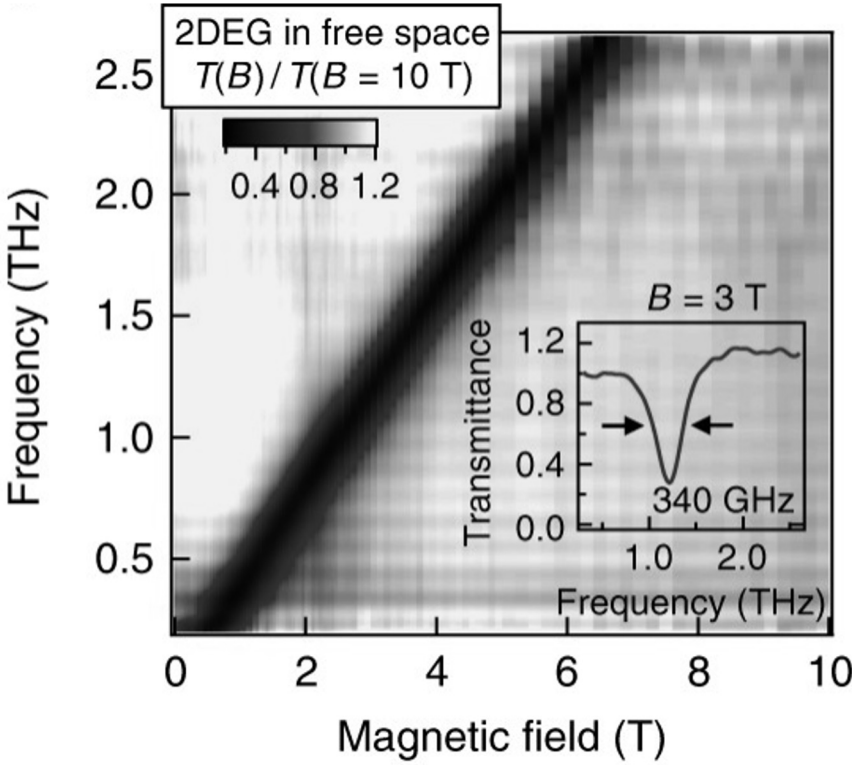

Li, X., Manfra, M., Kono, J., et. al. Nature Photonics (2018)

Semiconductor-Quantum-Well Axion Radiometer Experiment

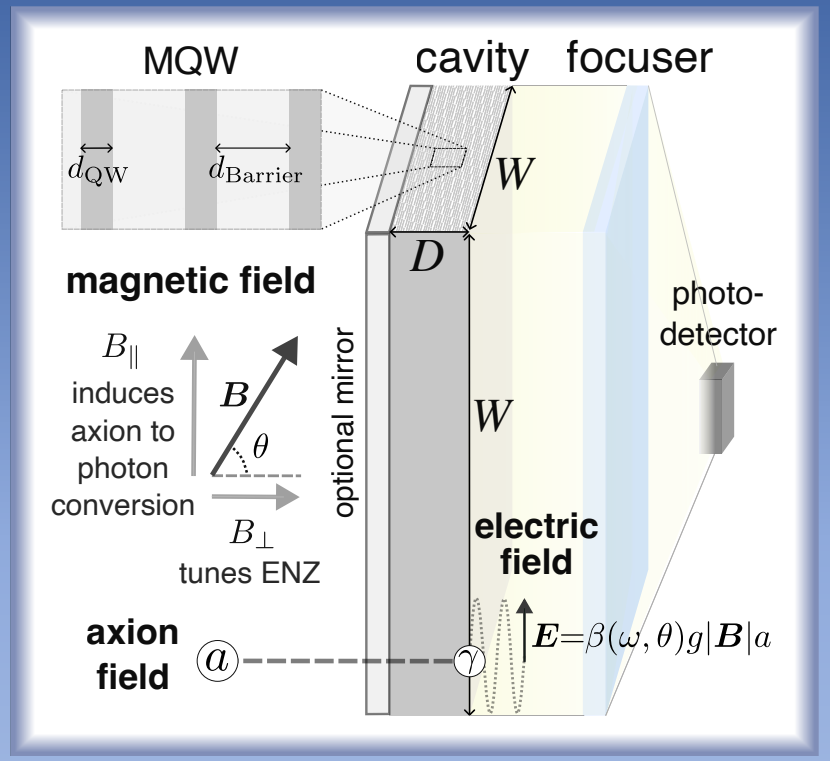

logo by Haaniya

Axion Response from MQW Cavity

- Axion-induced electric field

$$E_{\text{vac}} = g_{\alpha\gamma} B a$$

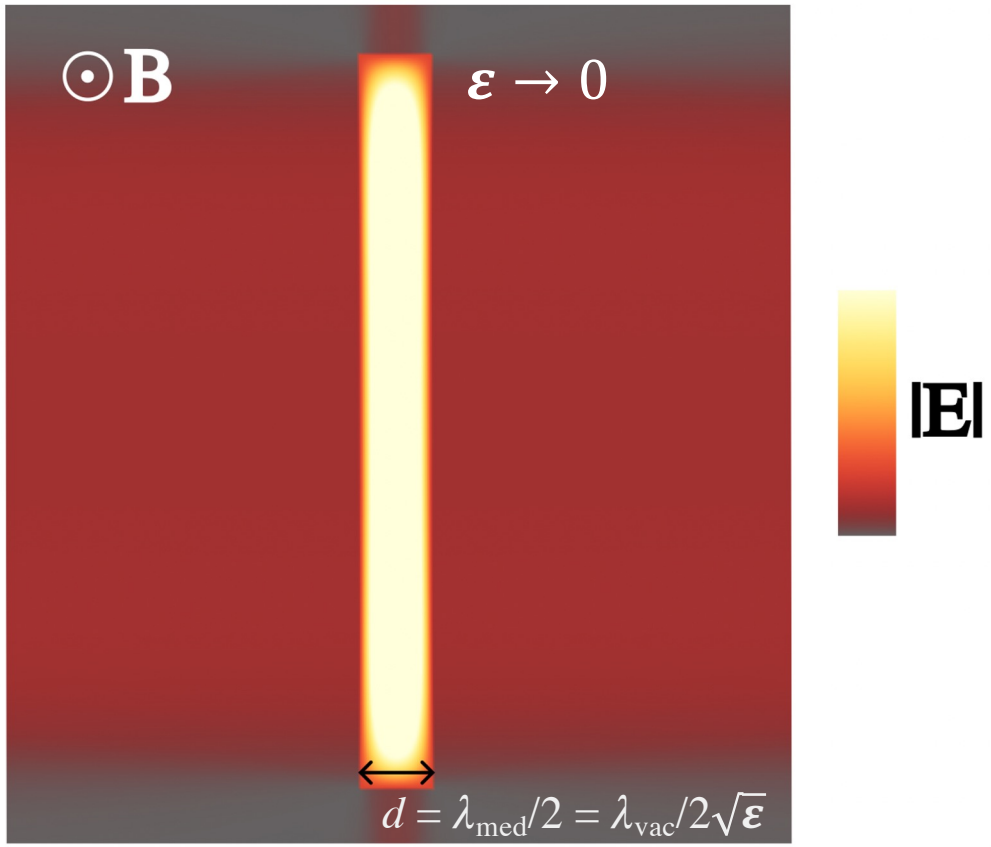

COMSOL Simulation

Mehrani, arXiv:2509.14320

Axion Response from MQW Cavity

- Axion-induced electric field

$$E_{\text{vac}} = g_{a\gamma} B a$$

- Plasmonic cavities generate surface radiation with boost β

$$E_{\text{prop}} = \beta E_{\text{vac}}$$

$$\beta = \left| \frac{-\sin \frac{\sqrt{\varepsilon}\omega d}{2}(1-\varepsilon)}{\varepsilon \sin \frac{\sqrt{\varepsilon}\omega d}{2} + i\sqrt{\varepsilon}\cos \frac{\sqrt{\varepsilon}\omega d}{2}} \right|$$

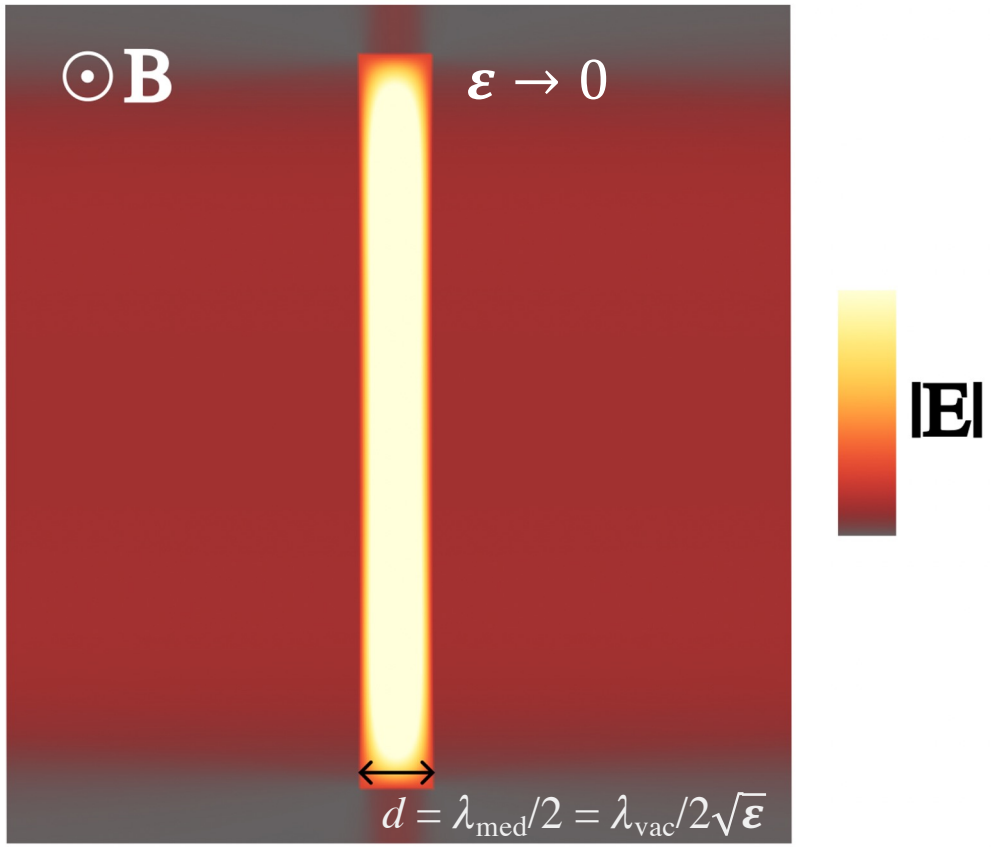

COMSOL Simulation

Mehrani, arXiv:2509.14320

Axion Response from MQW Cavity

- Axion-induced electric field

$$E_{\text{vac}} = g_{\alpha\gamma} B a$$

- Plasmonic cavities generate surface radiation with boost β

$$E_{\text{prop}} = \beta E_{\text{vac}}$$

$$\beta = \left| \frac{-\sin\frac{\sqrt{\varepsilon}\omega d}{2}(1-\varepsilon)}{\varepsilon \sin\frac{\sqrt{\varepsilon}\omega d}{2} + i\sqrt{\varepsilon}\cos\frac{\sqrt{\varepsilon}\omega d}{2}} \right|$$

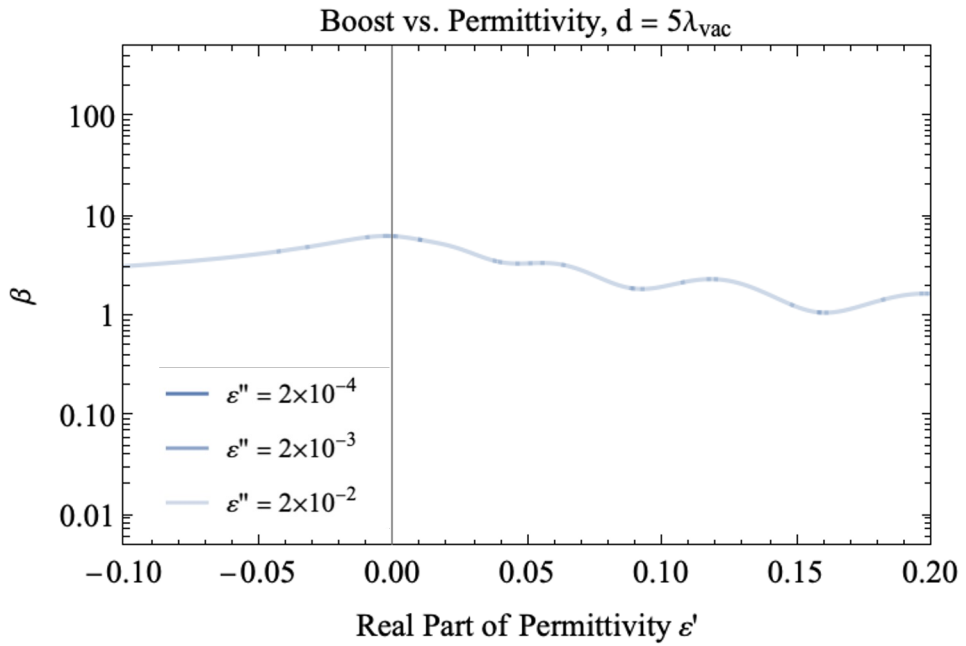

Mehrani, arXiv:2509.14320

Axion Response from MQW Cavity

- Axion-induced electric field

$$E_{\text{vac}} = g_{\alpha\gamma} B a$$

- Plasmonic cavities generate surface radiation with boost β

$$E_{\text{prop}} = \beta E_{\text{vac}}$$

$$\beta = \left| \frac{-\sin\frac{\sqrt{\varepsilon}\omega d}{2}(1-\varepsilon)}{\varepsilon \sin\frac{\sqrt{\varepsilon}\omega d}{2} + i\sqrt{\varepsilon}\cos\frac{\sqrt{\varepsilon}\omega d}{2}} \right|$$

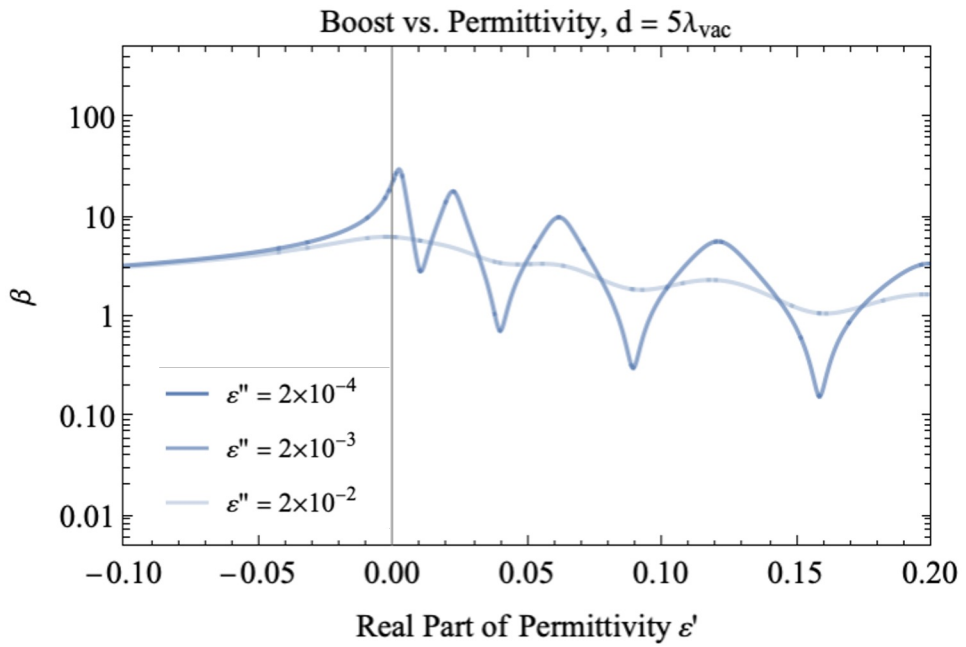

Mehrani, arXiv:2509.14320

Axion Response from MQW Cavity

- Axion-induced electric field

$$E_{\text{vac}} = g_{\alpha\gamma} B a$$

- Plasmonic cavities generate surface radiation with boost β

$$E_{\text{prop}} = \beta E_{\text{vac}}$$

$$\beta = \left| \frac{-\sin \frac{\sqrt{\varepsilon}\omega d}{2}(1-\varepsilon)}{\varepsilon \sin \frac{\sqrt{\varepsilon}\omega d}{2} + i\sqrt{\varepsilon}\cos \frac{\sqrt{\varepsilon}\omega d}{2}} \right|$$

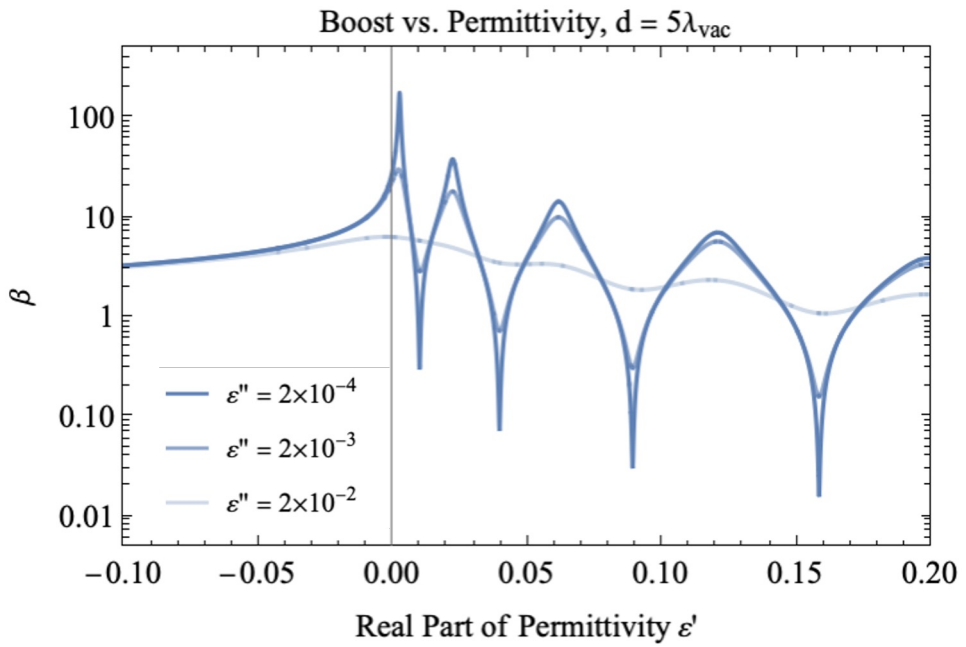

Mehrani, arXiv:2509.14320

Axion Response from MQW Cavity

- Axion-induced electric field

$$E_{\text{vac}} = g_{\alpha\gamma} B a$$

- Plasmonic cavities generate surface radiation with boost β

$$E_{\text{prop}} = \beta E_{\text{vac}}$$

$$\beta = \left| \frac{-\sin \frac{\sqrt{\varepsilon}\omega d}{2}(1-\varepsilon)}{\varepsilon \sin \frac{\sqrt{\varepsilon}\omega d}{2} + i\sqrt{\varepsilon}\cos \frac{\sqrt{\varepsilon}\omega d}{2}} \right|$$

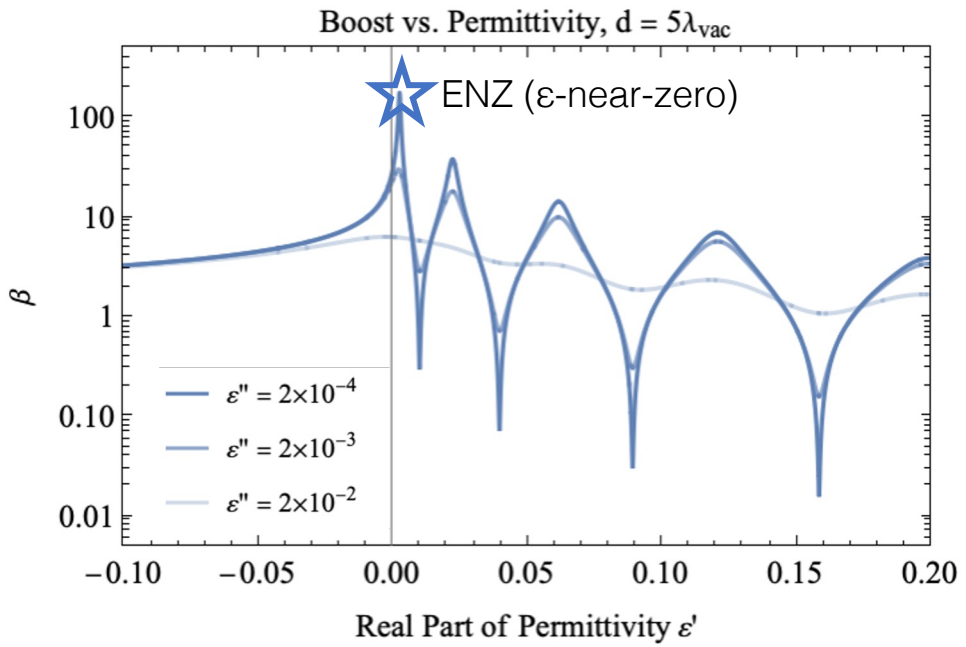

Mehrani, arXiv:2509.14320

ENZ Tunability in MQW

- A magnetic field tunes the ENZ point with cyclotron resonance

$$\hat{m}^* \cdot \frac{d\mathbf{v}}{dt} + \hat{m}^* \cdot \frac{\mathbf{v}}{\tau} = e(\mathbf{E} + \mathbf{v}\times\mathbf{B}) \qquad \mathbf{J} = ne\mathbf{v} = \hat{\sigma} \cdot \mathbf{E}$$

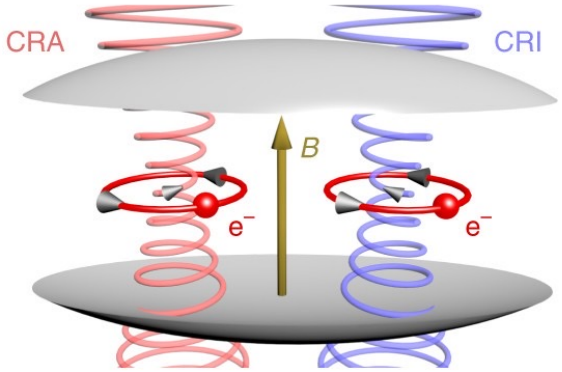

Li, X., Kono, J., et. al.
Nature Photonics (2018)

ENZ Tunability in MQW

- A magnetic field tunes the ENZ point with cyclotron resonance

$$\hat{m}^* \cdot \frac{d\mathbf{v}}{dt} + \hat{m}^* \cdot \frac{\mathbf{v}}{\tau} = e(\mathbf{E} + \mathbf{v}\times\mathbf{B}) \qquad \mathbf{J} = ne\mathbf{v} = \hat{\sigma} \cdot \mathbf{E}$$

- Conductivity

$$\sigma_{\mathrm{CRI}} = \sigma_{xx} - i\,\sigma_{xy} = \frac{\sigma_{\mathrm{DC}}}{1 - i(\omega + \omega_c)\tau}$$

$$\sigma_{\mathrm{CRA}} = \sigma_{xx} + i\,\sigma_{xy} = \frac{\sigma_{\mathrm{DC}}}{1 - i(\omega - \omega_c)\tau}$$

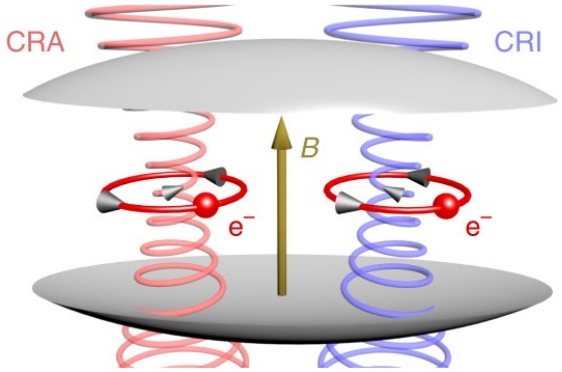

Li, X., Kono, J., et. al.
Nature Photonics (2018)

ENZ Tunability in MQW

- A magnetic field tunes the ENZ point with cyclotron resonance

$$\hat{m}^* \cdot \frac{d\mathbf{v}}{dt} + \hat{m}^* \cdot \frac{\mathbf{v}}{\tau} = e(\mathbf{E} + \mathbf{v}\times\mathbf{B}) \qquad \mathbf{J} = ne\mathbf{v} = \hat{\sigma} \cdot \mathbf{E}$$

- Conductivity

$$\sigma_{\mathrm{CRI}} = \sigma_{xx} - i\,\sigma_{xy} = \frac{\sigma_{\mathrm{DC}}}{1 - i(\omega + \omega_c)\tau}$$

$$\sigma_{\mathrm{CRA}} = \sigma_{xx} + i\,\sigma_{xy} = \frac{\sigma_{\mathrm{DC}}}{1 - i(\omega - \omega_c)\tau}$$

- Permittivity

$$\hat{\varepsilon} = \hat{\varepsilon}_{\mathrm{bg}} + i\frac{\hat{\sigma}}{\omega\varepsilon_0 d_{\mathrm{QW}}}$$

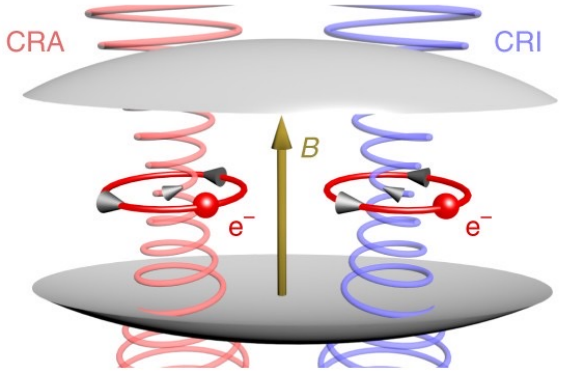

Li, X., Kono, J., et. al.
Nature Photonics (2018)

ENZ Tunability in MQW

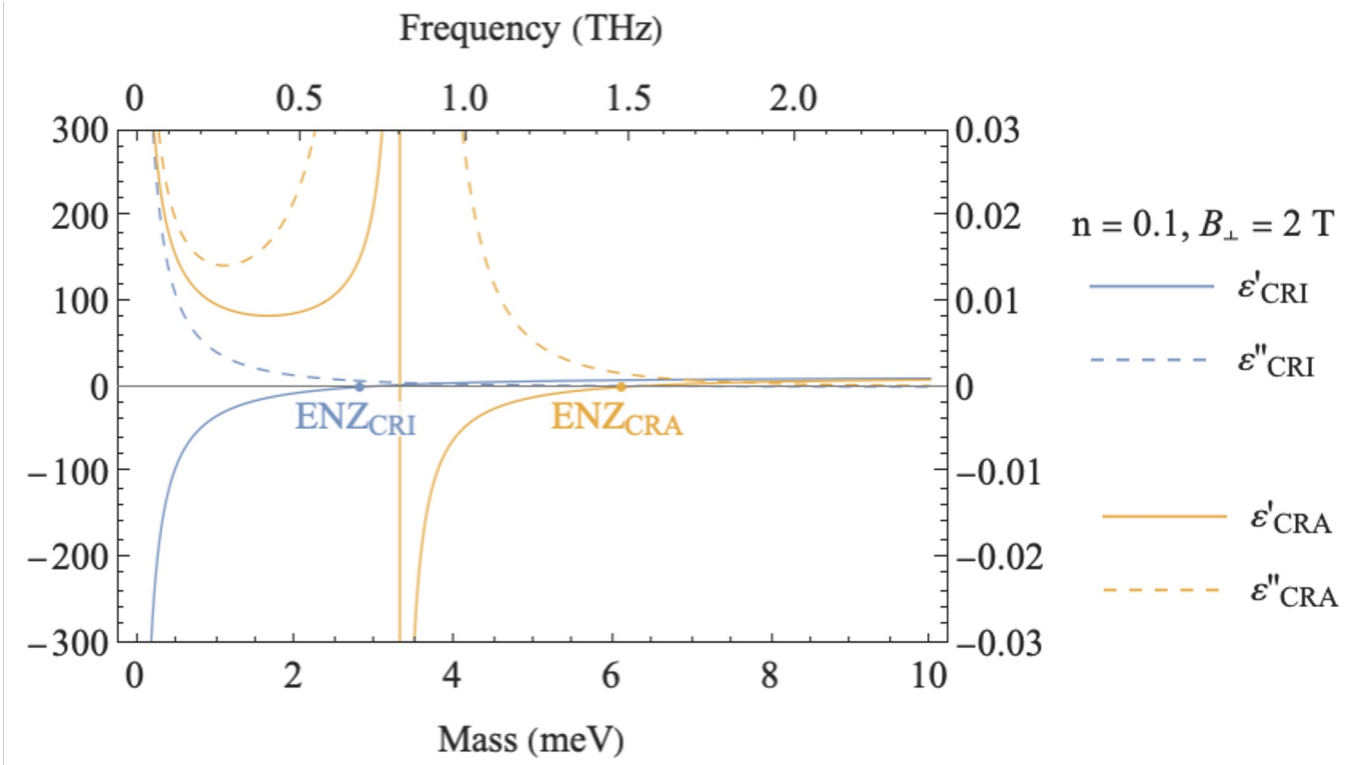

Mehrani, arXiv:2509.14320

ENZ Tunability in MQW

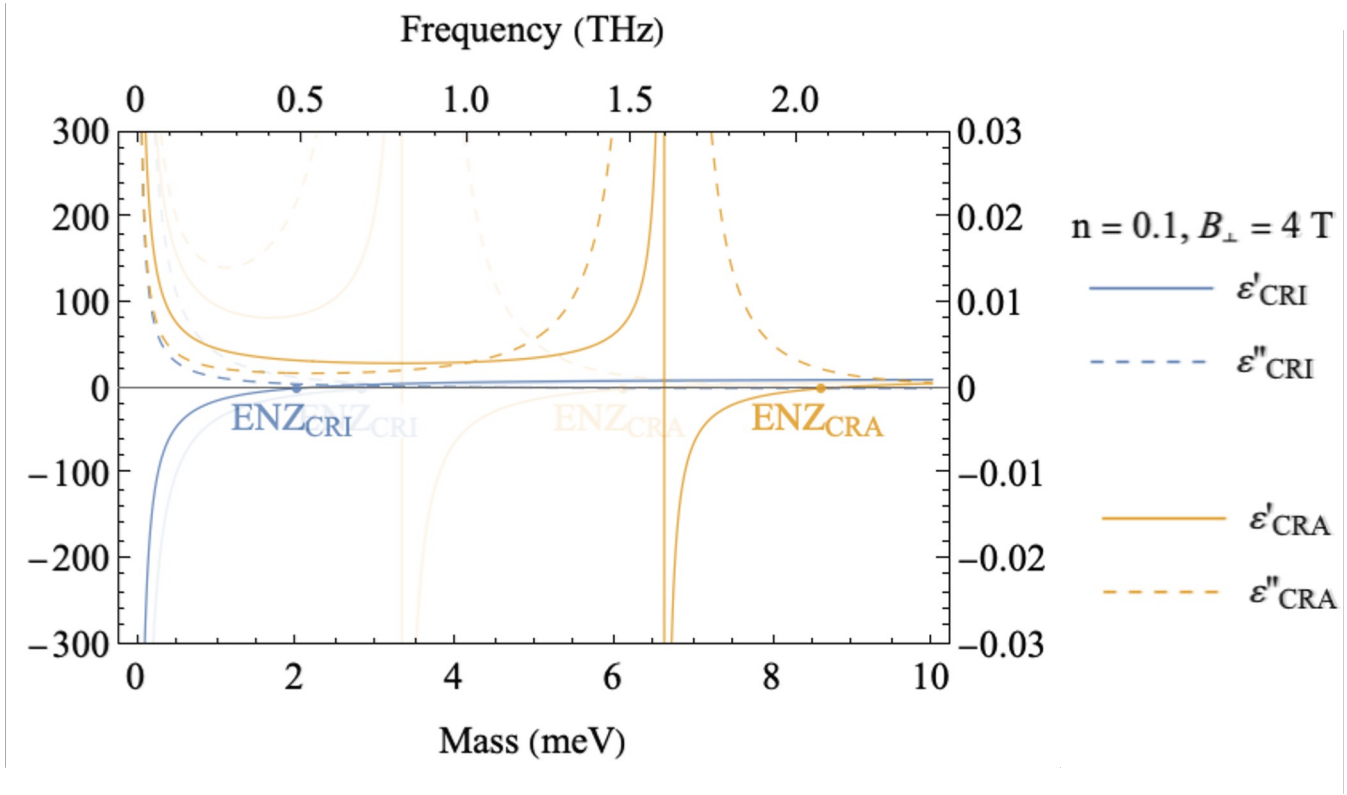

Mehrani, arXiv:2509.14320

ENZ Tunability in MQW

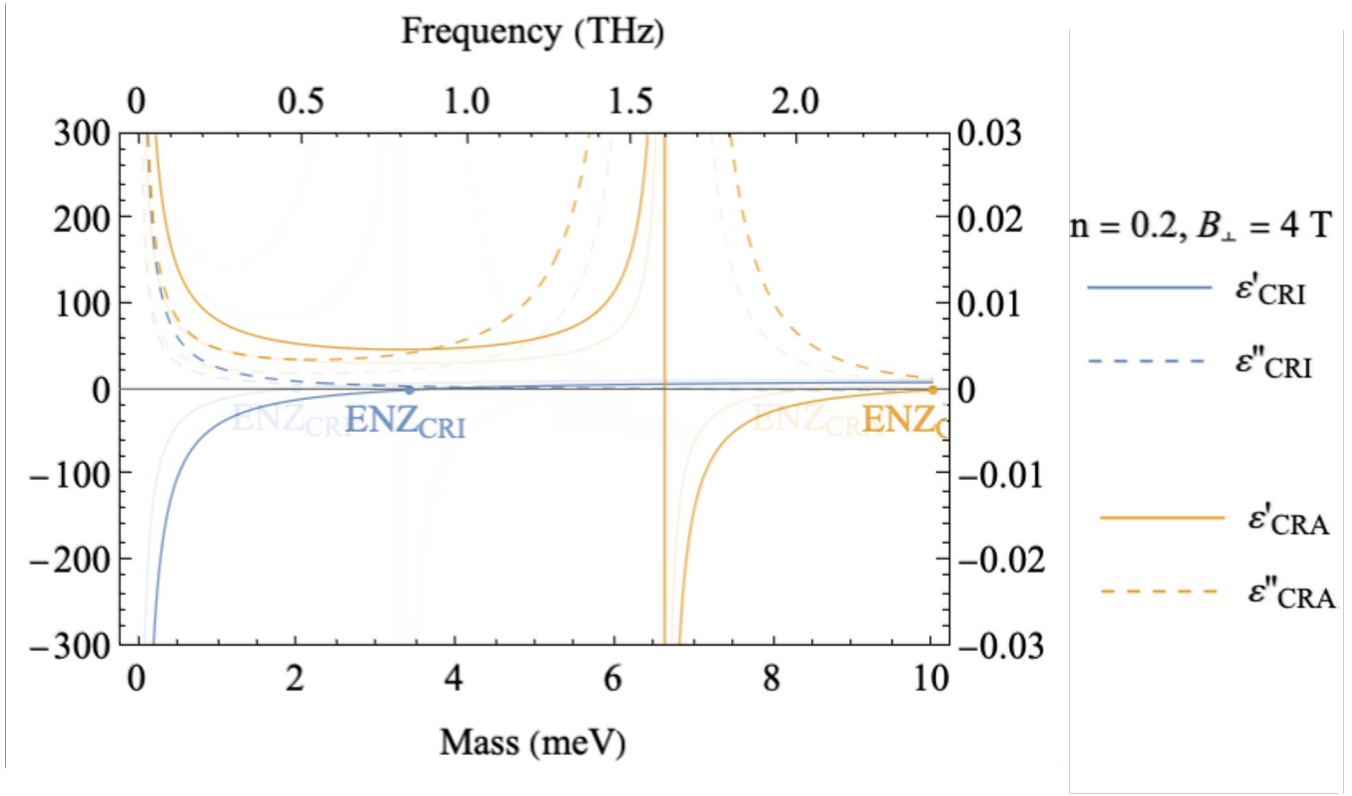

Mehrani, arXiv:2509.14320

ENZ Tunability in MQW

- CRI mode is lossless

$$\beta_{\mathrm{CRI}} \gg \beta_{\mathrm{CRA}}$$

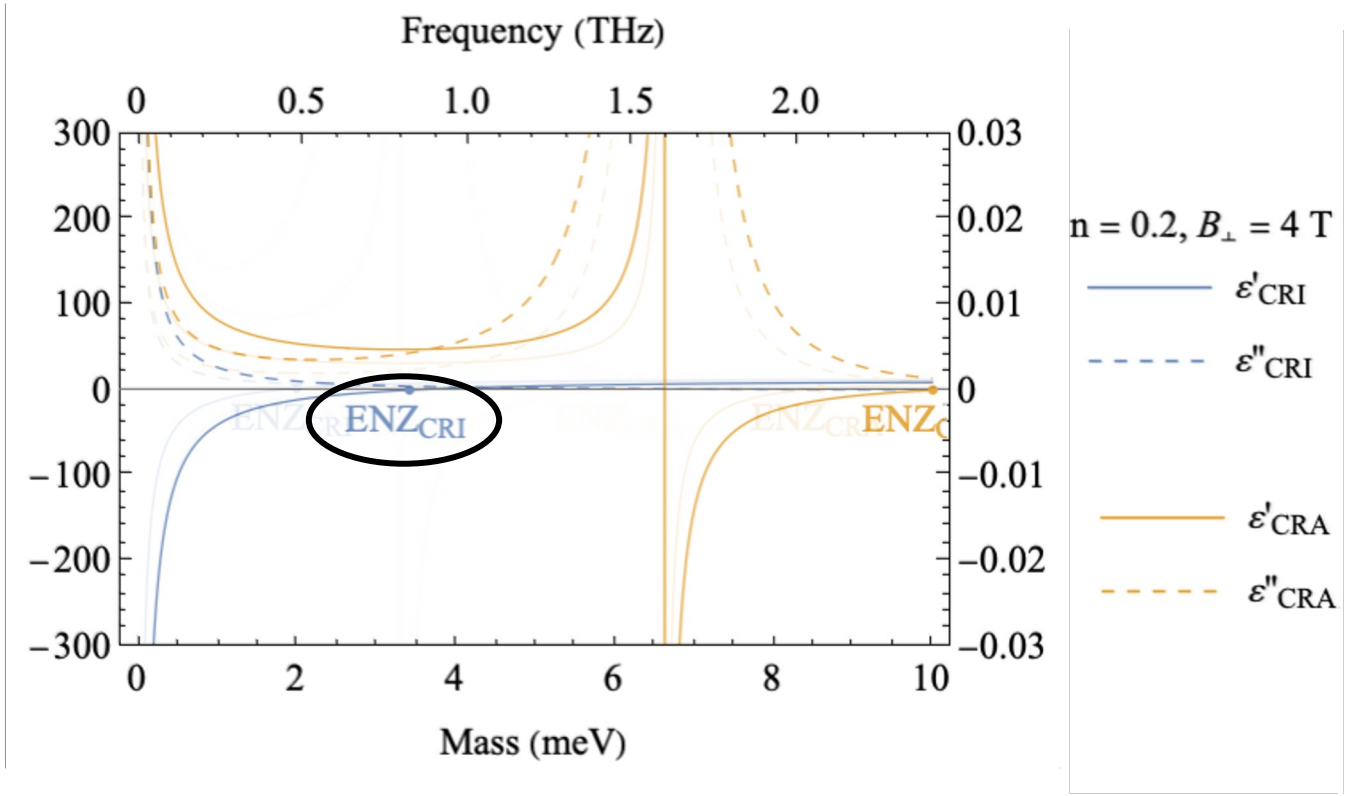

Mehrani, arXiv:2509.14320

ENZ Tunability in MQW

- CRI mode is lossless

$$\beta_{\mathrm{CRI}} \gg \beta_{\mathrm{CRA}}$$

- MQWs use effective medium theory (EMT)

$$\varepsilon_{\mathrm{eff}} = \frac{\varepsilon_{\mathrm{barrier}} d_{\mathrm{Barrier}} + \varepsilon_{\mathrm{QW}} d_{\mathrm{QW}}}{d_{\mathrm{Barrier}} + d_{\mathrm{QW}}}$$

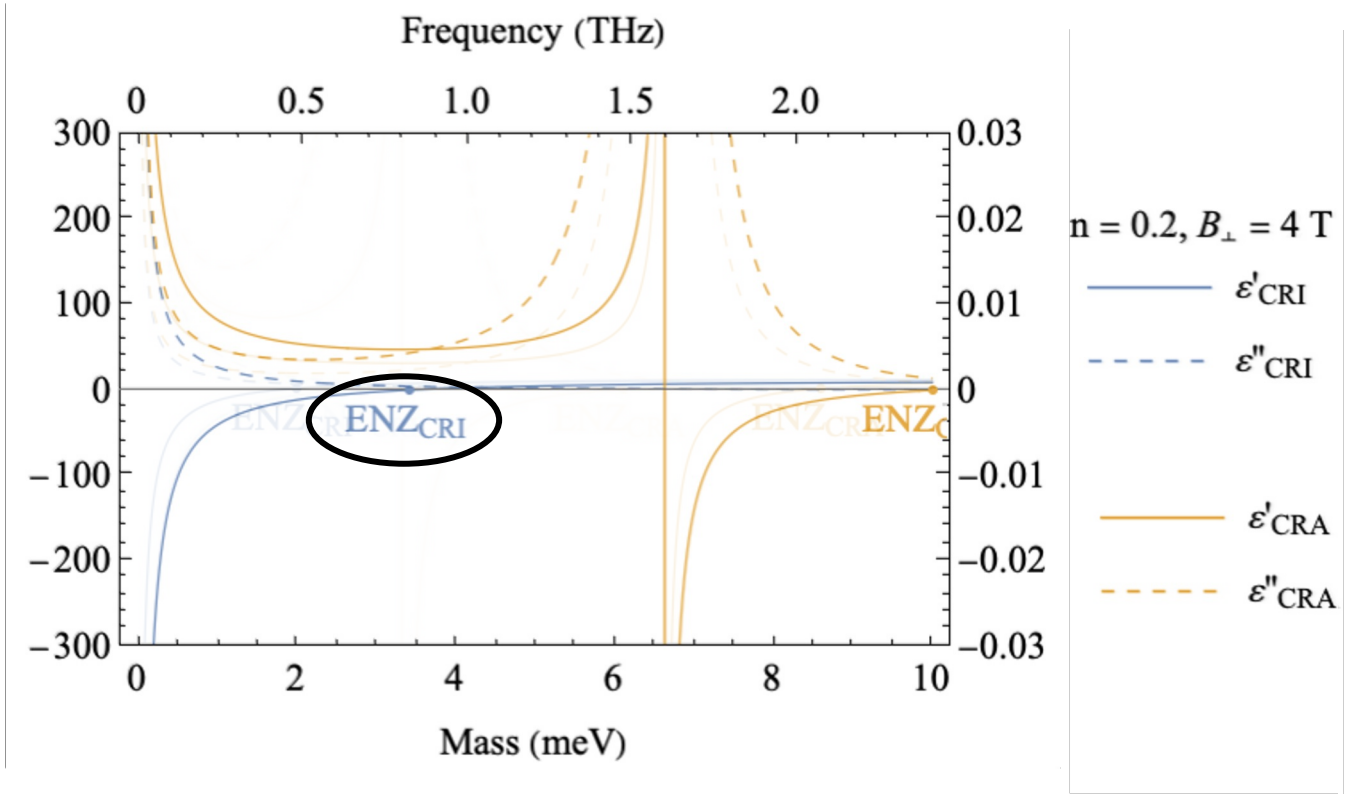

Mehrani, arXiv:2509.14320

Dual Magnetic Field Control

- $\boldsymbol{B}_\perp$, normal to MQW surface, tunes the ENZ, the permittivity component parallel to surface

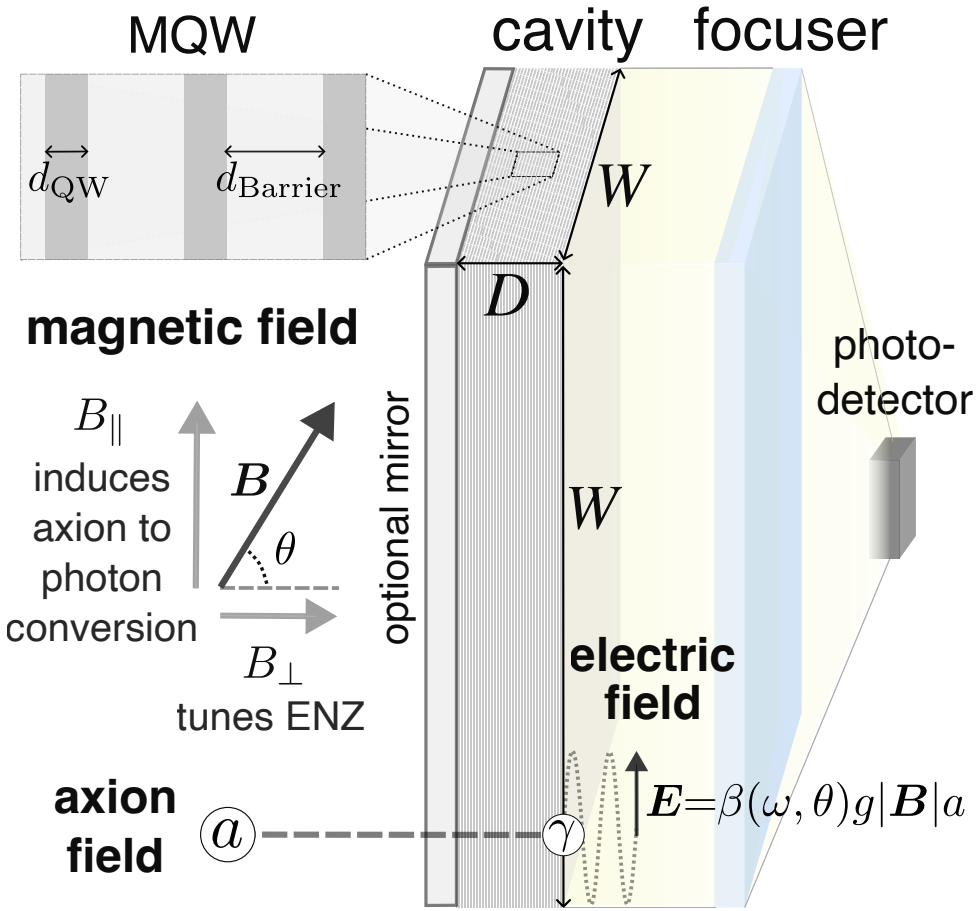

Mehrani, arXiv:2509.14320

Dual Magnetic Field Control

- $\boldsymbol{B}_{\perp}$, normal to MQW surface, tunes the ENZ, the permittivity component parallel to surface
- $\boldsymbol{B}_{\parallel}$, parallel to MQW surface, generates electric field component parallel to surface

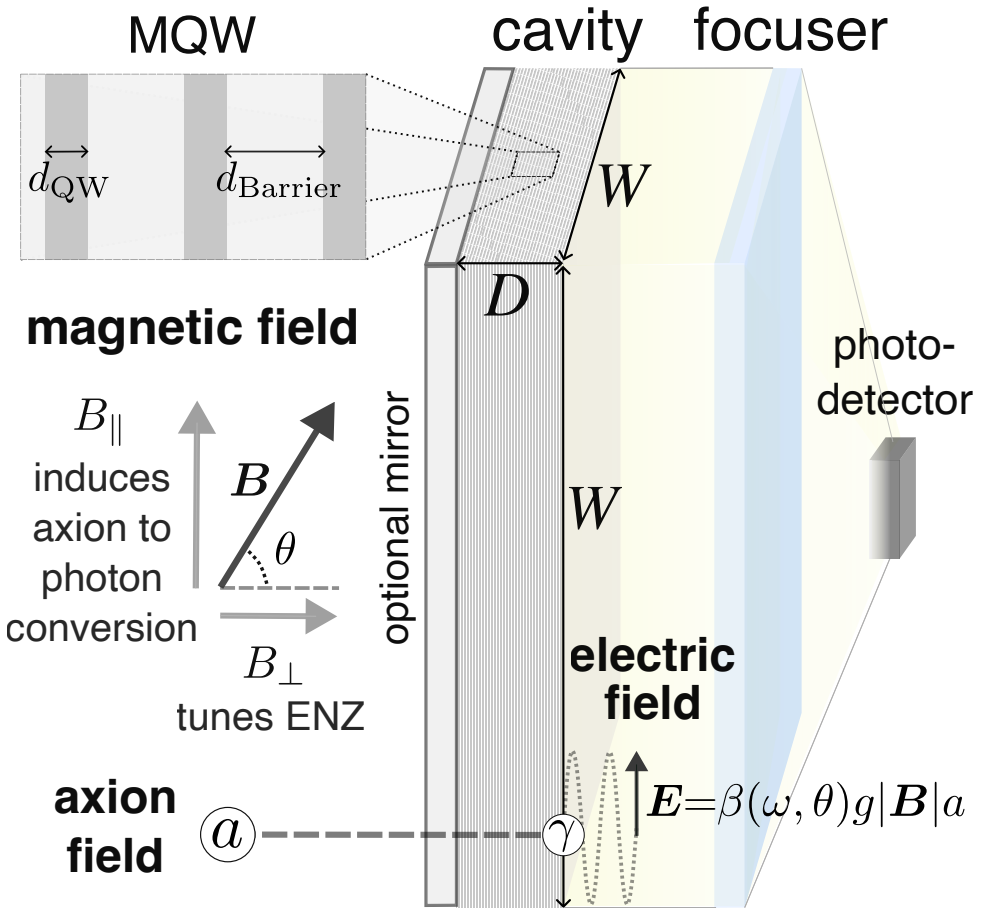

Mehrani, arXiv:2509.14320

Dual Magnetic Field Control

- $\boldsymbol{B}_{\perp}$, normal to MQW surface, tunes the ENZ, the permittivity component parallel to surface
- $\boldsymbol{B}_{\parallel}$, parallel to MQW surface, generates electric field component parallel to surface
- Tuning by tilting θ.

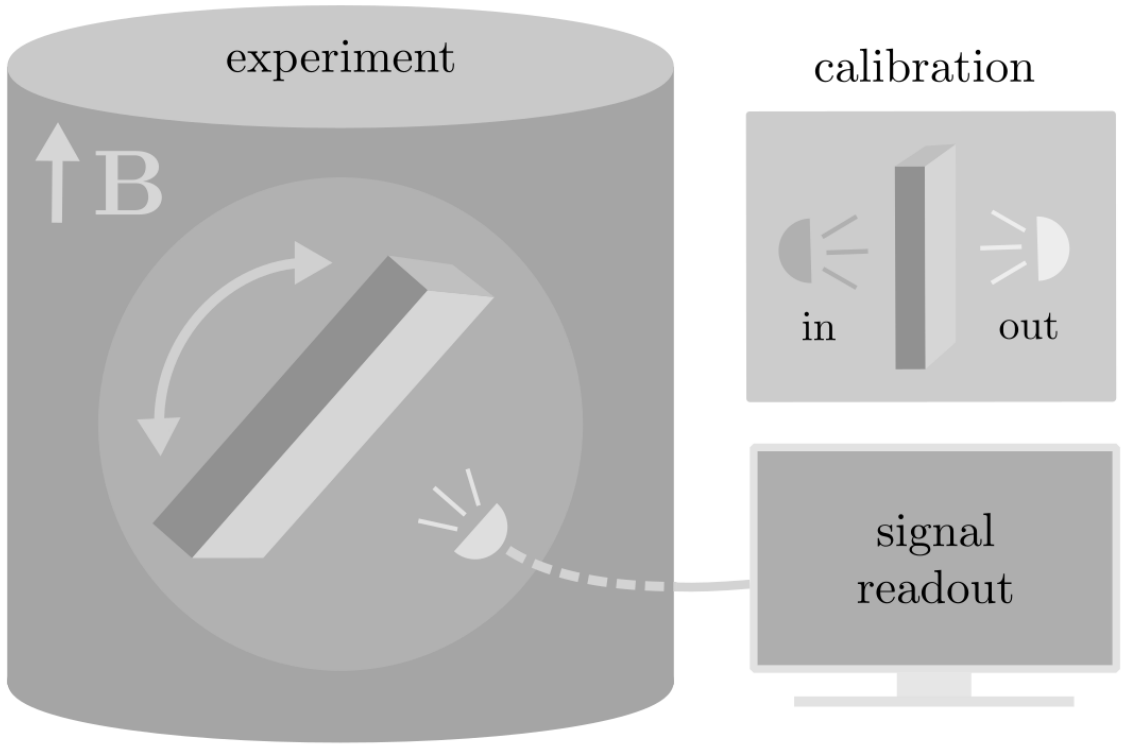

Mehrani, arXiv:2509.14320

Experimental Parameters

Parameter	Config. 1	Config. 2	Config. 3
B [T]	36	36	50
T [K]	0.3	0.3	0.3
n [10^{11} cm^{-2}]	3	3	3
τ [ns]	1.7	1.7	4
w [cm]	3	3	5
d [mm]	2	10	20
d_{QW} [nm]	30	30	30
d_{Barrier} [nm]	90	150	90
Γ_{dark} [mHz]	1	1	0.1
η [%]	7	20	35

Mehrani, arXiv:2509.14320

Experimental Parameters

	Realistic ⟷		Optimistic
Parameter	Config. 1	Config. 2	Config. 3
B [T]	36	36	50
T [K]	0.3	0.3	0.3
n [10^{11} cm^{-2}]	3	3	3
τ [ns]	1.7	1.7	4
w [cm]	3	3	5
d [mm]	2	10	20
d_{QW} [nm]	30	30	30
d_{Barrier} [nm]	90	150	90
Γ_{dark} [mHz]	1	1	0.1
η [%]	7	20	35

Mehrani, arXiv:2509.14320

Experimental Parameters: Magnetic field

	Realistic ⟷		Optimistic
Parameter	Config. 1	Config. 2	Config. 3
B [T]	36	36	50
T [K]	0.3	0.3	0.3
n [10^{11} cm^{-2}]	3	3	3
τ [ns]	1.7	1.7	4
w [cm]	3	3	5
d [mm]	2	10	20
d_{QW} [nm]	30	30	30
d_{Barrier} [nm]	90	150	90
Γ_{dark} [mHz]	1	1	0.1
η [%]	7	20	35

Mehrani, arXiv:2509.14320

NATIONAL HIGH MAGNETIC FIELD LABORATORY

- **Field strength:** 36 tesla
- **Bore size:** 40 mm
- **Power:** 14 MW
- **Homogeneity**: 1 ppm (in NMR Configuration)
- **Number of input and output leads possible**: 36
- **Frequency**: 0-1.5 GHz
- **Temperature Range**: 0.3-300K
- **Uniformity Over 10 mm DSV**: 1 ppm (NMR configuration)
- **Open for users who would pay for magnet time**: Yes

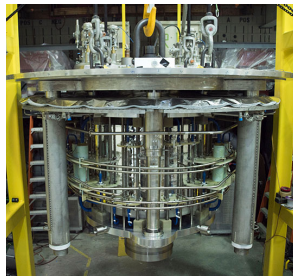

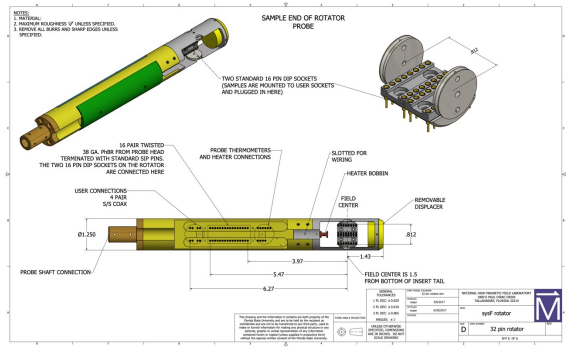

Experimental Parameters: Photodetector

Realistic ⟷ Optimistic

Parameter	Config. 1	Config. 2	Config. 3
B [T]	36	36	50
T [K]	0.3	0.3	0.3
n [10^{11} cm^{-2}]	3	3	3
τ [ns]	1.7	1.7	4
w [cm]	3	3	5
d [mm]	2	10	20
d_{QW} [nm]	30	30	30
d_{Barrier} [nm]	90	150	90
Γ_{dark} [mHz]	1	1	0.1
η [%]	7	20	35

Mehrani, arXiv:2509.14320

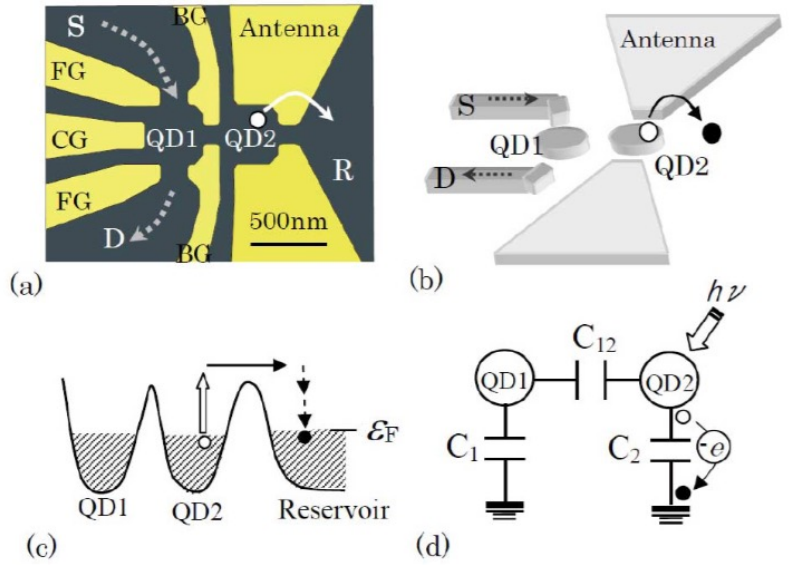

Komiyama S., IEEE Journal of Selected Topics in Quantum Electronics (2011)

Experimental Parameters: MQW

	Realistic ⟷		Optimistic
Parameter	Config. 1	Config. 2	Config. 3
B [T]	36	36	50
T [K]	0.3	0.3	0.3
n [10^{11} cm^{-2}]	3	3	3
τ [ns]	1.7	1.7	4
w [cm]	3	3	5
d [mm]	2	10	20
d_{QW} [nm]	30	30	30
d_{Barrier} [nm]	90	150	90
Γ_{dark} [mHz]	1	1	0.1
η [%]	7	20	35

Mehrani, arXiv:2509.14320

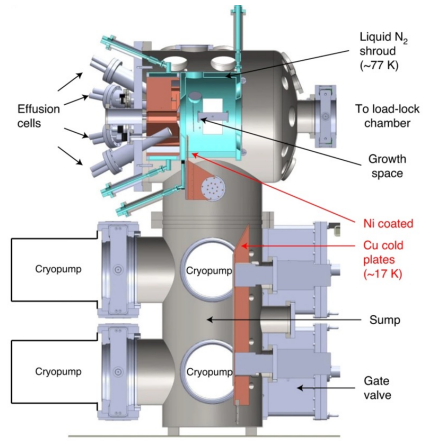

Nature Materials 20 632-637 (2021)

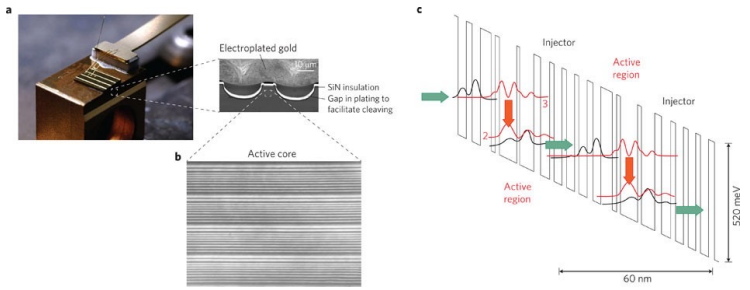

Nature Photonics 6 432-439 (2012)

Experimental Parameters: MQW

	Realistic ⟷		Optimistic
Parameter	Config. 1	Config. 2	Config. 3
B [T]	36	36	50
T [K]	0.3	0.3	0.3
n [10^{11} cm^{-2}]	3	3	3
τ [ns]	1.7	1.7	4
w [cm]	3	3	5
d [mm]	2	10	20
d_{QW} [nm]	30	30	30
d_{Barrier} [nm]	90	150	90
Γ_{dark} [mHz]	1	1	0.1
η [%]	7	20	35

Mehrani, arXiv:2509.14320

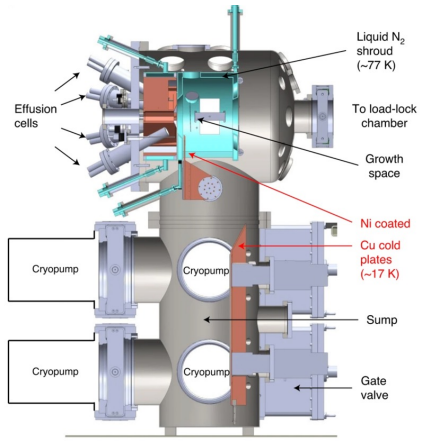

Nature Materials 20 632-637 (2021)

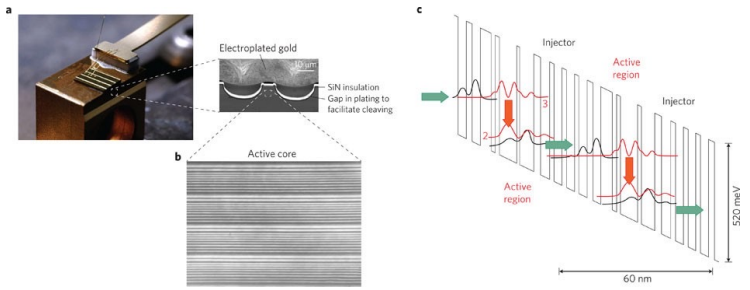

Nature Photonics 6 432-439 (2012)

Axion Proposed Sensitivity

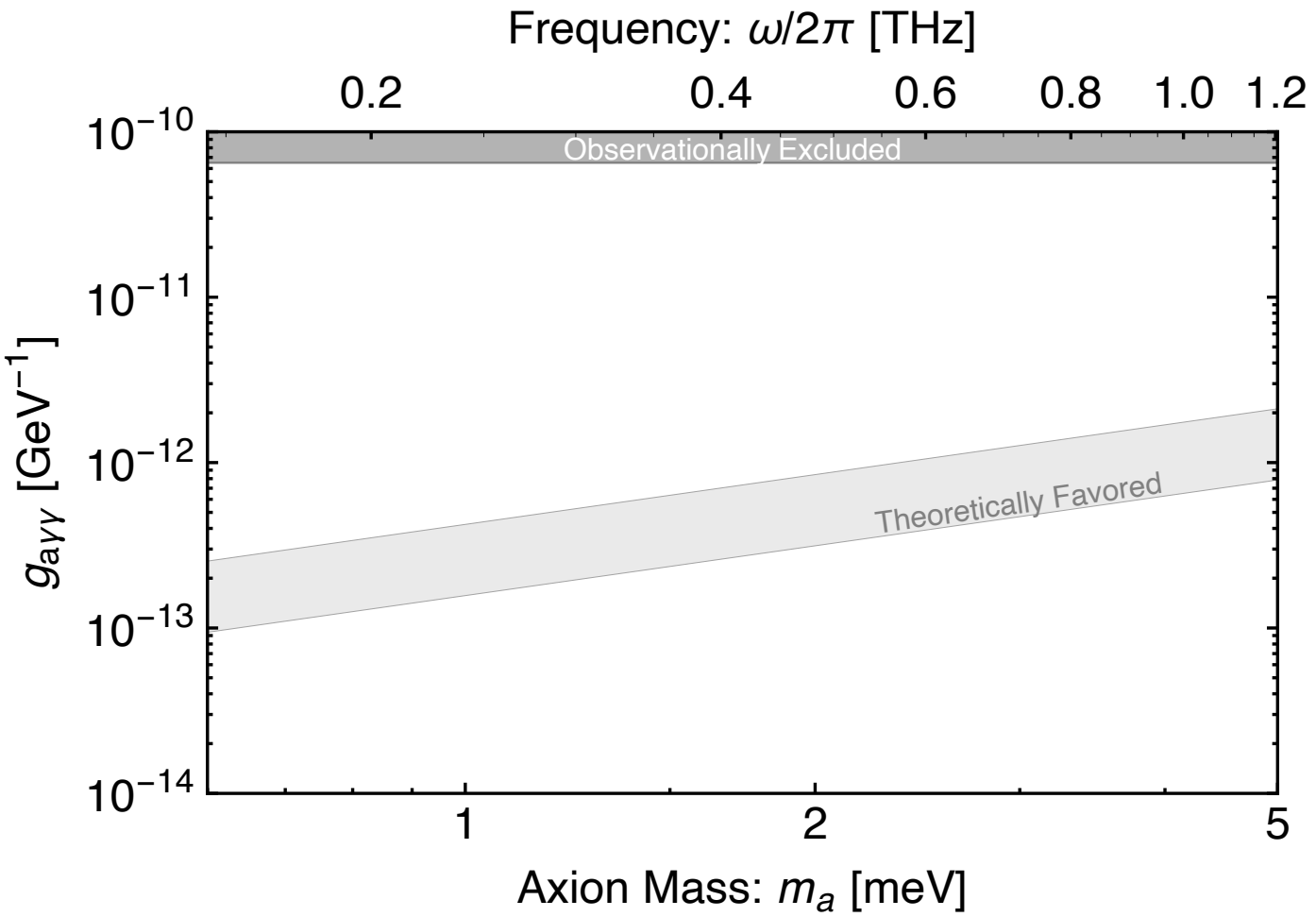

Mehrani, arXiv:2509.14320

Axion Proposed Sensitivity

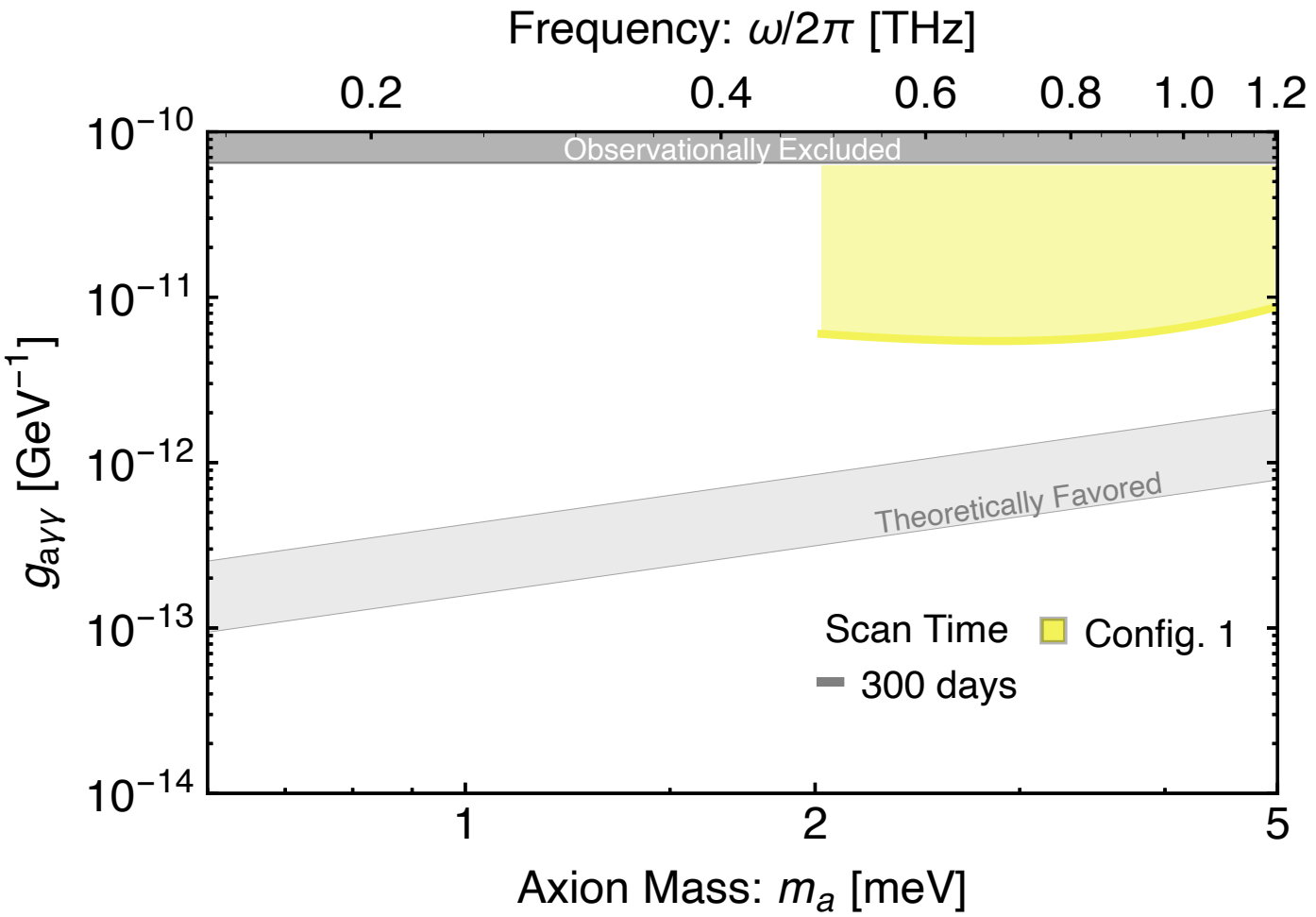

Mehrani, arXiv:2509.14320

Axion Proposed Sensitivity

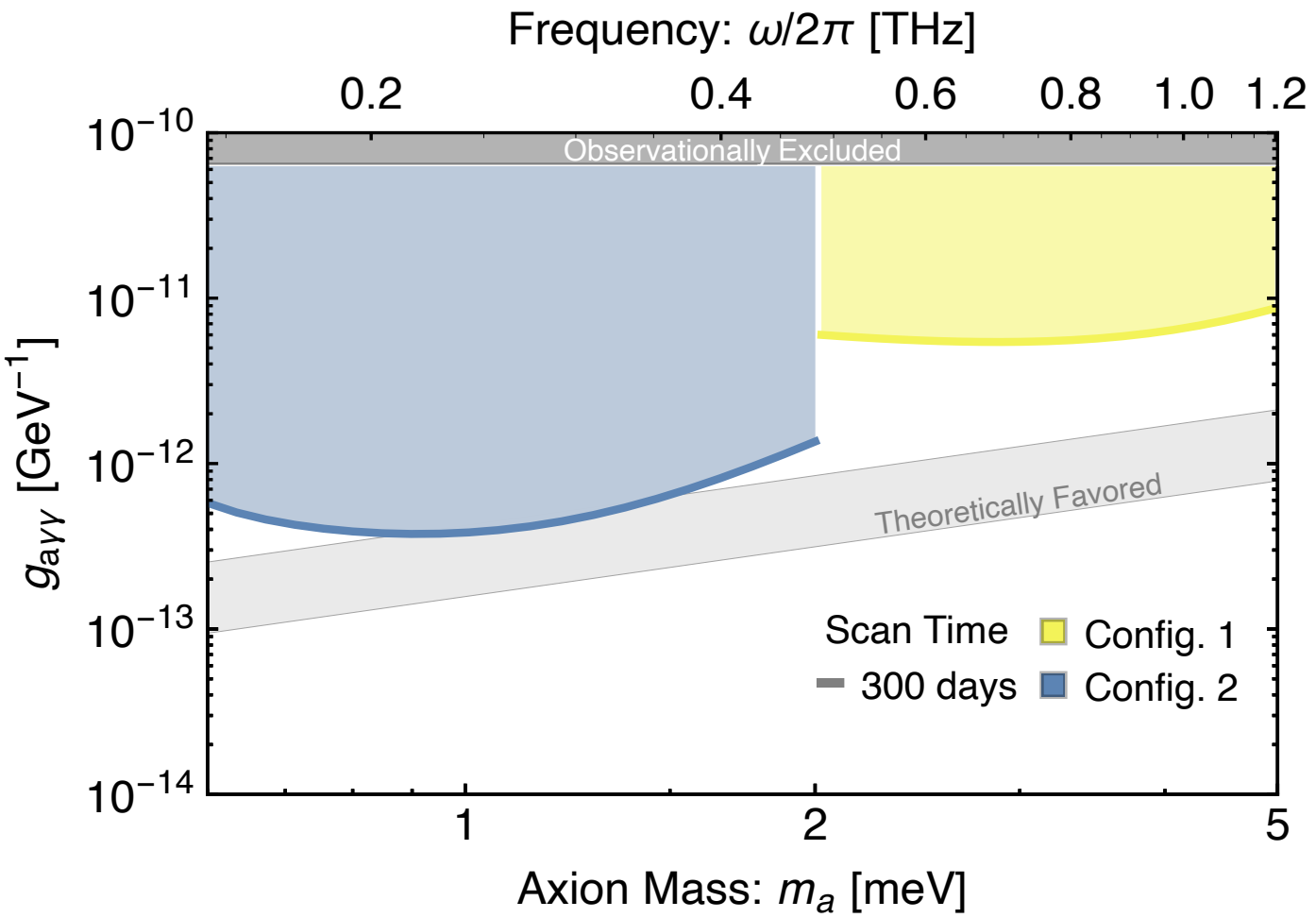

Mehrani, arXiv:2509.14320

Axion Proposed Sensitivity

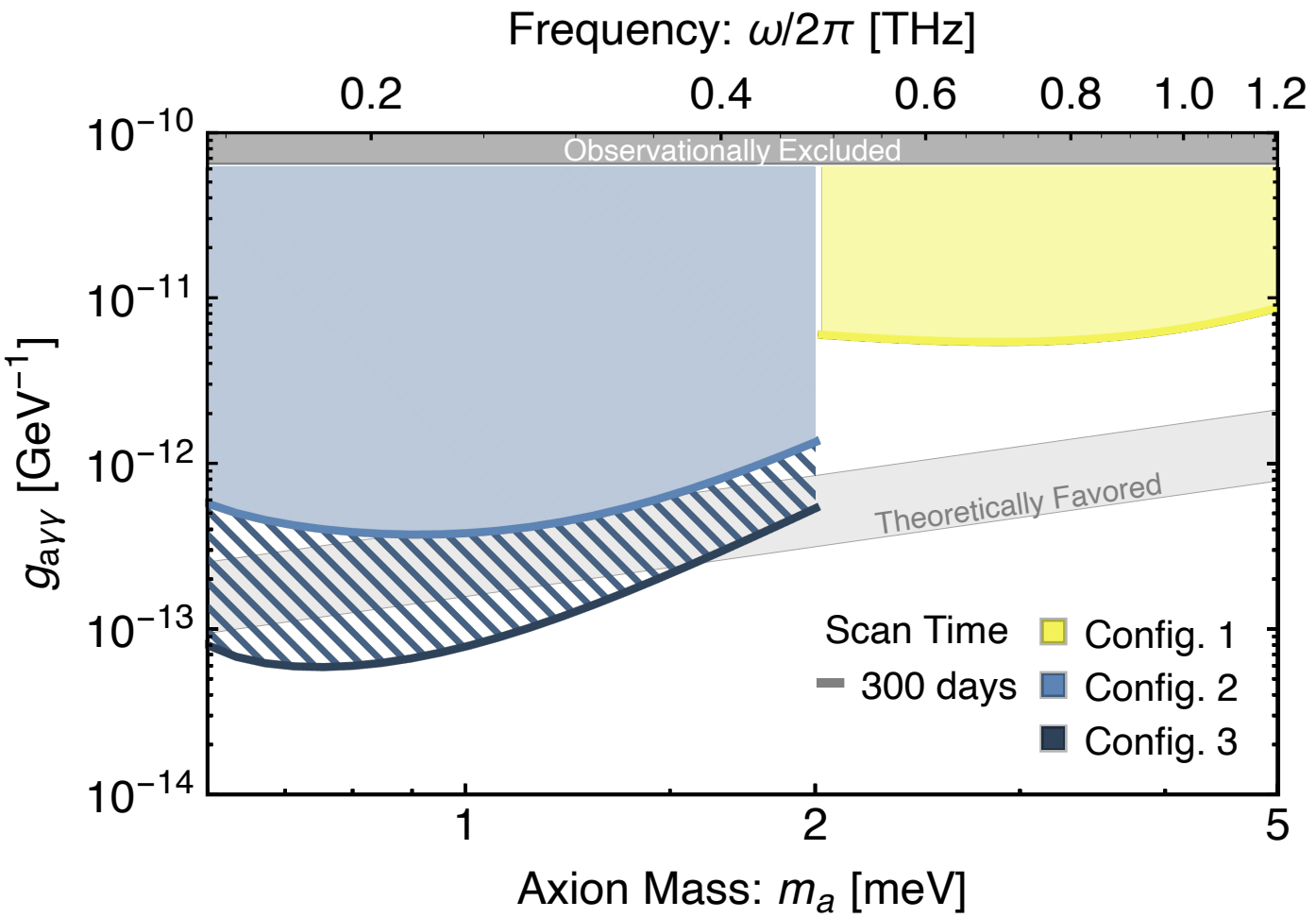

Mehrani, arXiv:2509.14320

Axion Proposed Sensitivity

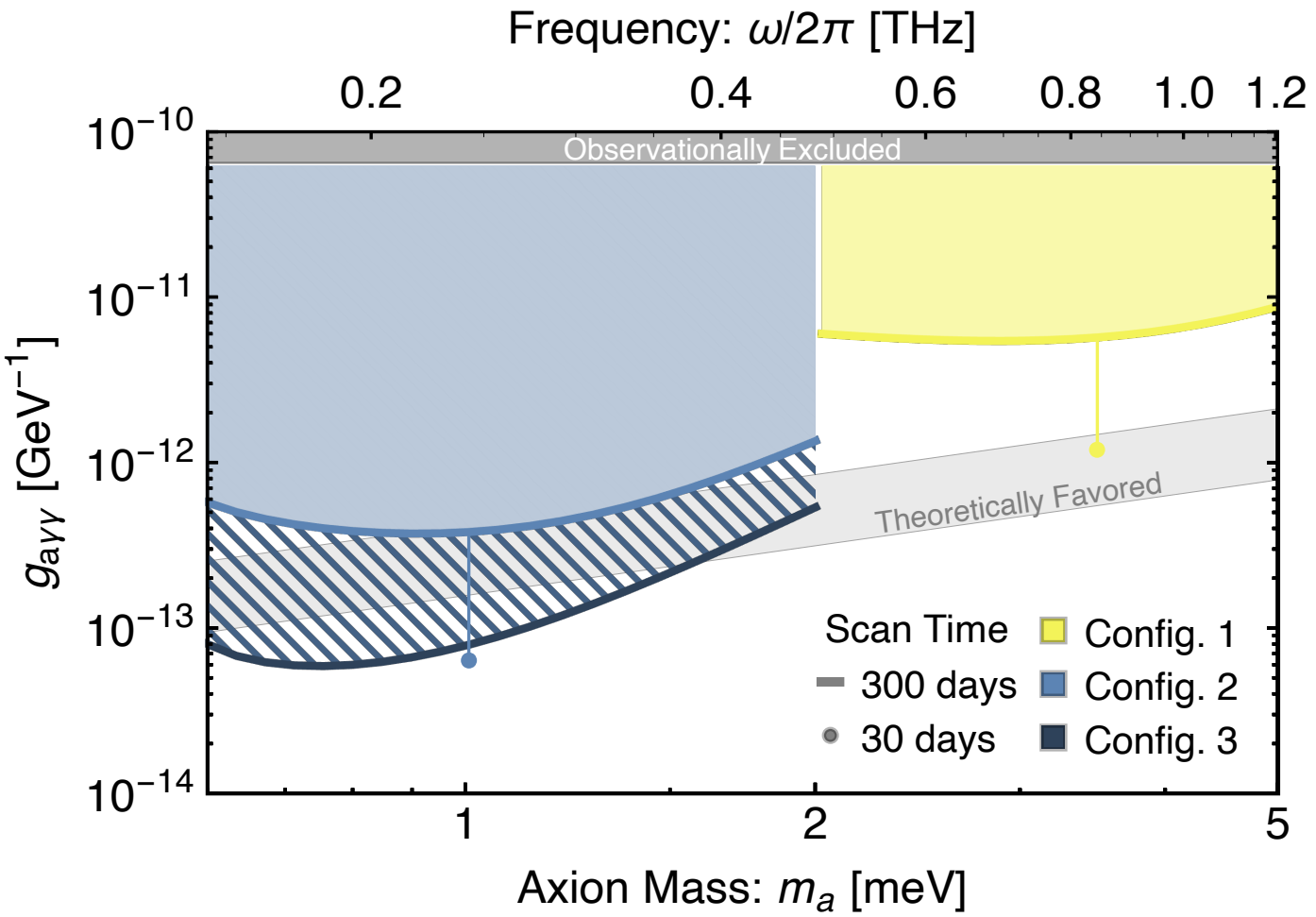

Mehrani, arXiv:2509.14320

Simulating Experimental Conditions in COMSOL

Finite MQW area reduces collimation of surface radiation.

- Aspect ratio of at least ~1.5 for 50% boost.

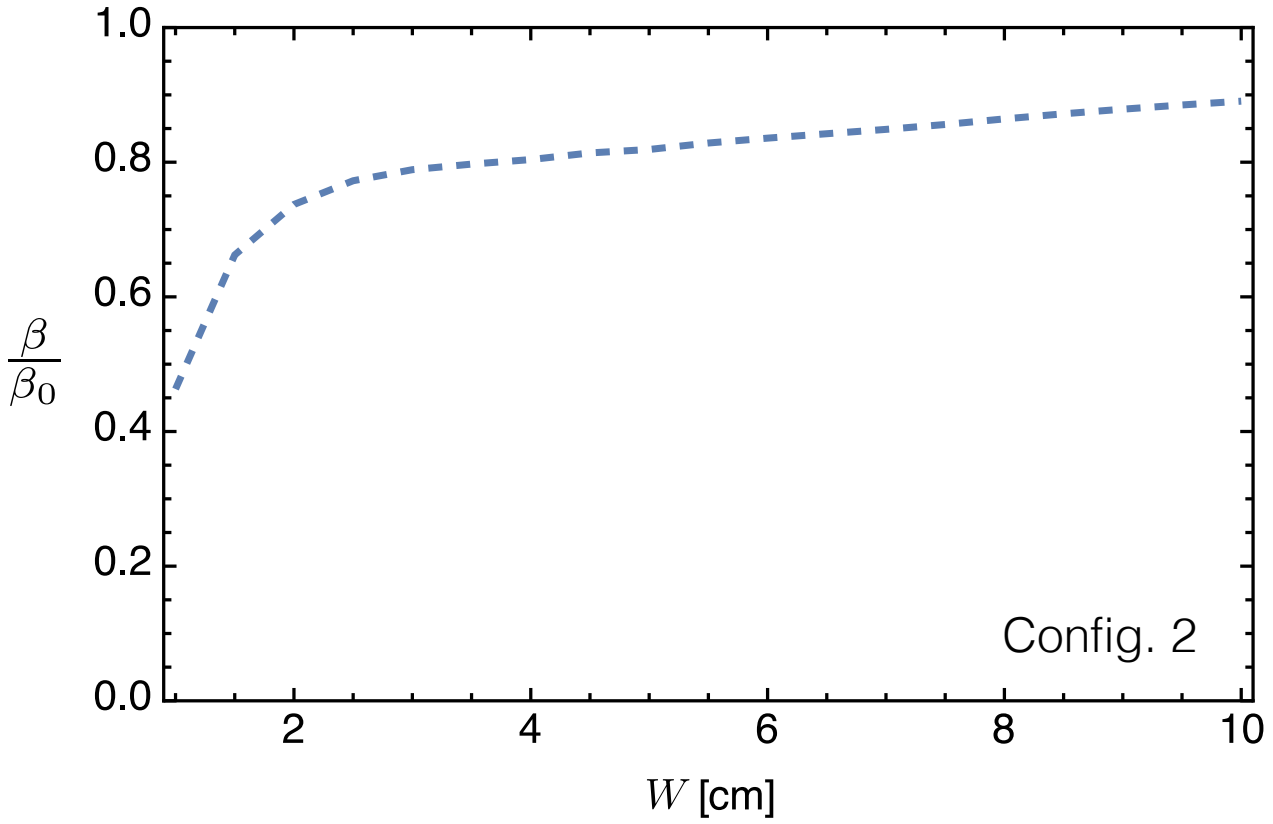

Mehrani, arXiv:2509.14320

Finite axion coherence can reduce photon coherence.

1 meV axion has a 40 cm coherence length ($\lambda_{\text{de Broglie}}$) and 2 μs coherence time

- Detector size is on the order of a few cm
- Detector response is on the order of ns

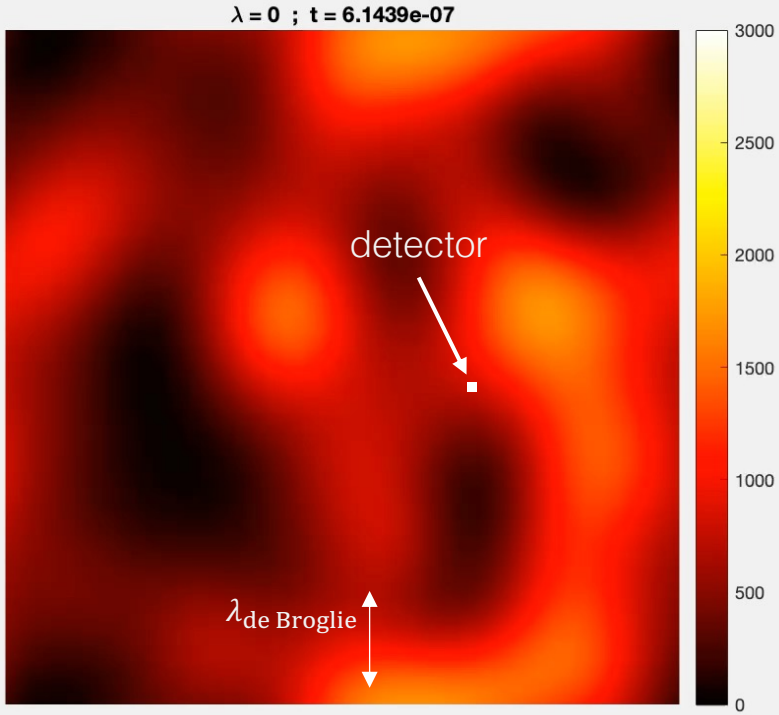

Axion field model provided by Mudit Jain.

Mehrani, arXiv:2509.14320

Finite axion coherence can reduce photon coherence.

- No significant reduction in boost.

Config. 2

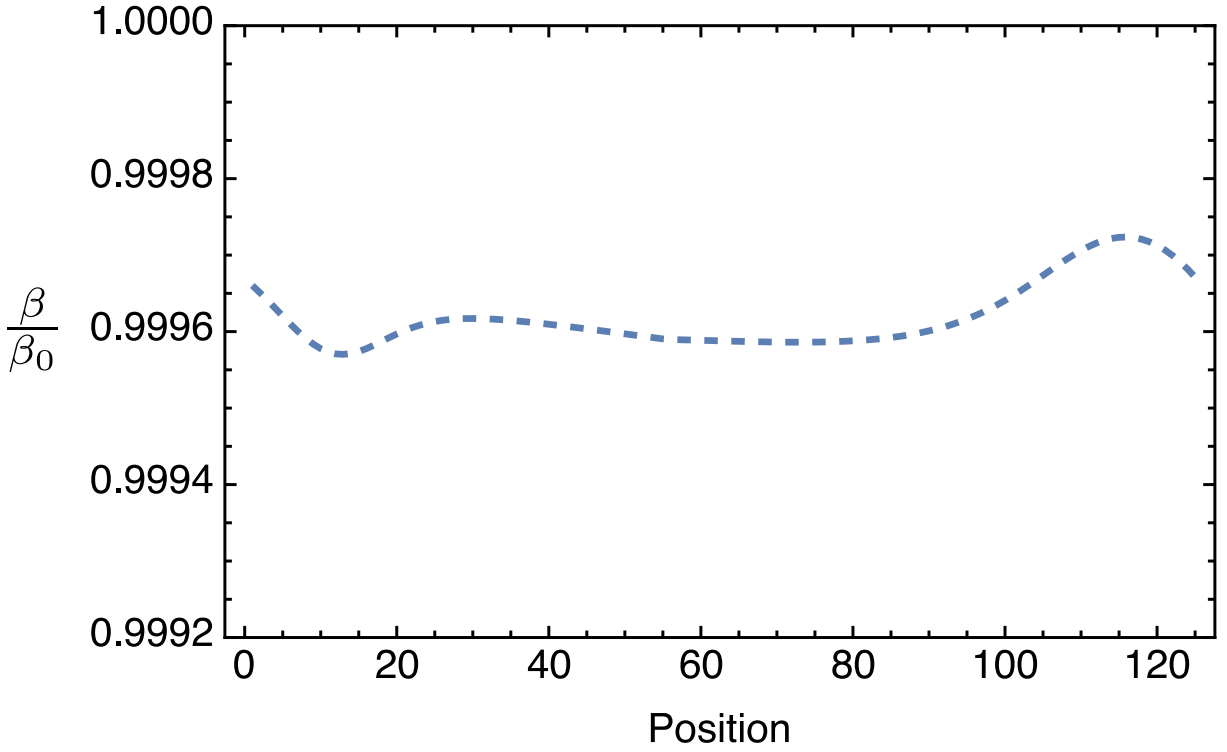

Mehrani, arXiv:2509.14320

Magnetic field and electron density inhomogeneities broaden resonance.

- The boost is extremely sensitive to B field and e^- density.

Magnetic field and electron density inhomogeneities broaden resonance.

- The boost is extremely sensitive to B field and e^- density.

Config. 2

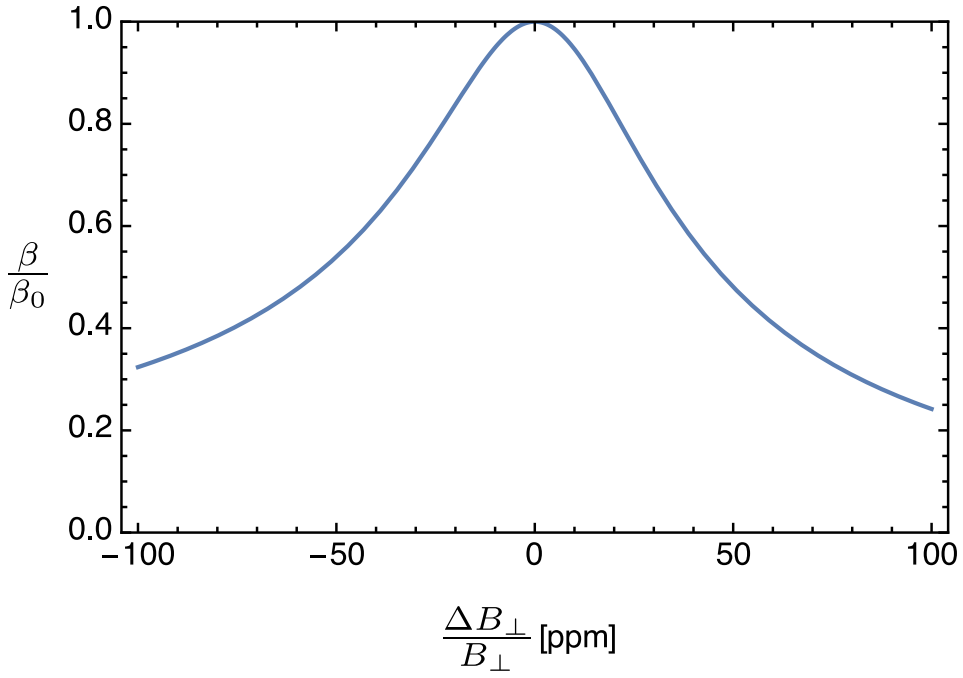

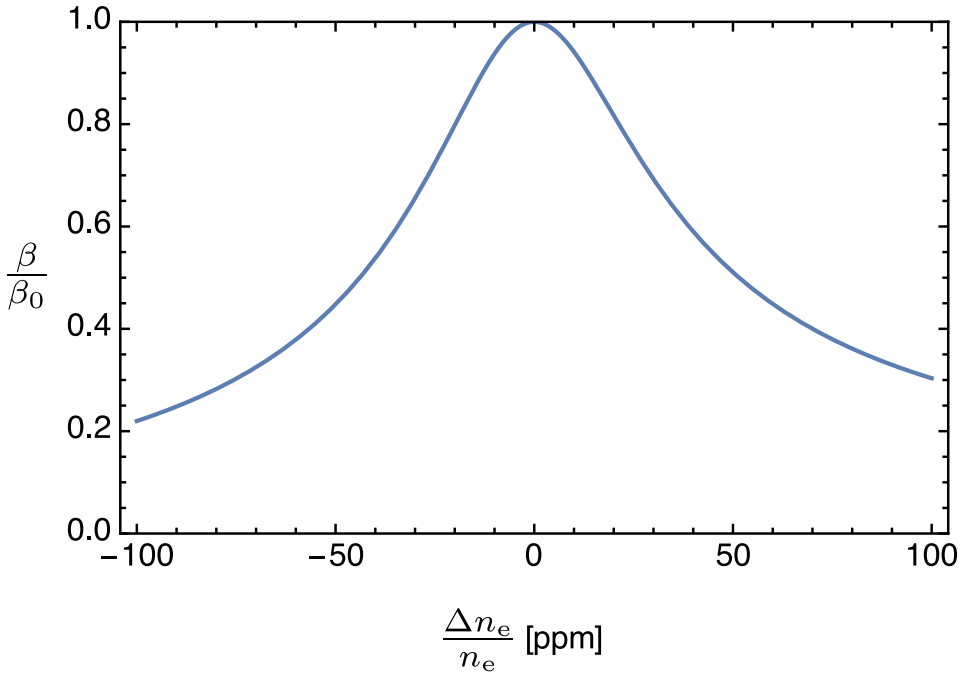

Mehrani, arXiv:2509.14320

Magnetic field and electron density inhomogeneities broaden resonance.

- The boost is extremely sensitive to B field and e^- density.

Config. 2

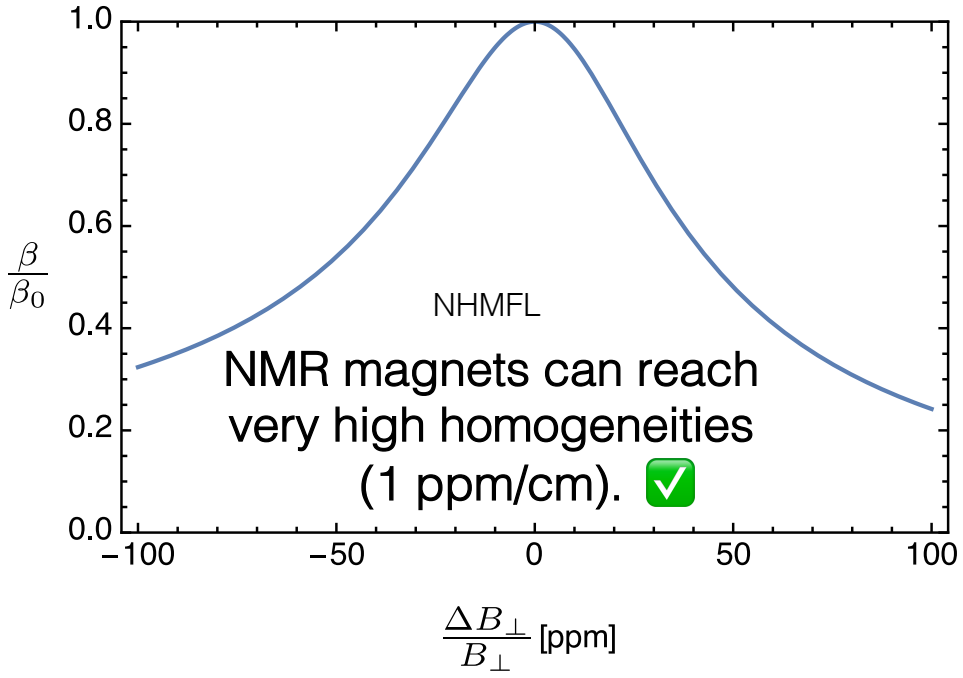

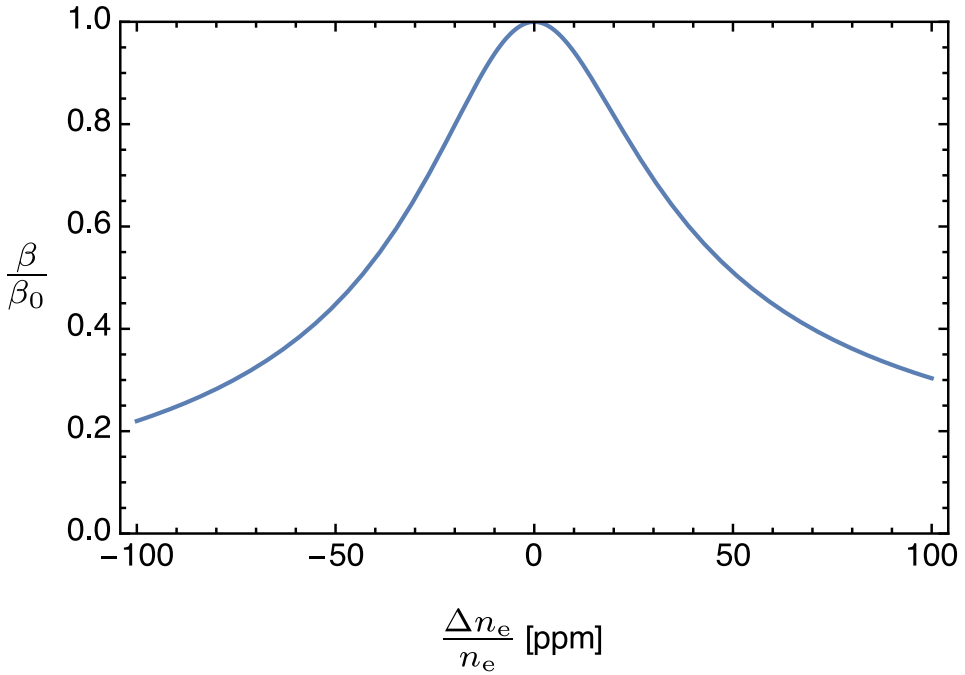

Mehrani, arXiv:2509.14320

Magnetic field and electron density inhomogeneities broaden resonance.

- The boost is extremely sensitive to B field and e^- density.

Config. 2

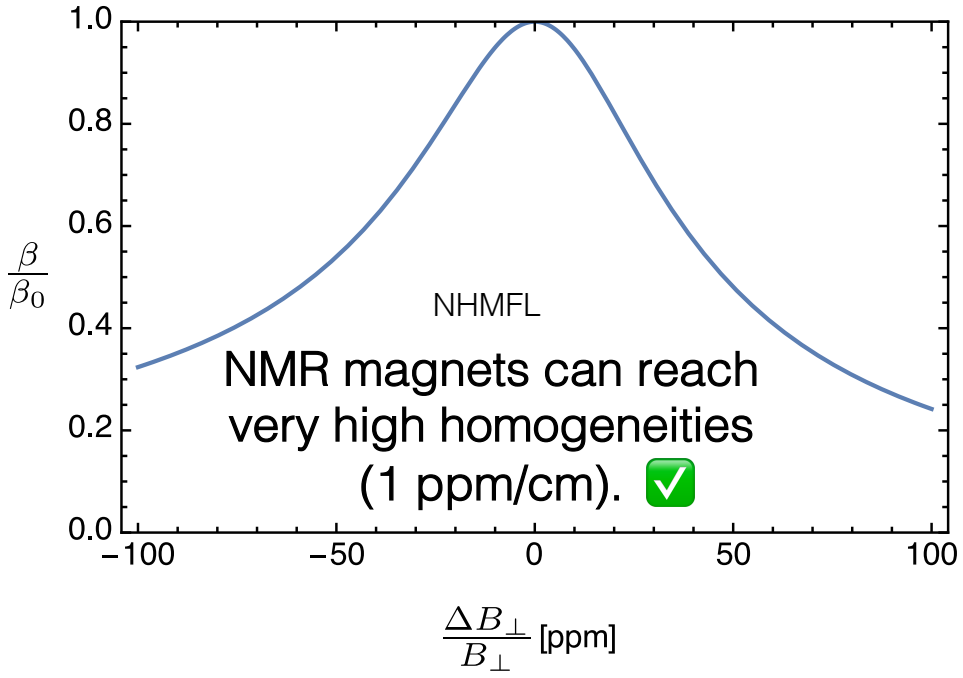

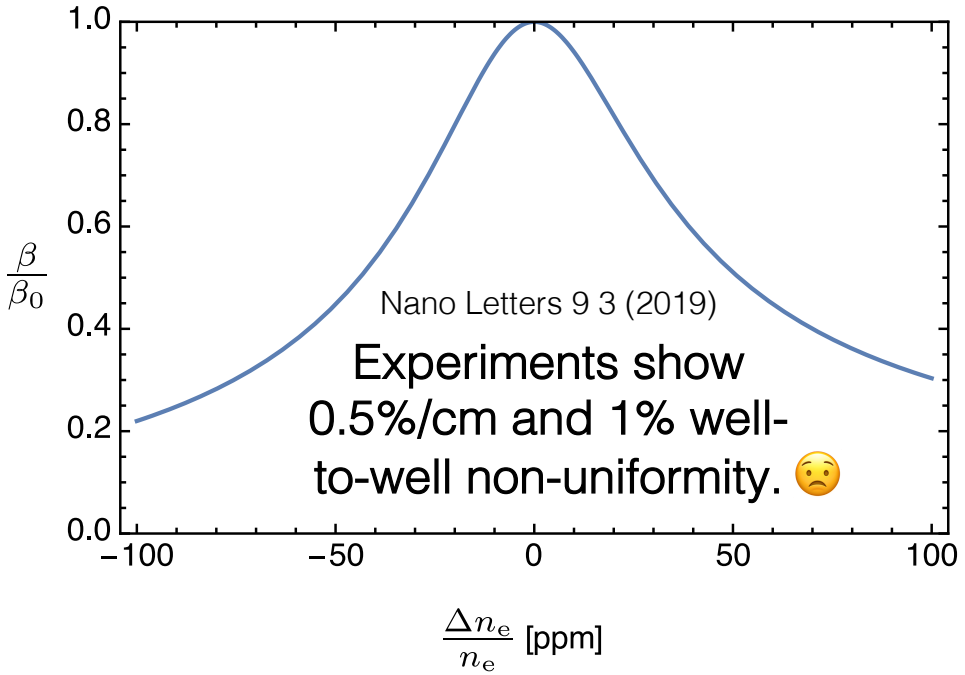

Mehrani, arXiv:2509.14320

Magnetic field and electron density inhomogeneities broaden resonance.

- The boost is extremely sensitive to B field and e^- density.

Config. 2

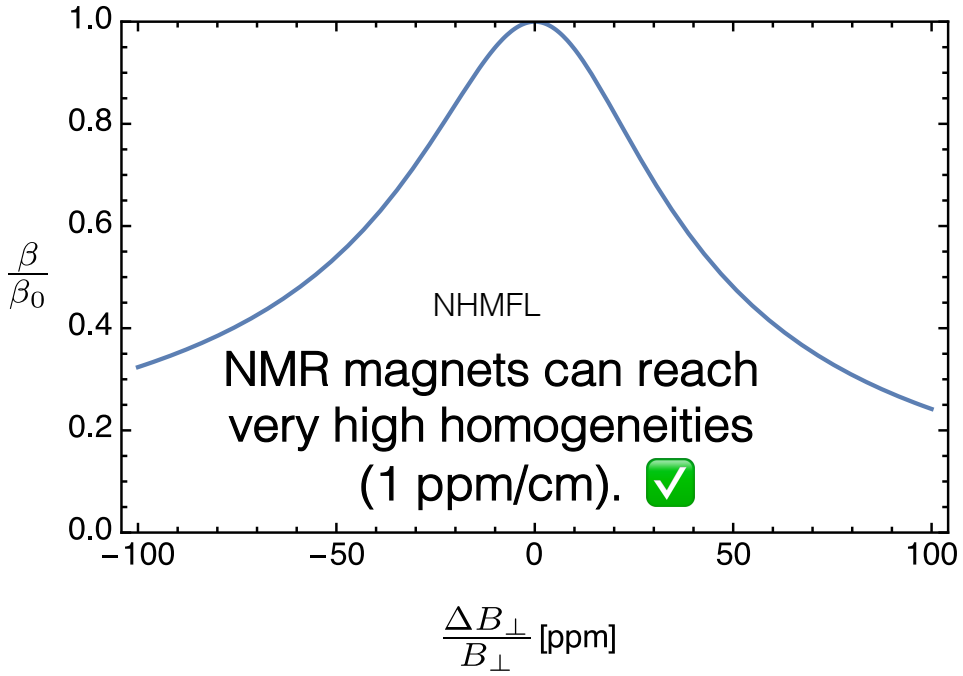

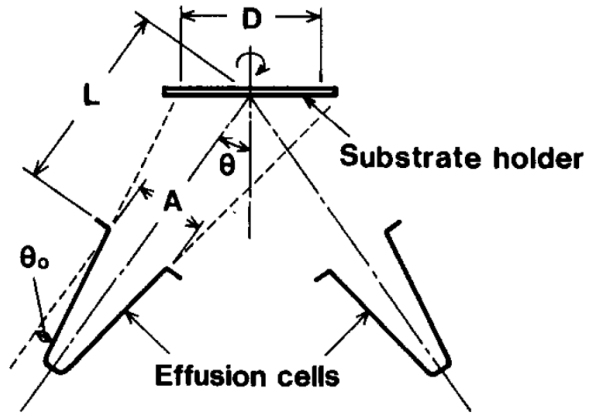

Journal of Crystal Growth 81 188-192 (1987)

Mehrani, arXiv:2509.14320

Magnetic field and electron density inhomogeneities broaden resonance.

- The boost is extremely sensitive to B field and e^- density.

Config. 2

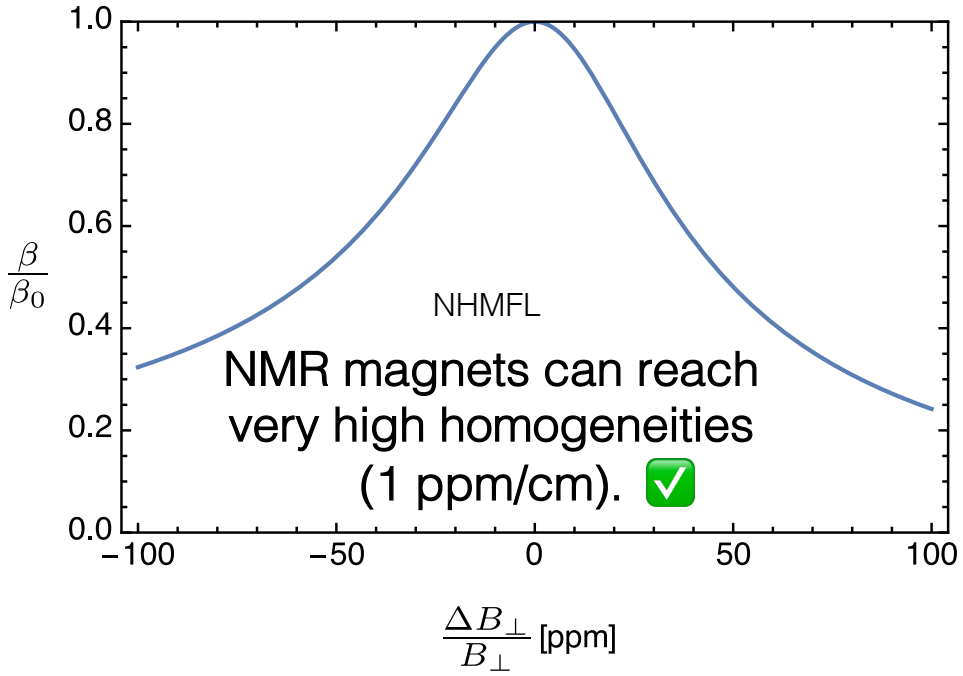

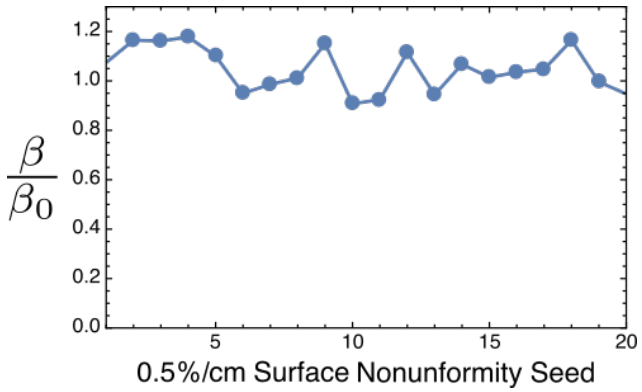

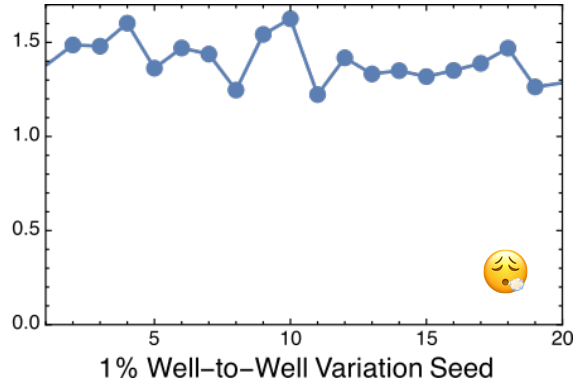

Mehrani, arXiv:2509.14320

Magnetic field and electron density inhomogeneities broaden resonance.

- The boost is extremely sensitive to B field and e^- density.

Config. 2

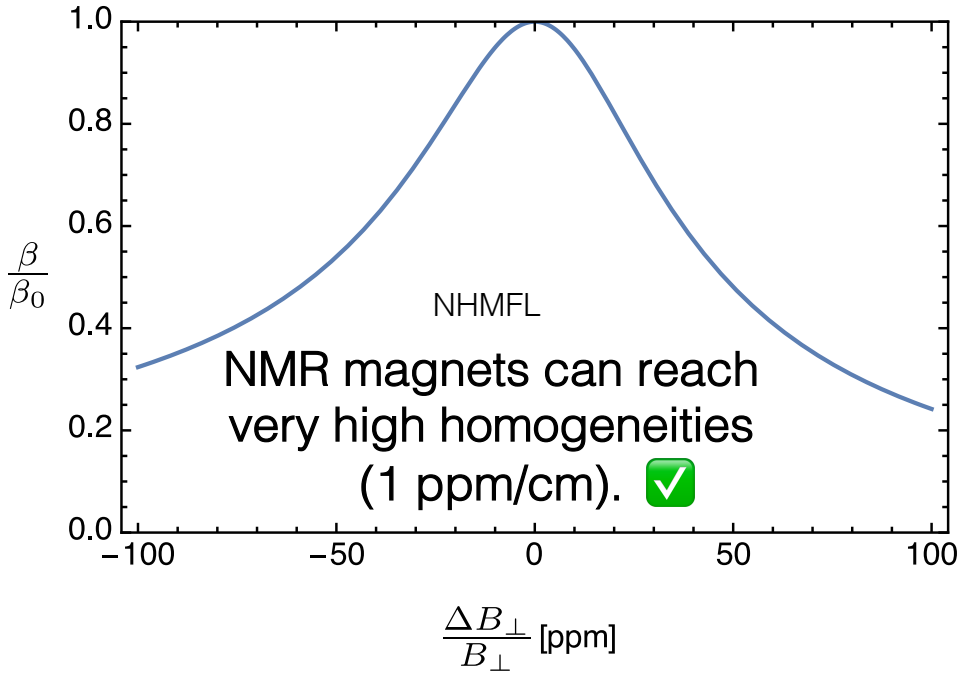

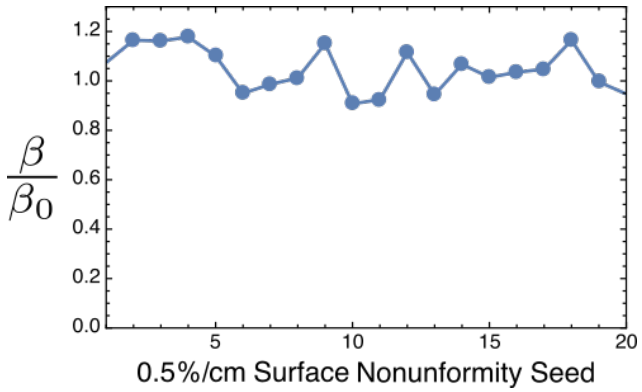

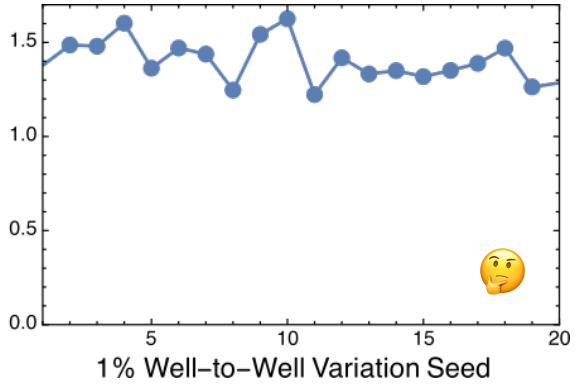

Mehrani, arXiv:2509.14320

Magnetic field and electron density inhomogeneities broaden resonance.

- The boost is extremely sensitive to B field and e^- density.

Config. 2

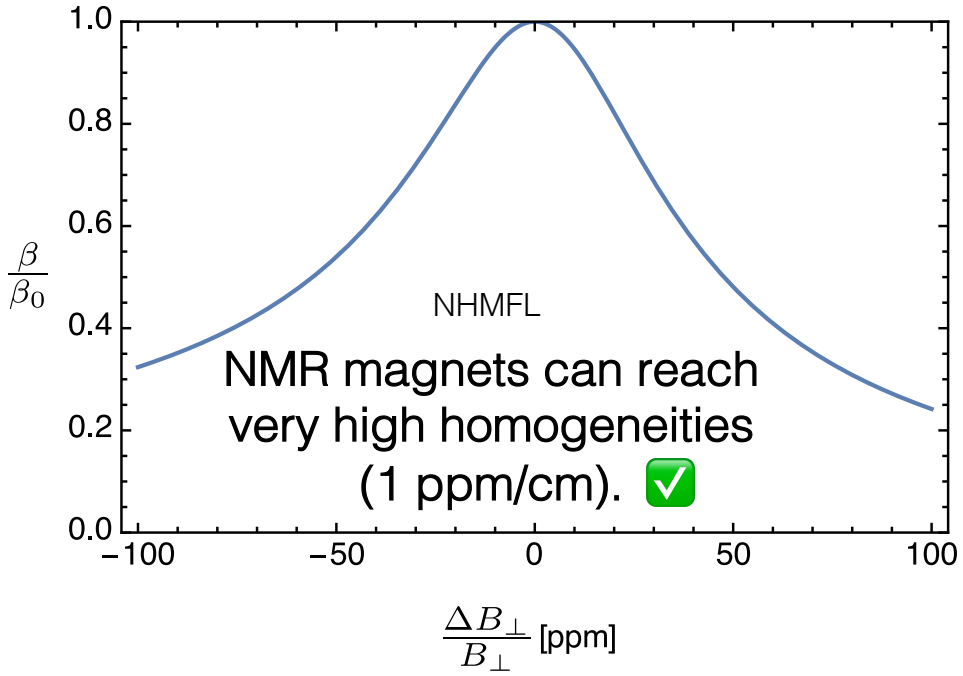

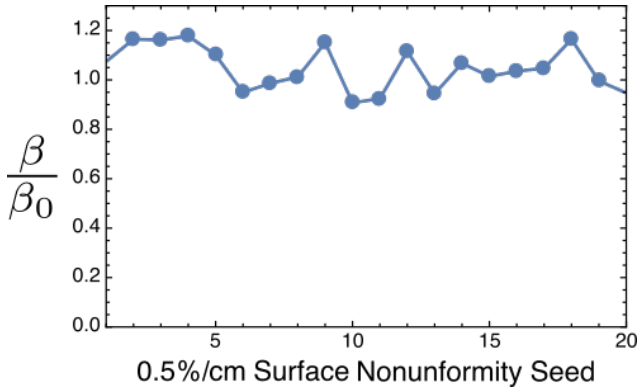

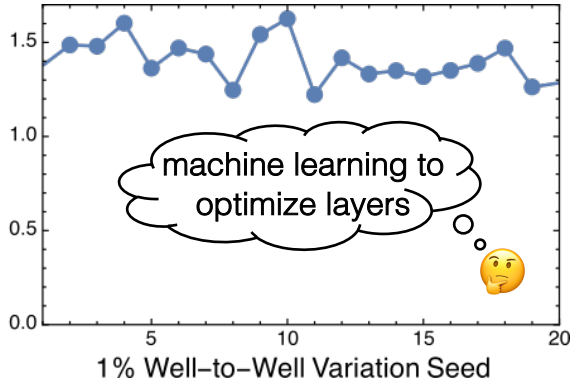

Mehrani, arXiv:2509.14320

Validation Experimental Conditions

Summary: 50% of maximum boost is maintained when testing a variety of experimental conditions.

Conclusion

SQWARE is a new tabletop, electromagnetically-tunable, and highly-sensitive axion detection scheme that may probe meV axions.

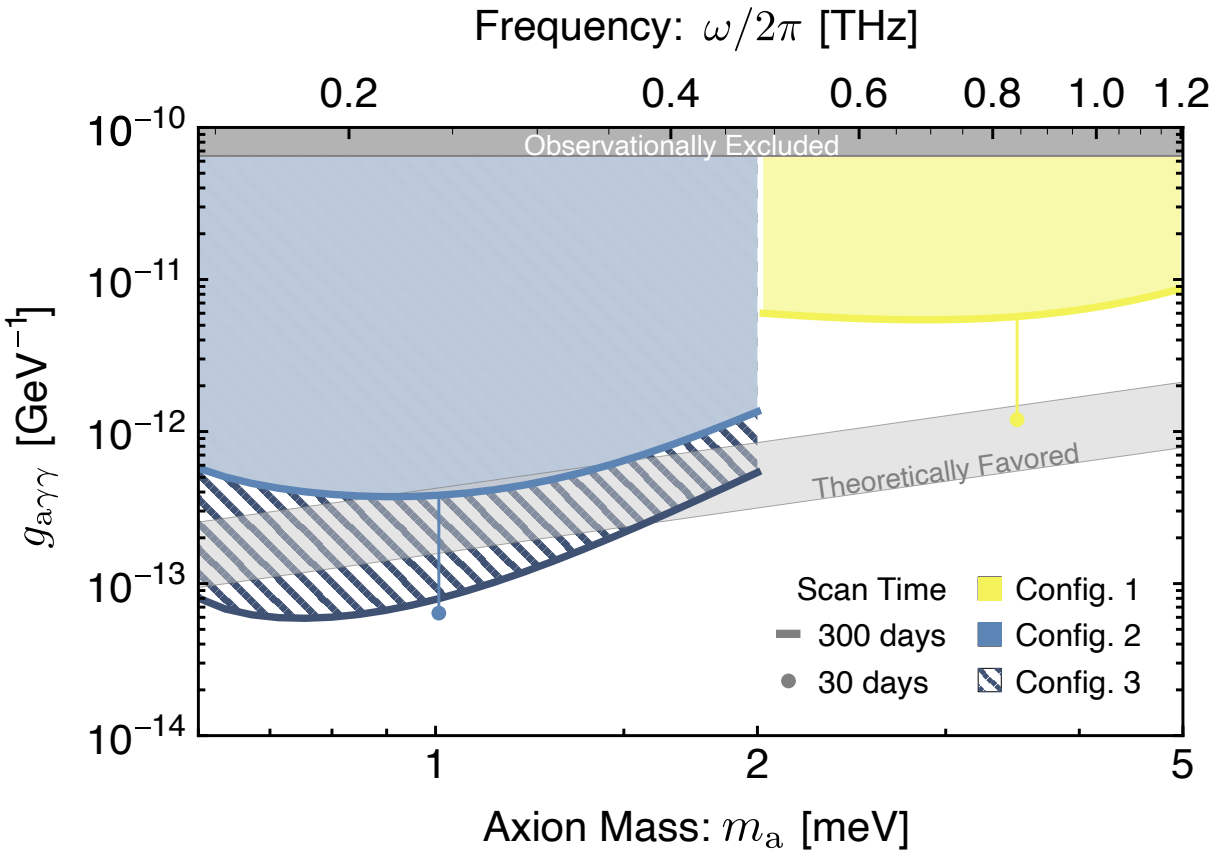

Mehrani, arXiv:2509.14320

Conclusion

SQWARE is a new tabletop, electromagnetically-tunable, and highly-sensitive axion detection scheme that may probe meV axions.

We are working on material characterization experiments and Config-0 design that could give preliminary constraints!

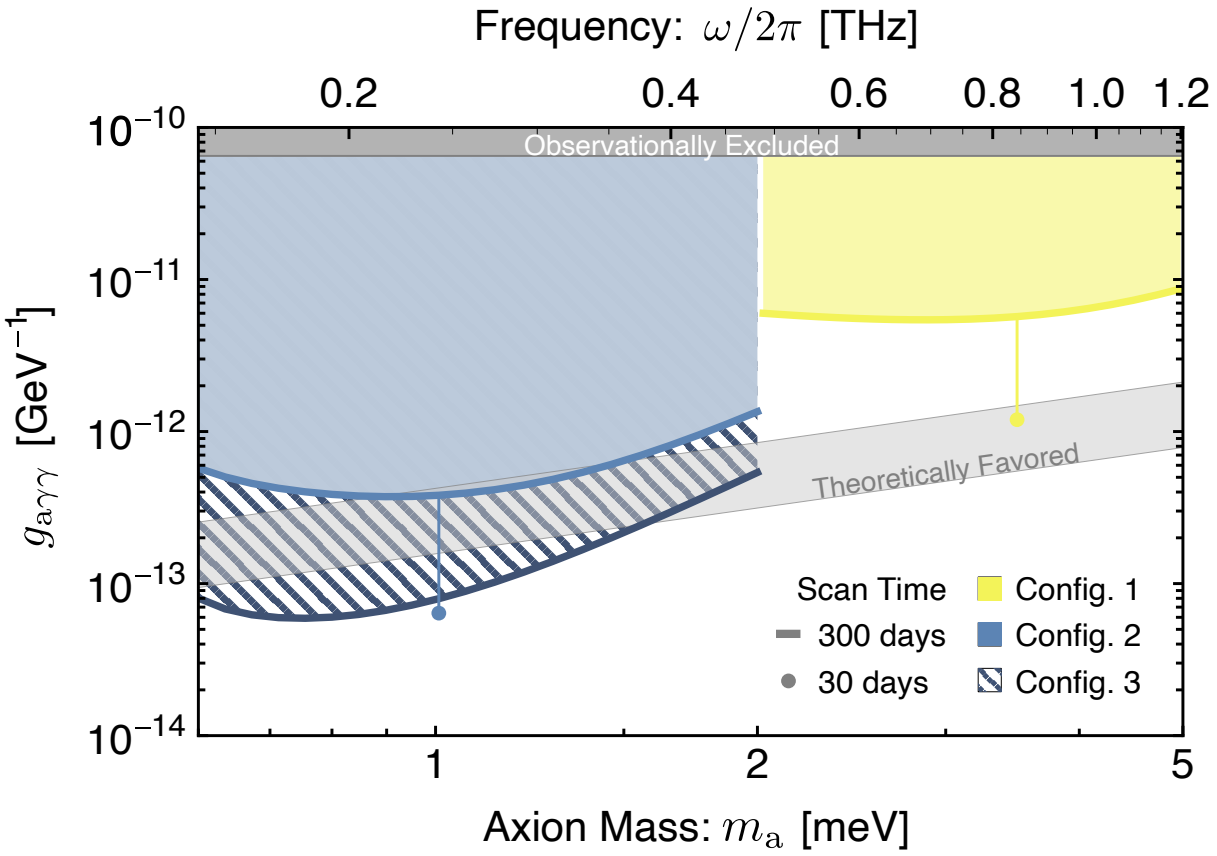

Mehrani, arXiv:2509.14320

Acknowledgements

Co-authors

- Shengxi Huang (advisor), Jun Kono (advisor), Andrew Long, Henry Everitt, Andrey Baydin, Kuver Sinha, Tao Xu, Michael Manfra

Helpful discussions!

- Alexey Belyanin, Amin Mustafa, Mudit Jain, Dorian Amaral, R. C. Woods

SCOPE + KONO + CAP lab members!

Pheno 2026 organizers!

Conclusion

SQWARE is a new tabletop, electromagnetically-tunable, and highly-sensitive axion detection scheme that may probe meV axions.

We are working on material characterization experiments and Config-0 design that could give preliminary constraints!

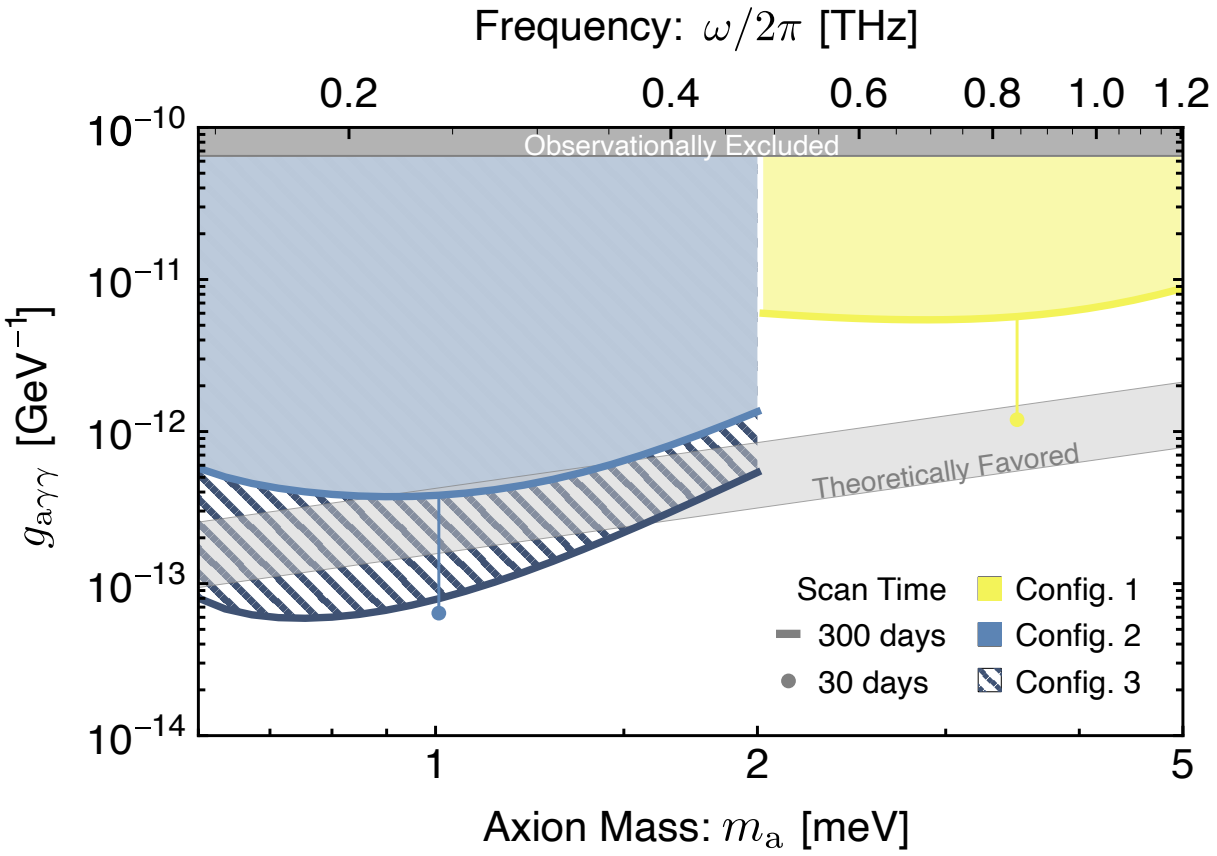

Thank you for listening!

Mehrani, arXiv:2509.14320

Config-0 Preliminary Estimates

- 2000 layers (200 um) ~ 10x state-of-the-art (N = 166) MQWs
- 10 T field, e^- density = 4.5 x 10^{11}/ cm^{-2}
- CRA polarization (lower loss at higher frequency)
- $\beta cos\theta$ = 20 at 16 meV (compare 70 at 4 meV for Config 1)

$$g > 1.4\times10^{-13}\,\mathrm{GeV}^{-1}\left[\frac{36\ \mathrm{T}}{|\mathbf{B}|\cos\theta(m_a)}\right]\left[\frac{100}{\beta(m_a)}\right]\left[\frac{0.2}{\eta}\right]^{\frac{1}{2}}\left[\frac{9\ \mathrm{cm}^2}{W^2}\right]^{\frac{1}{2}}\left[\frac{\Gamma_{\mathrm{dark}}}{1\ \mathrm{mHz}}\right]^{\frac{1}{4}}\left[\frac{m_a}{1\ \mathrm{meV}}\right]^{\frac{3}{2}}\left[\frac{30\ \mathrm{days}}{t_{\mathrm{obs}}}\right]^{\frac{1}{4}}$$

- Working on N = 100 with optimal layer density configuration (machine learning integrated in COMSOL)

Effective Medium Theory (EMT) is valid when layer thickness << λ_{med}.

$$\varepsilon_{\mathrm{eff}} = \frac{\varepsilon_{\mathrm{barrier}} d_{\mathrm{Barrier}} + \varepsilon_{\mathrm{QW}} d_{\mathrm{QW}}}{d_{\mathrm{Barrier}} + d_{\mathrm{QW}}}$$

- COMSOL simulations of boost validate EMT.

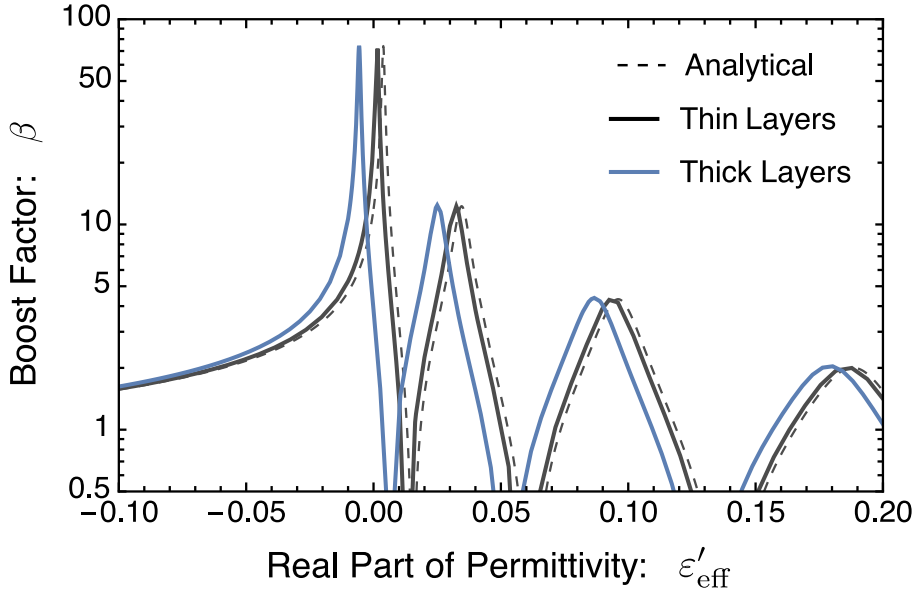

Mehrani, arXiv:2509.14320

Dark Photon Proposed Sensitivity

- Dark photon mixes with massless photon
- Parallel magnetic field component irrelevant
- Mixing parameter χ instead of coupling g

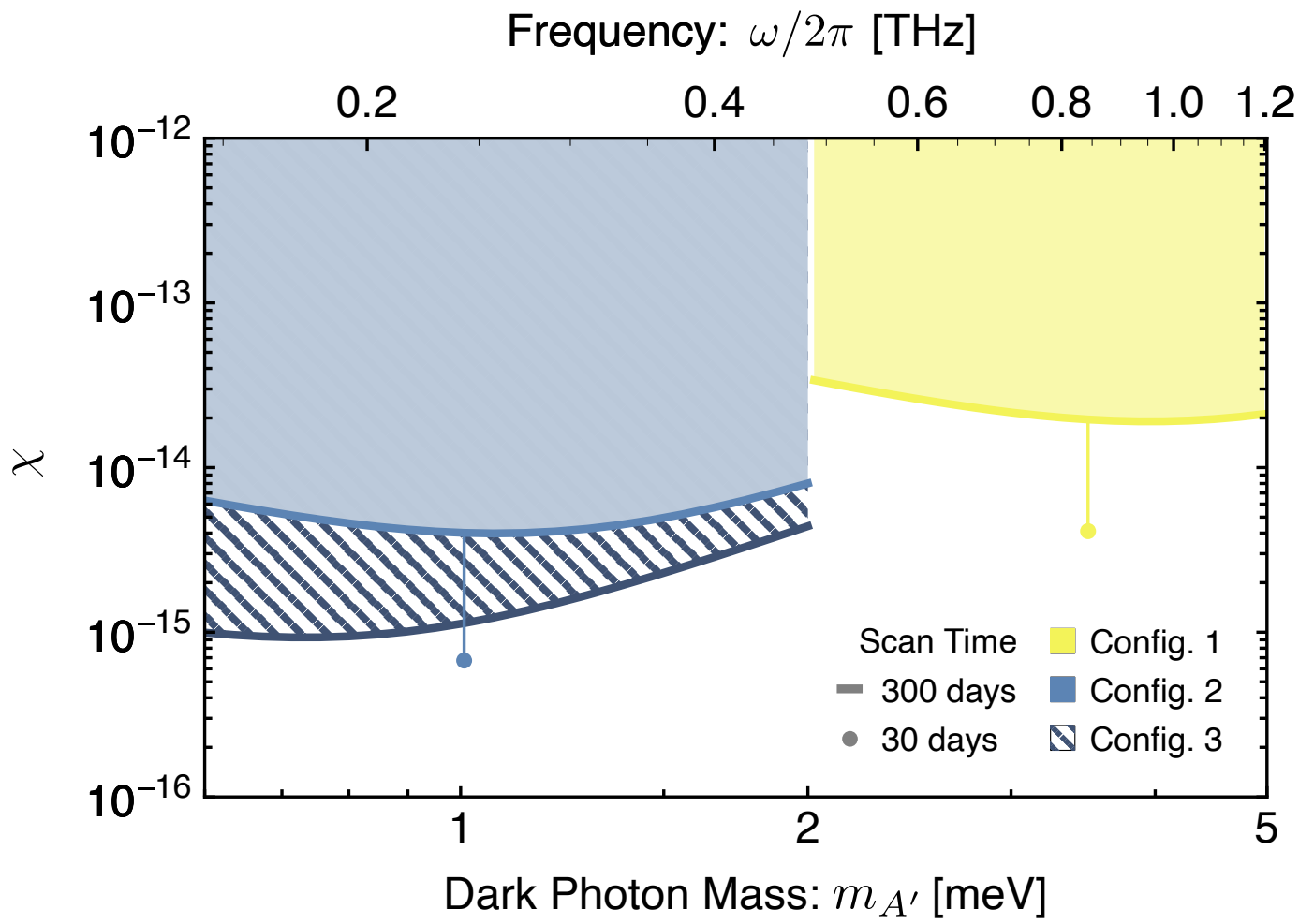

Why we don't use bulk semiconductor?

Bulk Doped Semiconductor

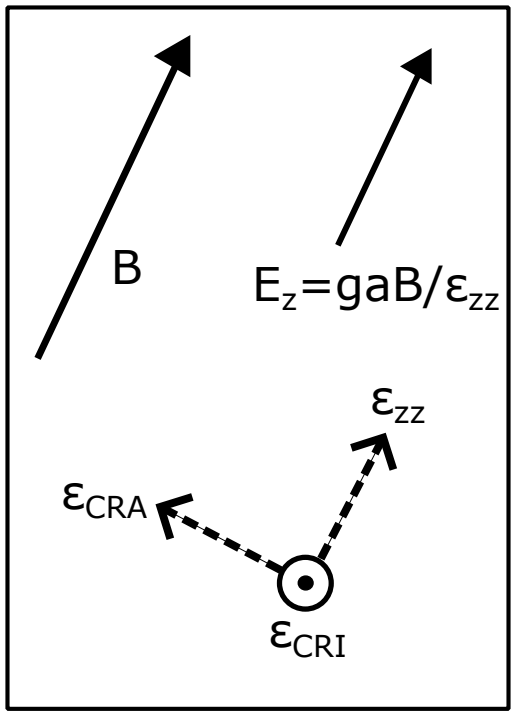

MQW (2DEGs)

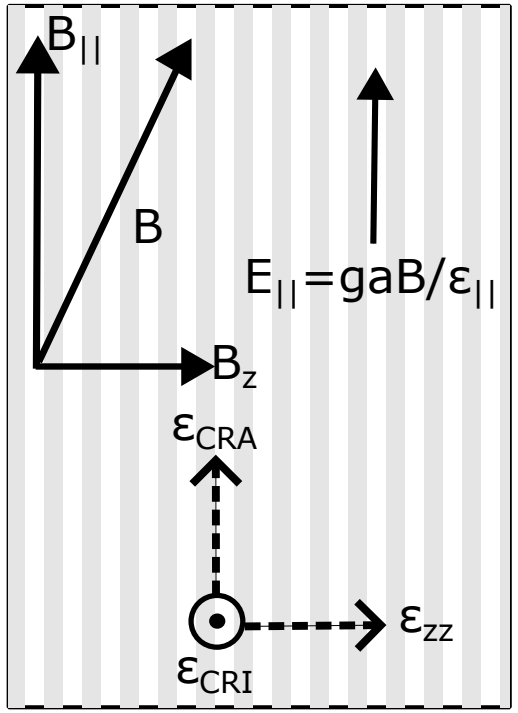

$E_z = gaB_z/\varepsilon_{zz}$ is negligible here compared to $E_{||}$ (on resonance)

EMT (1)

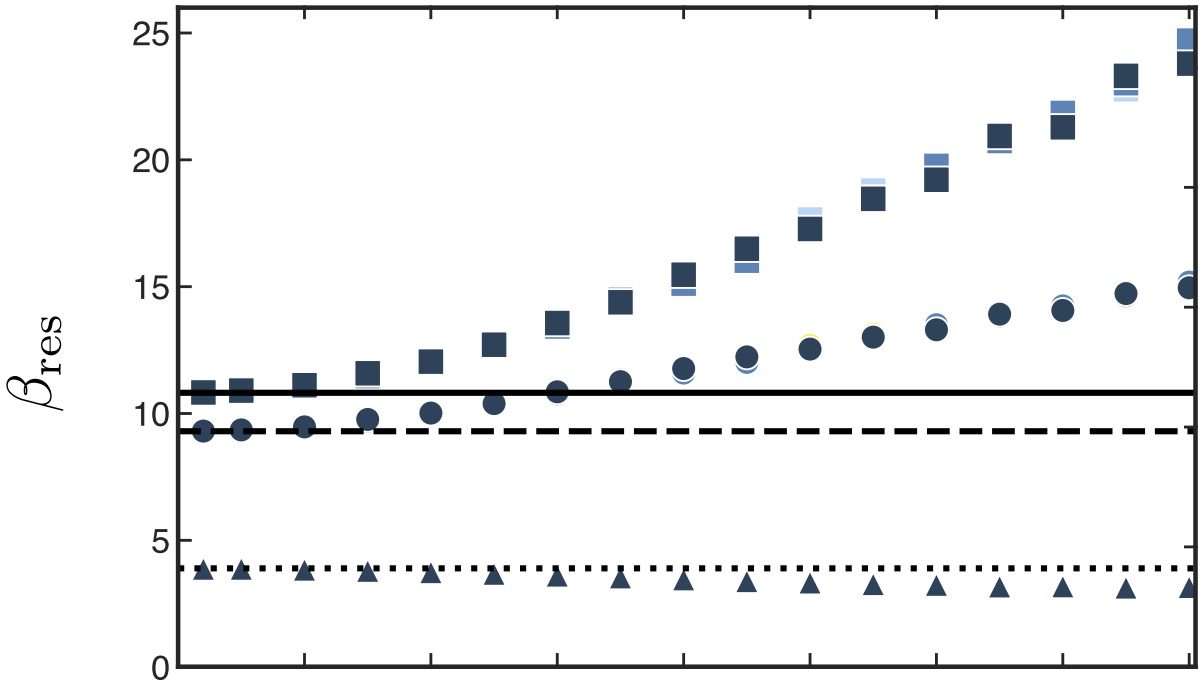
β_{res}
25
20
15
10
5
0

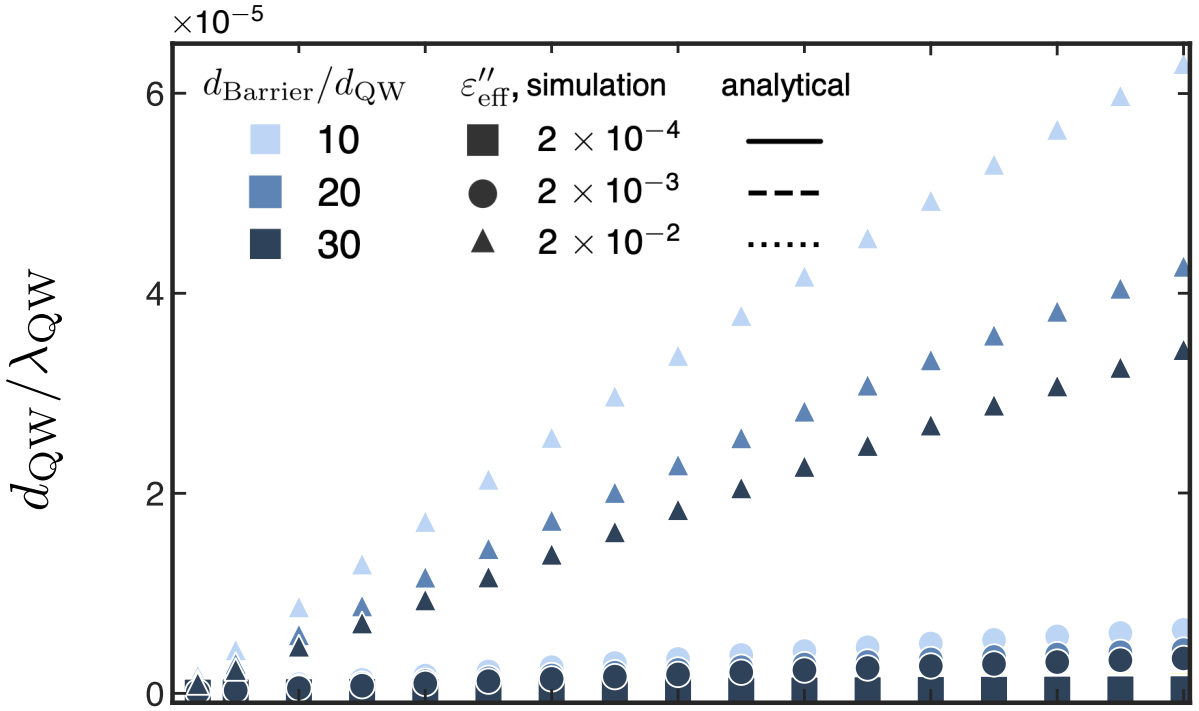
$\times 10^{-5}$
$d_{\mathrm{QW}}/\lambda_{\mathrm{QW}}$
6
4
2
0
$d_{\mathrm{Barrier}}/d_{\mathrm{QW}}$
10
20
30
$\varepsilon''_{\mathrm{eff}}$, simulation
2×10^{-4}
2×10^{-3}
2×10^{-2}
analytical

EMT (2)

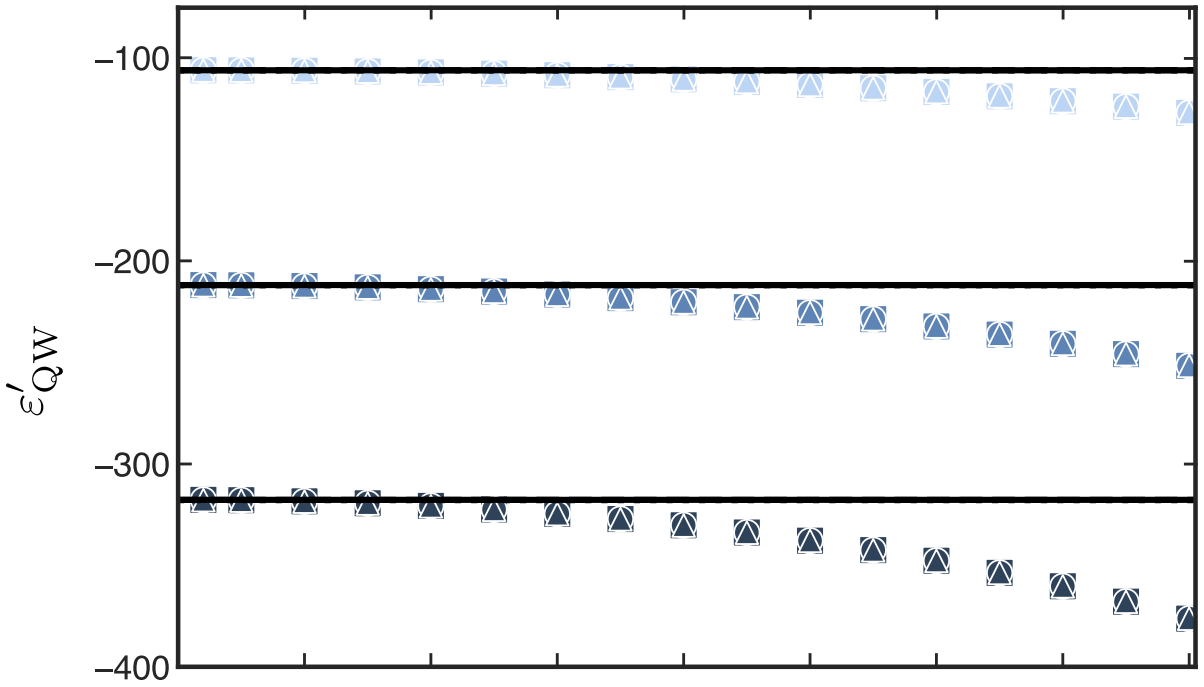
−100
−200
−300
−400
$\varepsilon'_{\mathrm{QW}}$

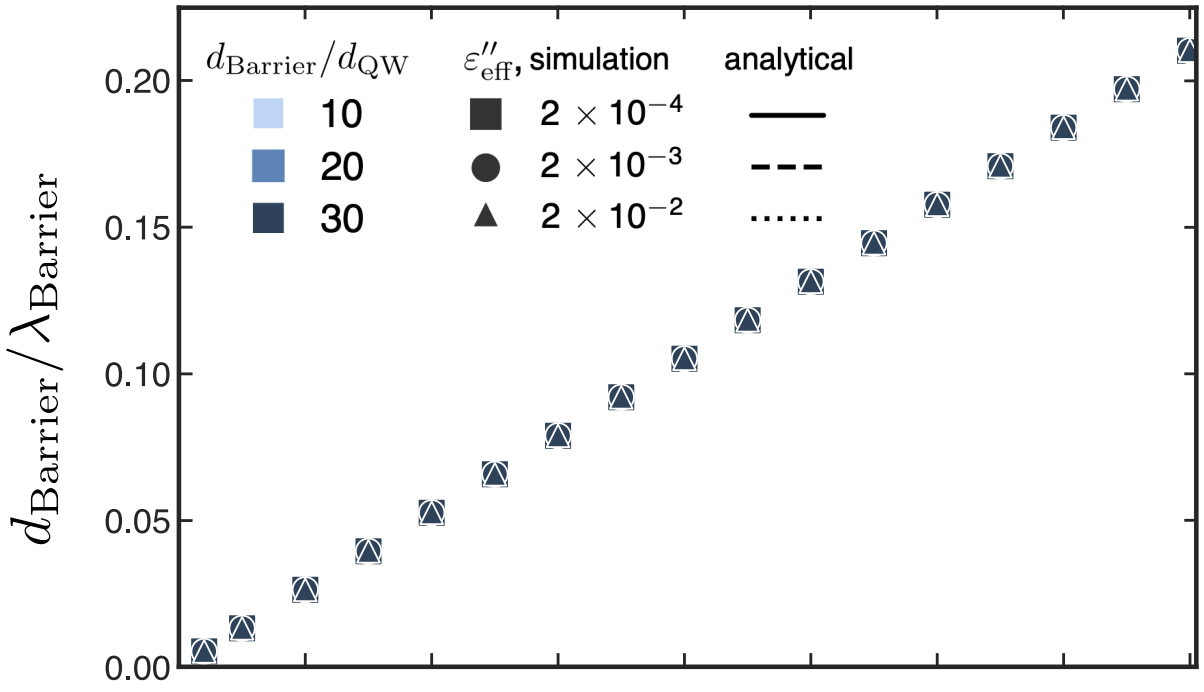
$d_{\mathrm{Barrier}}/d_{\mathrm{QW}}$
10
20
30
$\varepsilon''_{\mathrm{eff}}$, simulation
2×10^{-4}
2×10^{-3}
2×10^{-2}
analytical
0.20
0.15
0.10
0.05
0.00
$d_{\mathrm{Barrier}}/\lambda_{\mathrm{Barrier}}$

EMT (3)

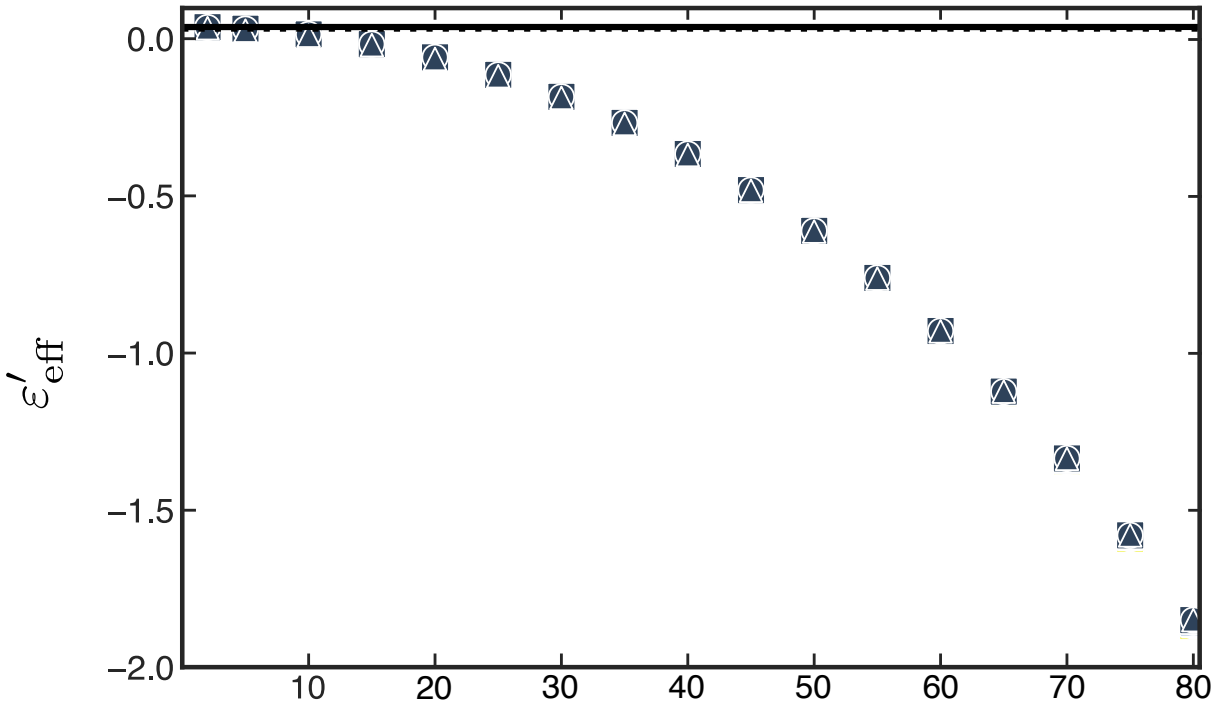
$\varepsilon'_{\mathrm{eff}}$
0.0
−0.5
−1.0
−1.5
−2.0
10
20
30
40
50
60
70
80

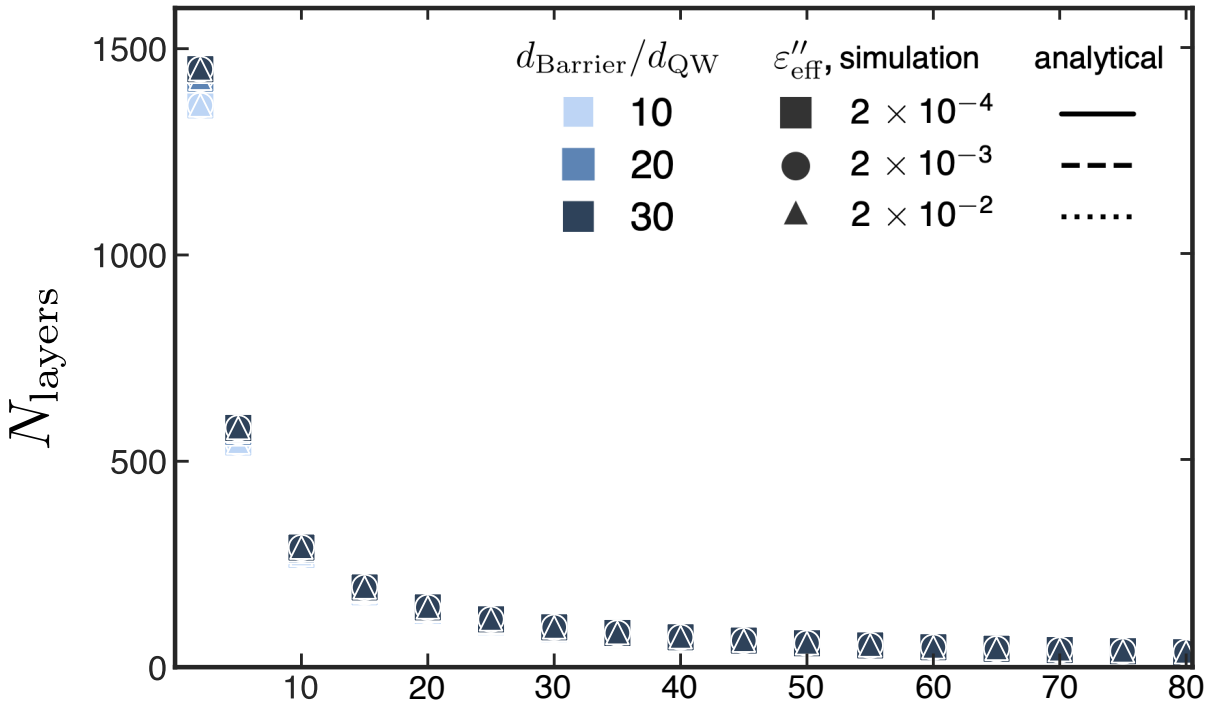
N_{layers}
1500
1000
500
0
10
20
30
40
50
60
70
80
$d_{\mathrm{Barrier}}/d_{\mathrm{QW}}$
10
20
30
$\varepsilon''_{\mathrm{eff}}$, simulation
2×10^{-4}
2×10^{-3}
2×10^{-2}
analytical

QW Permittivity and Boost

Config. 2

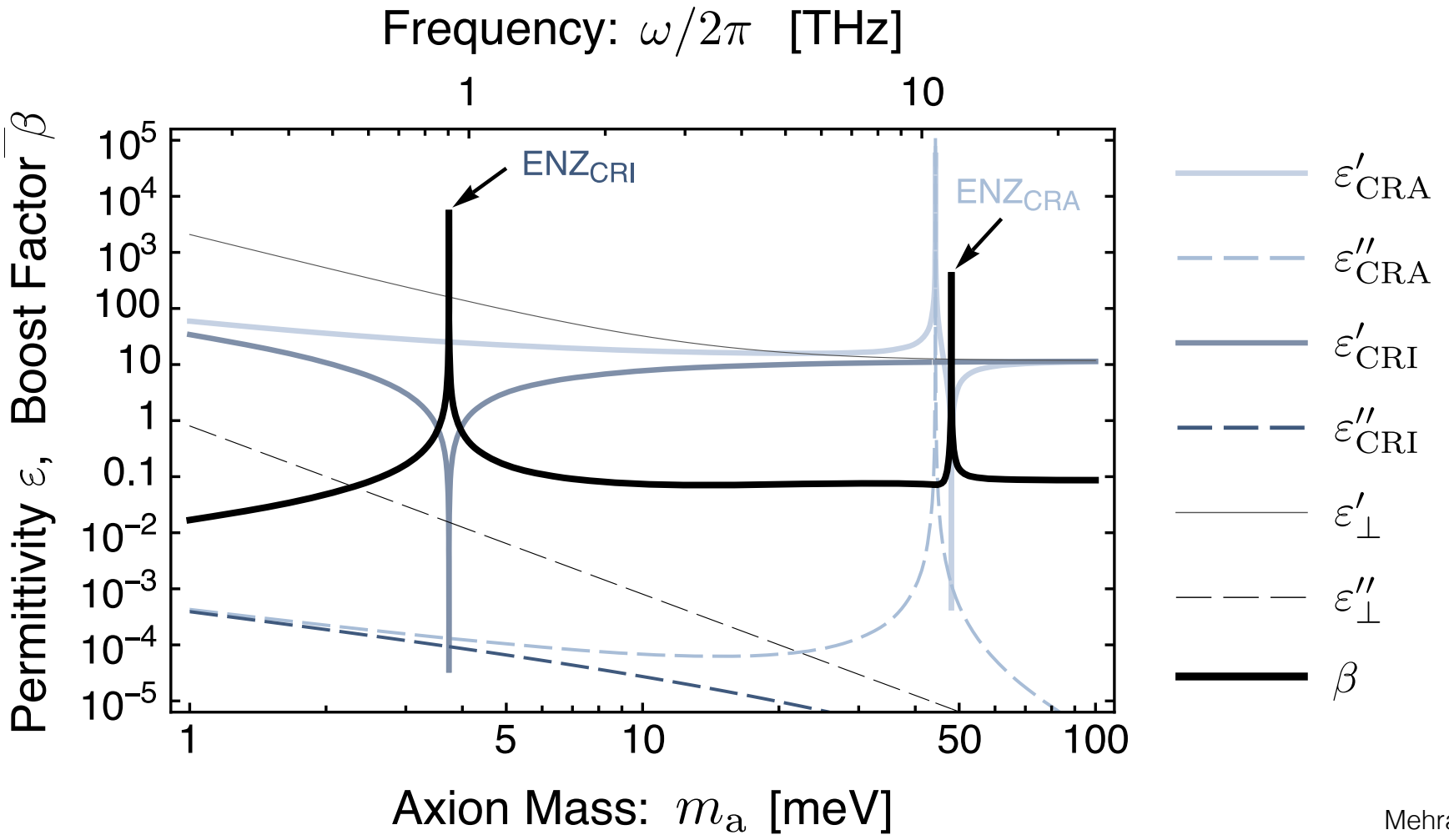

Mehrani, arXiv:2509.14320

MQW Angle and Boost

Config. 2

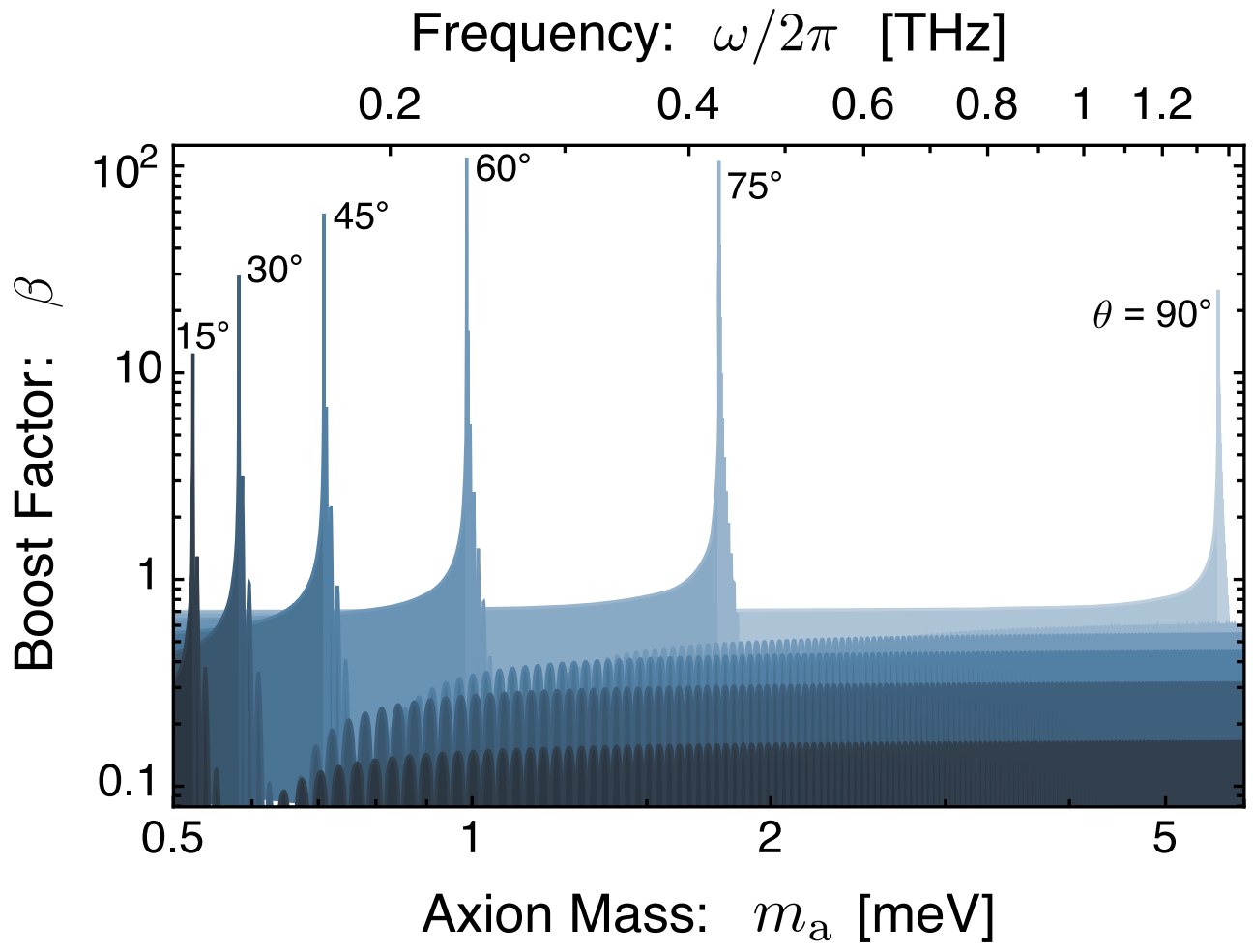

Mehrani, arXiv:2509.14320

MQW Angle, Quality Factor, and Boost

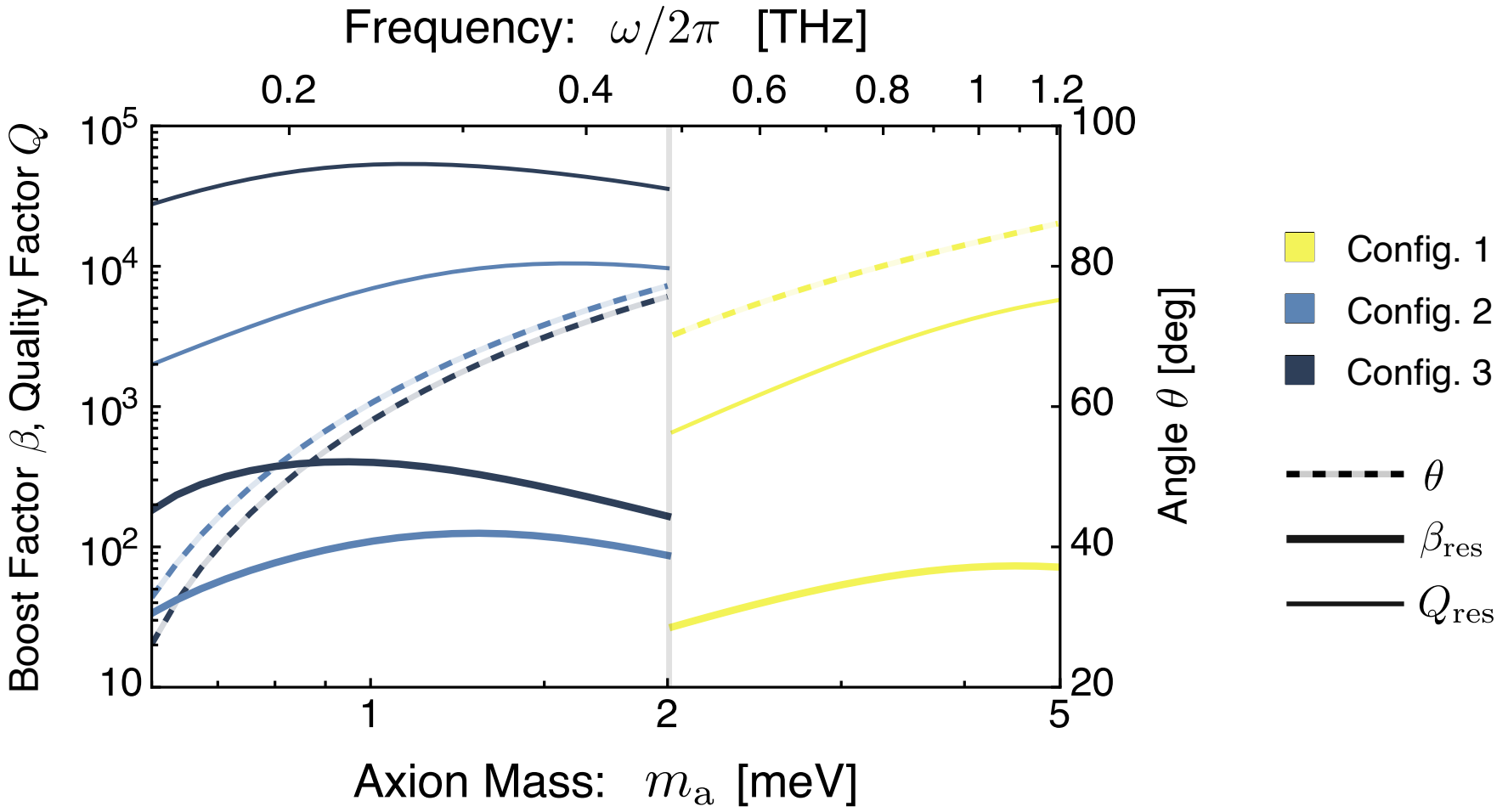

Axion Theory

- Peccei-Quinn Symmetry is a global U(1) symmetry which is spontaneously broken, generating a pseudo-goldstone boson: the axion!
- Tilt in the potential, due to coupling with gluon fields through either standard model quarks with PQ charge (DFSZ model) or exotic quarks (KSVZ).

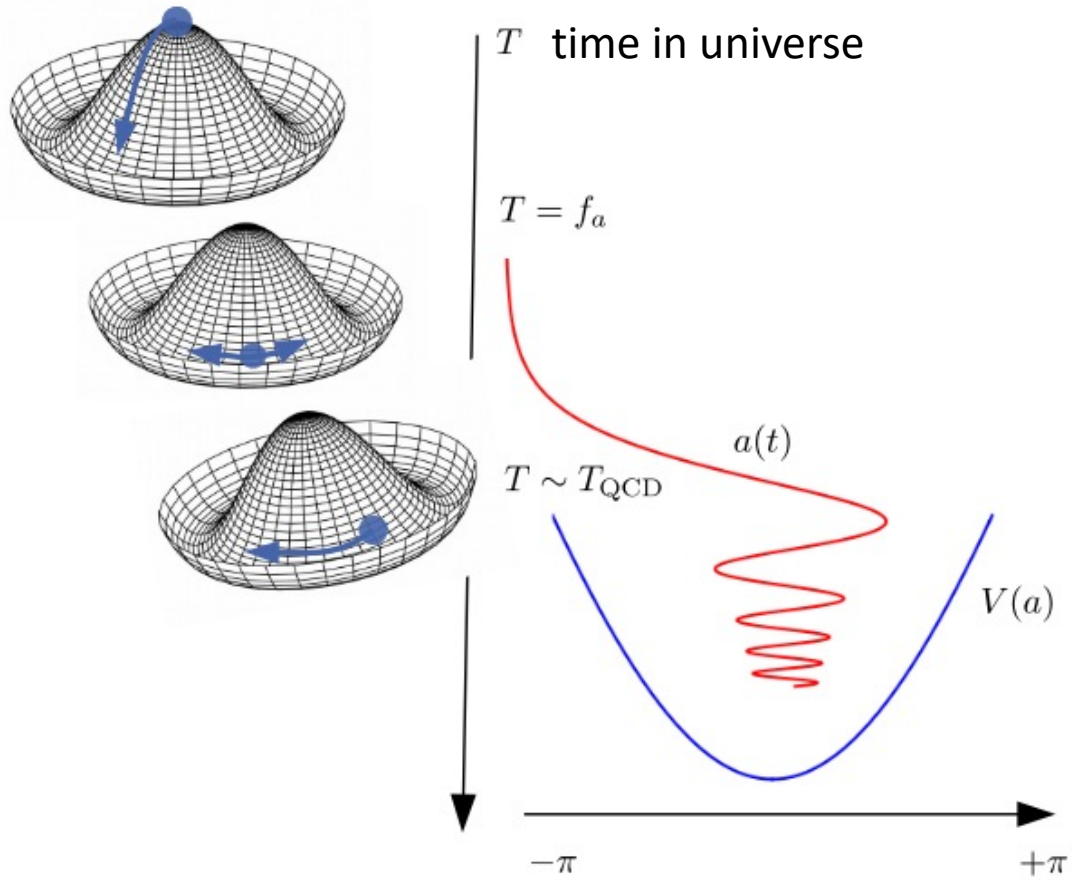

KIT Andreas Pargner (2019)

Axion Theory

- Post-inflation axion
  - The misalignment angle is a statistical average from all the Horizons.
- Pre-inflation axion
  - The misalignment angle is a quantum fluctuation and is stretched out by inflation.

$$\begin{aligned}
\boldsymbol{\nabla}\cdot\mathbf{E} &= \rho - g_{a\gamma}\mathbf{B}\cdot\boldsymbol{\nabla}a\,,\\
\boldsymbol{\nabla}\times\mathbf{B} - \dot{\mathbf{E}} &= \mathbf{J} + g_{a\gamma}(\mathbf{B}\,\dot{a} - \mathbf{E}\times\boldsymbol{\nabla}a)\,,\\
\boldsymbol{\nabla}\cdot\mathbf{B} &= 0\,,\\
\boldsymbol{\nabla}\times\mathbf{E} + \dot{\mathbf{B}} &= 0\,,\\
\boldsymbol{\nabla}^2 a + m_a^2 a &= g_{a\gamma}\mathbf{E}\cdot\mathbf{B}\,.
\end{aligned}$$

$$\mathcal{L} = -\frac{1}{4}F_{\mu\nu}F^{\mu\nu} - J^\mu A_\mu + \frac{1}{2}\partial_\mu a\partial^\mu a - \frac{1}{2}m_a^2 a^2 - \frac{g_{a\gamma}}{4}F_{\mu\nu}\widetilde{F}^{\mu\nu}a$$

Magnets at Rice

- Oxford 10 T Continuous
  - Constrain QCD axion with thinner prototype for higher frequencies at lower magnetic fields
- RAMBO 30 T Pulsed
  - Characterization of MQW

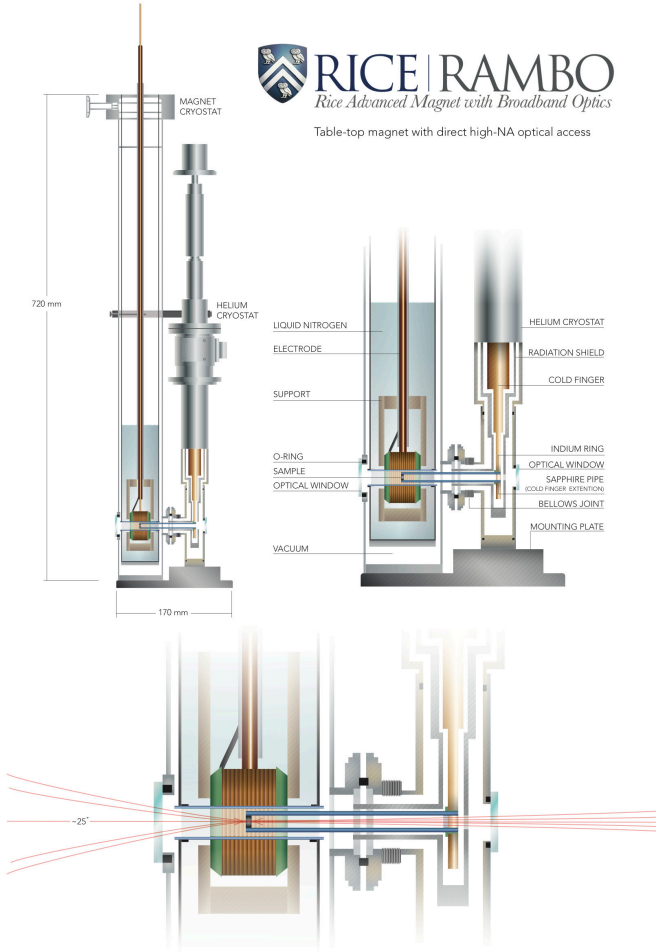

Quantum Dot (QD) Photodetector

- Coulomb Blockade: Photon exciting a QD is measured as a change in capacitance within a circuit
- QD Landau level system is tunable with a magnetic field (cyclotron resonance)!
- Experimentally tested at 2 meV and 6 meV resonances

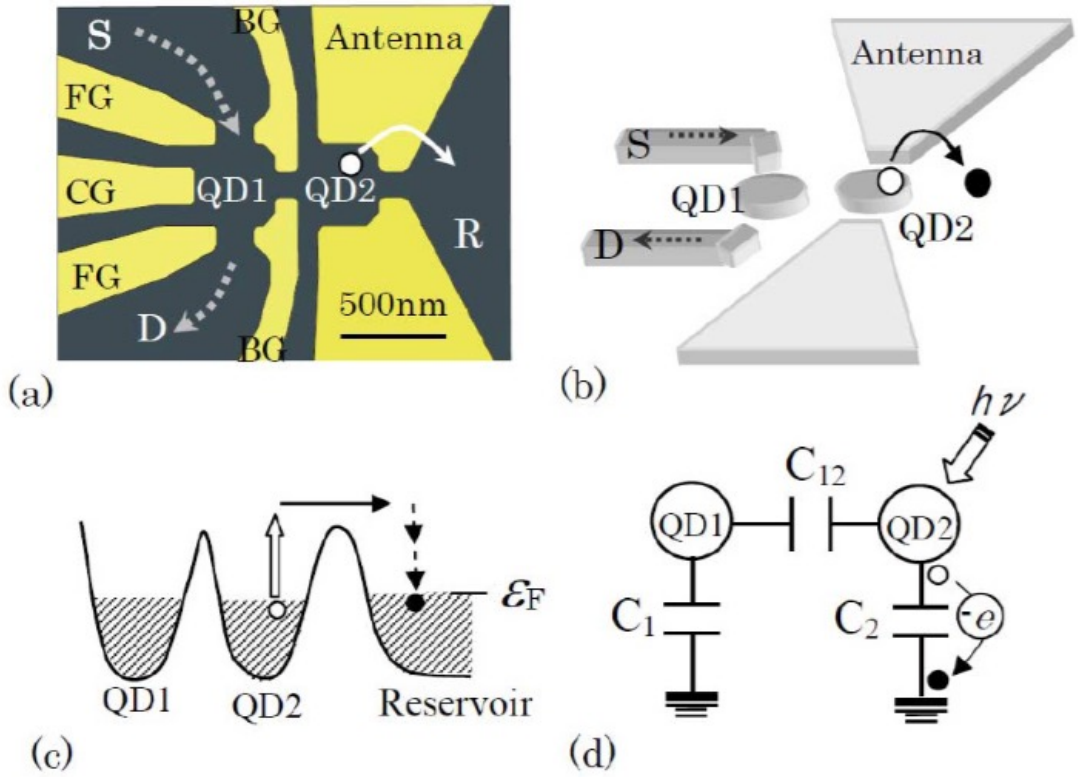

Komiyama S., IEEE Journal of Selected Topics in Quantum Electronics (2011)

Quantum Dot (QD) Photodetector

- Improvements with RF-SET
  - Using RF instead of DC conductance in circuit
  - Removing 1/f noise and better impedance matching
- Useful for broad range axion experiments

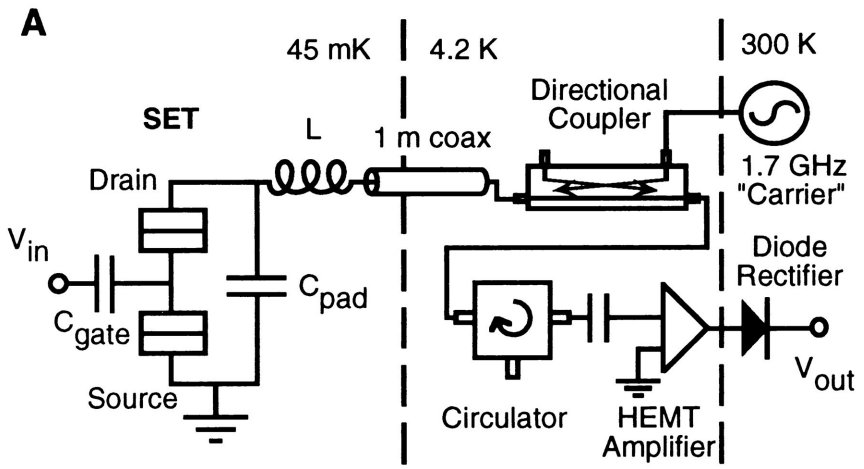

Science 280,1238-1242 (1998).

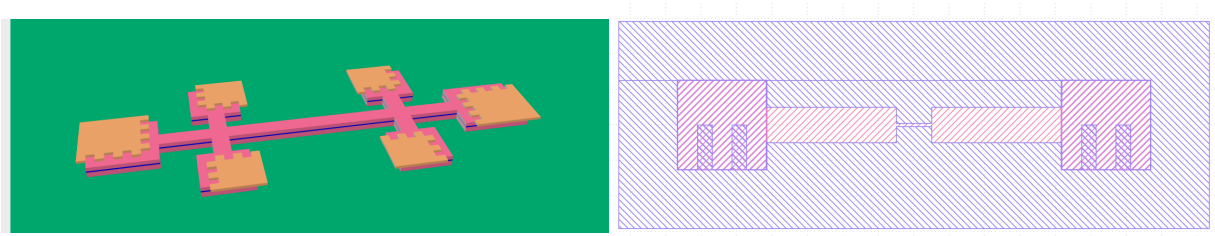

KLayout Designs

Axions are a promising DM model

- Several theoretical dark matter models with unique properties of mass, spin, charge, couplings!
- Axions could additionally solve the strong charge parity problem in quantum chromodynamics (QCD)
  - Peccei-Quinn theory:

$$\mathcal{L}_{\text{QCD}} = -\frac{1}{4} G^{a\mu\nu} G^{a}{}_{\mu\nu} - \frac{\boldsymbol{g_s^2 \theta}}{\boldsymbol{32\,\pi^2}}\, \boldsymbol{G^{a\mu\nu}\,\widetilde{G}^{a}_{\mu\nu}} + \sum_q \bar{q}\left(i\not{D} - m_q e^{i\theta_q \gamma_5} \right) q$$

$$\mathcal{L}_{\text{a}} = \frac{1}{2}\left(\partial_\mu a\right)^2 + \frac{\boldsymbol{a}}{\boldsymbol{f_a}} \frac{\boldsymbol{g_s^2}}{\boldsymbol{32\pi^2}} \boldsymbol{G\widetilde{G}} + \frac{1}{4} g^0_{a\gamma}\, a\, F\tilde{F} + \frac{\partial_\mu a}{2 f_a}\, \bar{q} c_q^0\, \gamma^\mu\, \gamma_5\, q - \bar{q}_L M_q q_R + \text{h.c.} + \cdots$$

Multiple Quantum Wells

- Studying ENZ resonance and homogeneity of multiple quantum wells at high magnetic fields
- Using pulsed THz transmission to characterize ENZ
- TMM simulations on the right

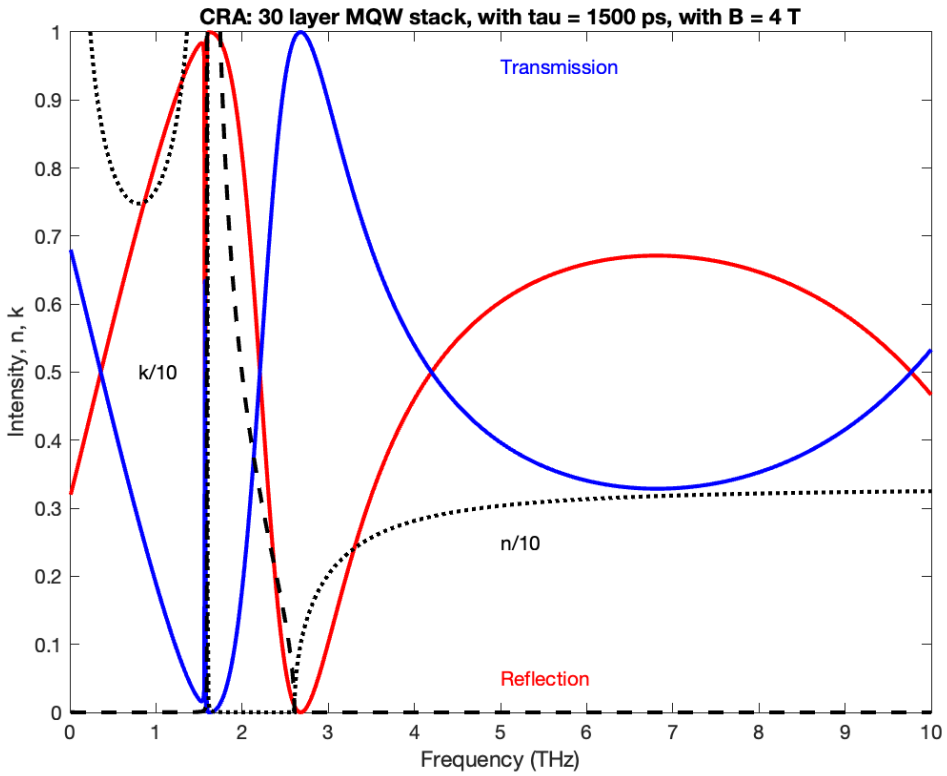

Material's Plasmonic Response to Axion

- Material response ($\hat{\varepsilon}$)

$$\mathbf{D}_a = \mathbf{E}_a + \mathbf{P}_a - \frac{i}{\omega}\boldsymbol{J}_a$$

$$= \mathbf{E}_a + \hat{\chi}\mathbf{E}_a - \frac{i\hat{\sigma}}{\omega}\mathbf{E}_a$$

$$= \hat{\varepsilon}\mathbf{E}_a = -g_{a\gamma}\mathbf{B}a(t)$$

- Plasmonic material ($|\varepsilon| \to 0$)

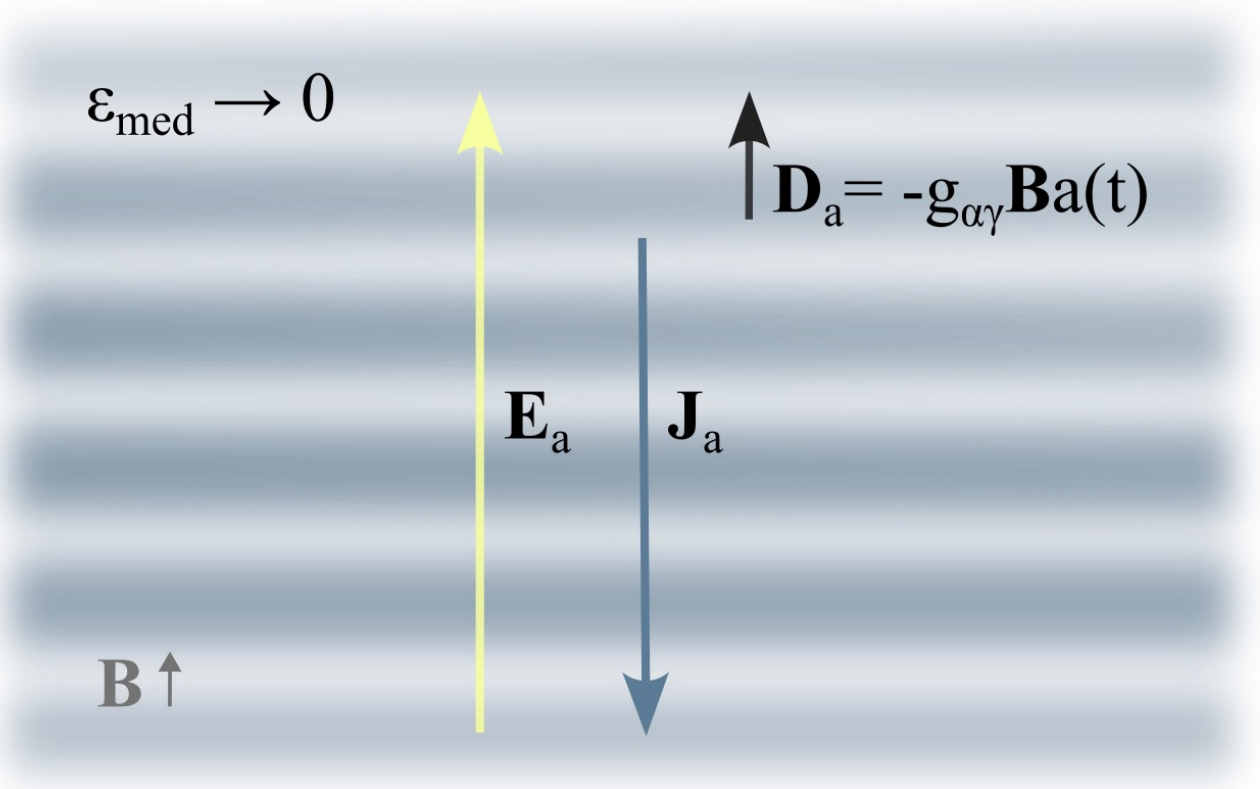

Electron Density Non-Uniformity

- The boost is extremely sensitive to the electron density.
- Experiments show 0.5%/cm and 1% well-to-well non-uniformity.

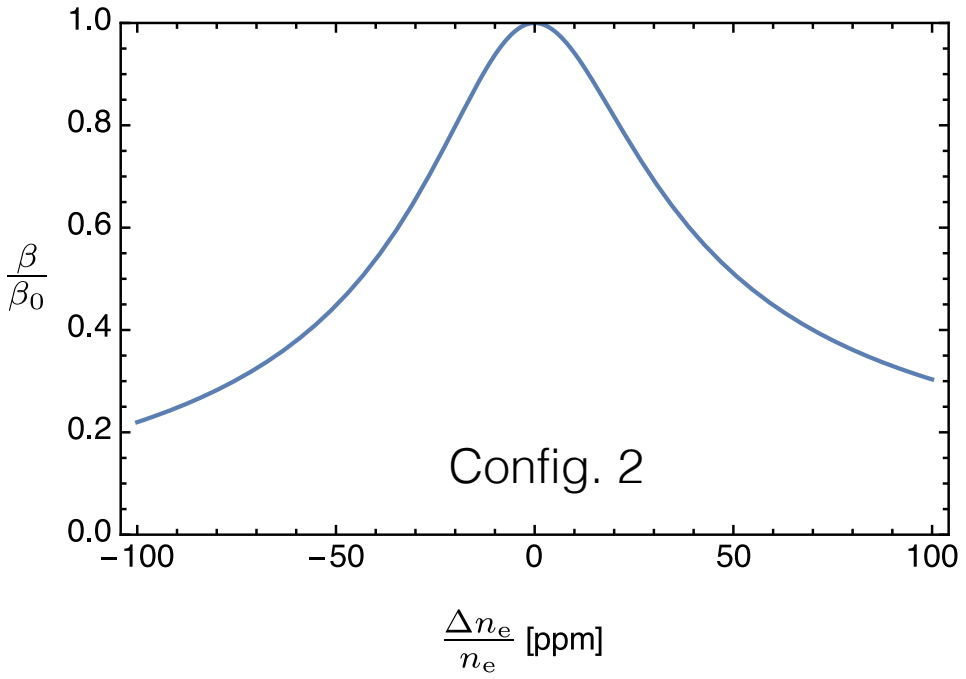

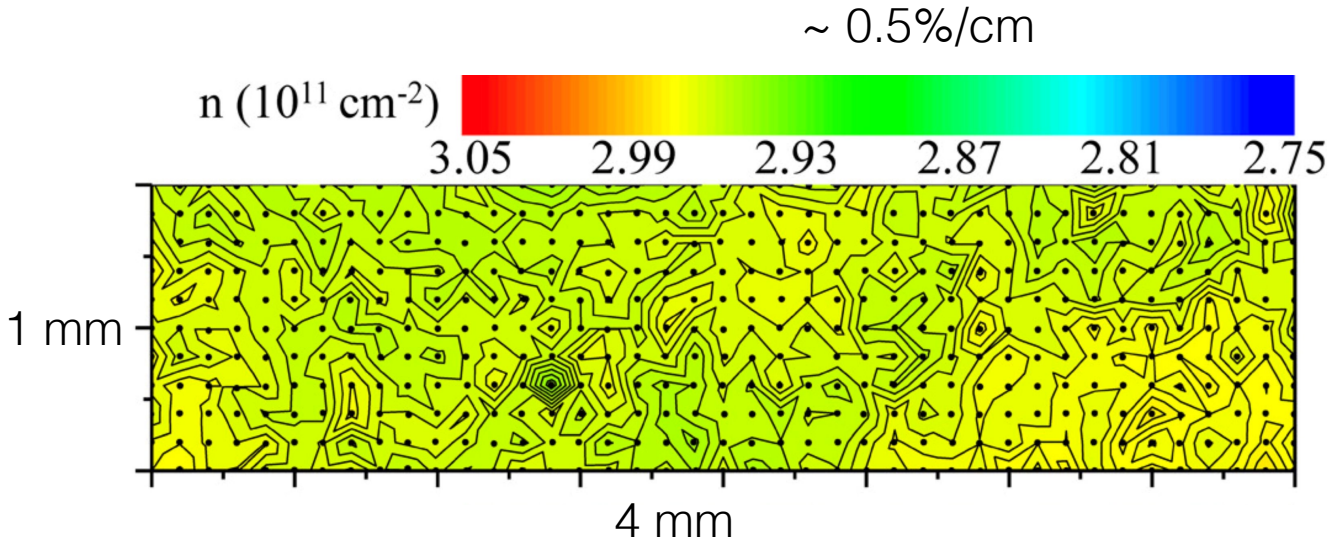

Nano Letters 9 3 (2019)

Electron density Non-Uniformity

- EMT comes to the rescue! Randomization across surface and well-to-well maintains boost ("best side" of MQW plotted).

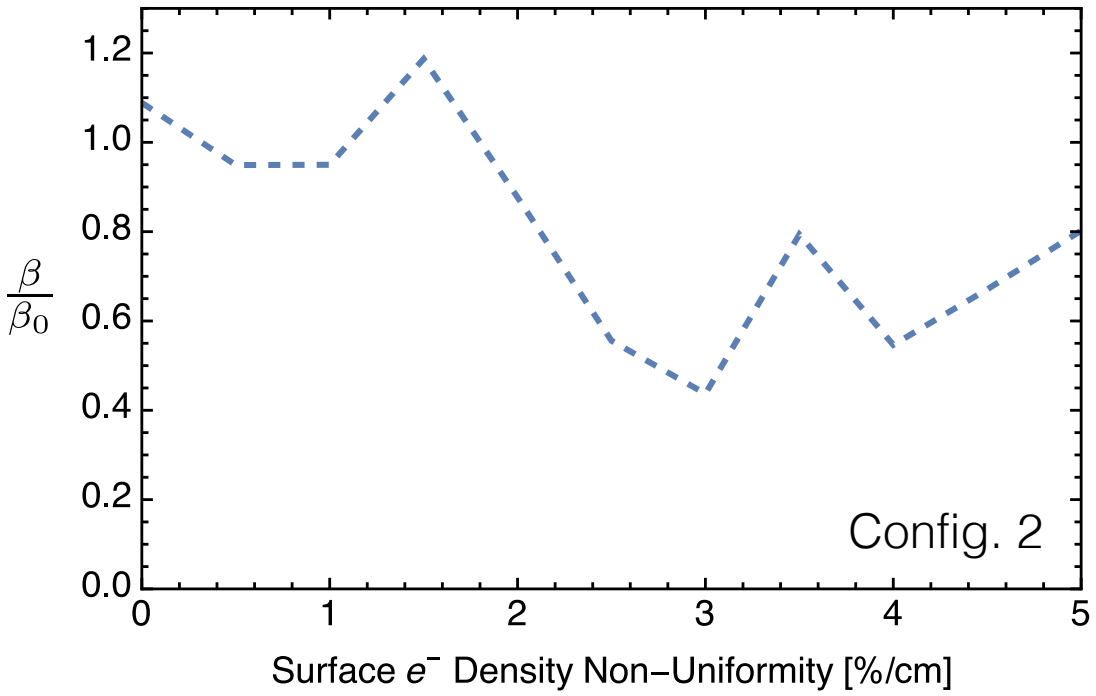

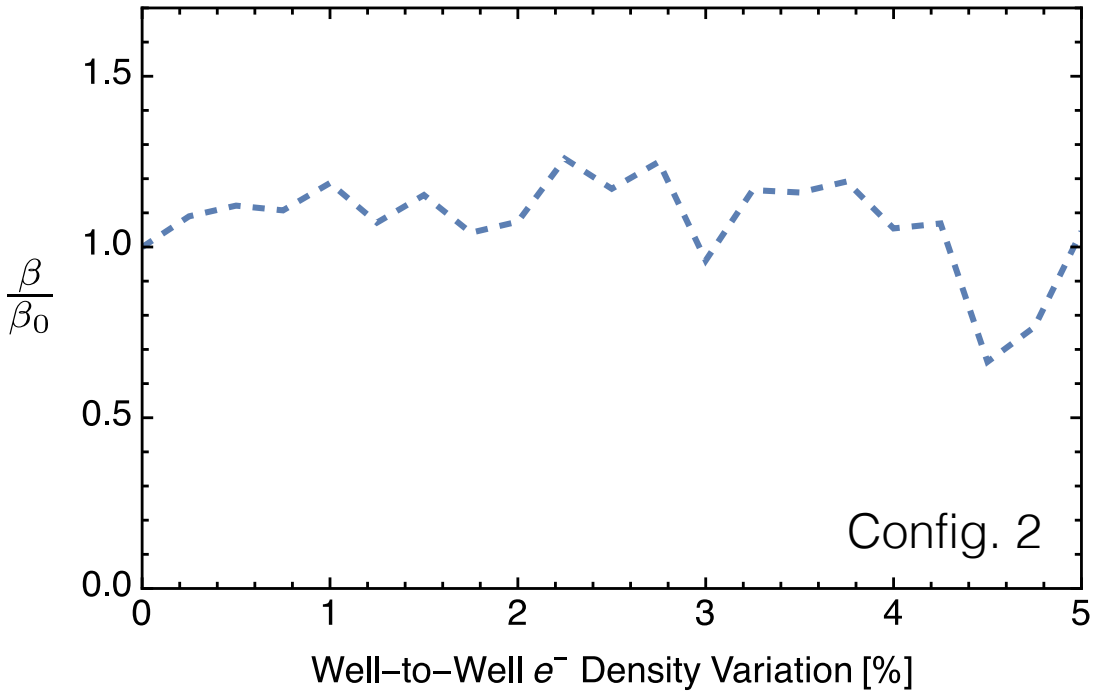

Mehrani, arXiv:2509.14320